Estimation of Geopotential Differences Over Intercontinental Locations Using Satellite and Terrestrial Measurements

by
N. K. Pavlis

Report No. 409

Department of Geodetic Science and Surveying
The Ohio State University
Columbus, Ohio 43210-1247

August 1991

Estimation of Geopotential Differences Over Intercontinental Locations Using Satellite and Terrestrial Measurements

by
N. K. Pavlis

Report No. 409

Department of Geodetic Science and Surveying
The Ohio State University
Columbus, Ohio 43210-1247

August 1991

ABSTRACT

An error analysis study was conducted in order to assess the currently achievable accuracies and the future anticipated improvements in the estimation of geopotential differences over intercontinental locations. Extending the ideas put forward by Colombo (1980), an observation/estimation scheme was proposed and studied, whereby gravity disturbance measurements on the Earth's surface, in caps surrounding the estimation points, are combined with corresponding data in caps directly over these points at the altitude of a low orbiting satellite, for the estimation of the geopotential difference between the terrestrial stations. The gravity disturbance data at altitude are inferred from GPS measurements made from the low orbiter to the high-altitude GPS satellites, in a multiple-high-single-low Satellite-to-Satellite Tracking (SST) configuration.

The mathematical modeling required to relate the primary observables to the parameters to be estimated, was studied both for the terrestrial data and the data at altitude. Emphasis was placed on the examination of systematic effects and on the corresponding reductions that need to be applied to the measurements to avoid systematic errors. For the gravitational accelerations inferred from SST data, a mismodeling related to a centrifugal acceleration term was identified and corrected. Alternative formulations related to the sampling (or discretion) and the propagated errors arising in the truncation theory considerations were derived. Recurrence relations for the altitude generalized truncation coefficients implied by Hotine's kernel, and for the degree variances implied by a first-order Gauss-Markov covariance model were originally developed in this study.

The error estimation for the geopotential differences was performed using both truncation theory and least-squares collocation with ring-averages, in case observations on the Earth's surface only are used. The error analysis indicated that with the currently available global geopotential model OSU89B and with gravity disturbance data in 2° caps surrounding the estimation points, the error of the geopotential difference arising from errors in the reference model and the cap data is about 23 kgal cm, for 30° station separation. This error is expected to reduce to about 12 kgal cm, when the lower-degree harmonics of the reference model are improved by the incorporation of the global GPS-

tracking data on Gravity Probe-B. The incorporation of gravity disturbance data at altitude was studied using least-squares collocation with ring-averages. It was found that for a low-degree (Nmax = 45) reference model, the data at the altitude of GP-B (600 km) can improve the geopotential difference accuracy by about 7%, as compared to the use of terrestrial data only. However, additional high-frequency observables at lower altitude are needed to achieve the results obtainable when a high-degree reference model is used, and to this end the gradiometer data from ARISTOTELES will provide a significant contribution.

FOREWORD

This report was prepared by Mr. Nikolaos K. Pavlis, Graduate Research Associate, Department of Geodetic Science and Surveying, under the supervision of Professor Richard H. Rapp. This study was supported by NASA Grant NAG 5-1329, The Ohio State University Research Foundation Project No. 723194. This grant was administrated by the NASA Goddard Space Flight Center, Greenbelt Maryland 20771. The NASA Technical Officer for this grant is Dr. Jean Welker, Code 621. Substantial computer support was provided by the Academic Computing Services, The Ohio State University. Substantial support was also provided by the Ohio Supercomputer Center through grant pas 160.

A slightly modified version of this report was submitted to the Graduate School of The Ohio State University in partial fulfillment of the requirements for the degree Doctor of Philosophy.

The reproduction and distribution of this report was carried out with funds supplied, in part, by the Department of Geodetic Science and Surveying.

ACKNOWLEDGMENTS

I express my sincere appreciation to my adviser Professor Richard H. Rapp for his guidance, encouragement and support throughout this research work. Working under his supervision for this, as well as other, research projects has been a most educating experience. To him and to Professors Clyde C. Goad and Ivan I. Mueller I am most indebted for their constructive criticism on my work and their suggestions and comments.

Special thanks go to my friends from the Department of Geodetic Science and Surveying whose interaction and friendship has made my stay at The Ohio State University a most enjoyable experience. In particular, I offer sincere thanks to Dr. George Dedes, Dr. Petros Patias and Dr. Theodossios Engelis for their friendship and willingness to share with me their knowledge and experience on a variety of topics during the first years of my studies. The friendship of Mr. Jarir Saleh, Mr. Jeong-Hee Kim and Dr. Yan Ming Wang is gratefully acknowledged.

Last but not least, I am indebted to Miss Melanie Hennell who typed this manuscript. Her excellent typing and patience in making a number of modifications are largely responsible for the present form of this material.

TABLE OF CONTENTS

LIST OF TABLES

LIST OF FIGURES

CHAPTER I

INTRODUCTION

The fundamental objective of geodesy is the accurate determination of the position and the gravity potential of points on the surface of the Earth or in the space surrounding the Earth. Such information is essential to support research (as well as application) in a number of related disciplines such as geodynamics, geophysics and oceanography.

Historically, geodesists have divided the problem of position and gravity potential determination in two parts, due to the limitations imposed both by Nature and by the observational techniques available. In that sense, angle and distance measurements on the Earth would provide through triangulation and trilateration the "horizontal" coordinates (ϕ, λ) of a point. The reference surface employed in these determinations is the surface of an ellipsoid of revolution. The traditional practice in such determinations (as opposed to modern integrated approaches) emphasizes on geometric principles, while gravity field information is mainly used for the reduction of the surface measurements to the reference ellipsoid. However, since the reference ellipsoid is a surface not physically realizable, the third coordinate, the height of a point with respect to this surface, had to be determined indirectly.

A rather easily accessible and naturally provided surface, the Mean Sea Surface (MSS) or Mean Sea Level (MSL), would provide the reference surface with respect to which geopotential numbers and heights could be reckoned. As long as the MSL, as realized by tide gauge observations, was identified with a unique equipotential surface-the geoid, spirit leveling (a highly accurate geodetic measurement type) and gravity observations, would provide the geopotential number of a point. With certain approximations involved, geopotential numbers would yield orthometric heights, while gravimetry would provide the geoidal undulations (e.g. through Stokes' integral) required for the computation of heights with respect to the reference ellipsoid.

Under such operational procedures, the concepts of height and geopotential difference become heavily inter-related; their determination constitutes the second part of the problem mentioned in the beginning, where the physical properties of the Earth play a dominant role. The advantage of MSL is that it provides a natural connection between continents, enabling determination of height and geopotential differences between points which cannot be connected by leveling. In that sense, MSS becomes the natural reference surface for these determinations and establishes a world vertical datum. Obviously, the entire setup heavily depends on the assumption that MSS coincides with a unique equipotential surface of the Earth's gravity field, and on the accurate realization and monitoring of MSL.

1.1 Vertical Datum Inconsistencies and the Impact of Modern Space Techniques

Advances in a number of areas, that occurred during the last two decades, have caused geodesists to reconsider the classical procedures of vertical datum definition and height determination. Two main reasons are responsible for that:

(1) It has been well recognized by now that the MSS departs from an equipotential surface due to the presence of the Quasi-stationary Sea Surface Topography (QSST), whose magnitude is on the order of a meter. The presence of QSST affects the definition of vertical datums in two ways:

(a) Vertical datums established with respect to different tide gauge stations do not refer (in general) to the same equipotential surface, their offsets being on the order of $\pm \sqrt{2}$ kgal m (1 kgal m = 10 m^2/s^2).

(b) If in the adjustment of a vertical network, more than one tide gauge station were constrained to have zero elevations (e.g. the 1929 General Adjustment of the U.S. vertical reference system), the QSST differences at these stations will cause internal distortions that propagate throughout the adjusted network.

Laskowski (1983) has studied the effects of vertical datum inconsistencies on various gravimetric quantities by constructing certain models for the inconsistencies,

using also the oceanographic estimates of the QSST derived by Lisitzin (1965). Laskowski (ibid) also studied the likely distortions that the overconstraining of the 1929 adjustment of the U.S. leveling network might have caused. He concluded that the internal distortions are most severe near the tide gauges where incorrect zero-constraints were imposed. On a global basis, the gravity anomaly errors implied by the vertical datum inconsistency models he used, when analyzed harmonically, indicated that most of the power of the gravitational signatures is concentrated below spherical harmonic degree 60.

(2) The advent of modern space techniques, such as Very Long Baseline Interferometry (VLBI), Satellite Laser Ranging (SLR) and the Global Positioning System (GPS), has changed fundamentally the position determination procedures.

Laser ranging to the high-altitude LAser GEOdynamic Satellite (LAGEOS) has enabled the determination of geocentric coordinates for a number of globally (but not evenly) distributed permanent tracking sites to accuracies at the ± 5 cm level (Smith et al., 1985). VLBI measurements, on the other hand, are capable of determining baseline vectors between stations separated by 7000 km, accurate to a few centimeters, from 24-hour observing sessions (Herring, 1986). Being a geometric technique however, insensitive to the stations' locations with respect to the Earth's center of mass, VLBI requires that, at least one station's geocentric coordinates in the network, be defined from another source (e.g. from SLR observations). Finally, relative positioning using the GPS has already proved its capability to yield baseline components accurate to 2-3 ppm of the baseline length on a local or regional basis. With the full satellite constellation in orbit, dual frequency receivers and orbit determination using a fiducial network of tracking stations, it is expected that the system's performance will be at the 3 mm plus 0.01 ppm of the baseline length (Carter et al., 1989). Apart of the individual accuracy achievements in positioning, of each of the above techniques, the recent (January 1, 1988) establishment of the International Earth Rotation Service (IERS) (Mueller, 1988) enables the optimum combination of the results obtained by the above techniques (as well as Lunar Laser Ranging, and Doppler techniques), and the definition and maintenance of a Conventional Terrestrial Reference System (CTRS). The realization of such a system is accomplished through a network of stations whose geocentric coordinates are estimated

within a few centimeters and which constitute the Conventional Terrestrial Reference Frame (CTRF).

The main impact of the space techniques on the problem of height determination comes from their ability to provide all three components of the geocentric Cartesian coordinate vector, and thus geometric (ellipsoidal) heights as well. Hence, one of the two uses of leveling (that of providing vertical position information) becomes unnecessary. Consequently, in the context of modern position determination techniques, the concepts of height and geopotential difference may be well distinguished. Substantial effort has been made during the last few years, by a number of researchers (Engelis et al. (1985), Kearsley (1986), Schwarz et al. (1987), Rapp and Kadir (1988)) to investigate the data requirements and the attainable accuracies in deriving orthometric height differences from GPS-derived ellipsoidal height differences and gravimetric undulation differences. Such procedures aim to eliminate the need for spirit leveling in regional applications, essentially reversing the traditional geodetic practice in height determination. The aforementioned studies indicate that orthometric height differences accurate to about 2 ppm (of the baseline length), for lines 10-70 km long, are attainable, provided good gravity data coverage exists and one carefully accounts for topographic effects. Although such procedures may never reach the accuracy level of first-order spirit leveling, they certainly provide a promising cost-effective alternative for lower order vertical control on a regional basis.

1.2 The Task of Vertical Datum Unification and the Proposed Approaches

From the previous discussion, it becomes obvious that the internal inconsistencies in continental vertical networks, due to over-constraining of tide gauge stations, can be removed by re-adjusting the networks using only one geopotential number constraint (minimum constraint solution) (Laskowski, 1983). Such procedure was followed in the establishment of the United European Leveling Network 1973 (UELN-73), where the Normal Amsterdam Piel (NAP) was held fixed to an arbitrarily assigned geopotential number as the "origin" point of the network (Kelm, 1985). The same procedure is adopted for the definition and re-adjustment of the North American Vertical Datum 1988 (NAVD 88) (Zilkoski, 1986).

The removal of internal distortions from continental vertical networks does not pose any theoretical problems, nor does it require any additional observations other than the geopotential differences obtained from leveling and gravimetry. The implications however (e.g. in map-making) of changing the height system for an entire country or continent have to be considered carefully. In addition, even if a tide gauge were to be selected as the "origin" point of such network, the presence of the QSST would cause some points along the coast to be below, and some above, the MSL (Colombo, 1985a). Land "below sea level", shown on a coastal map, would be undesirable from the practical point of view; however, as Colombo (ibid) pointed out, such problems may be avoided using a local vertical reference for the region, based on a local tide gauge. Provided that at least one station is connected to both the local and the national (or international) network, both sets of "heights" may be converted to each other unambiguously. Such procedures are conceptually very similar to the use of local "best-fitting" ellipsoids as opposed to a global "Mean-Earth" ellipsoid (Heiskanen and Moritz, 1967, section 5-11) in "horizontal" network applications.

According to the above, the definition and realization of a global vertical network finally reduces to the task of accurate determination of geopotential differences between points that cannot be connected by spirit leveling (combined with gravity observations), i.e. between points separated by ocean. Once these geopotential differences are determined, e.g. between the "origins" of the various (internally consistent) continental networks, an arbitrary value for the potential at one "origin" point, is enough to provide a global uniform system of geopotential numbers.

Although the need for internally consistent continental networks arises from practical considerations, establishing intercontinental vertical connections is primarily of scientific, rather than operational interest, and the necessity of such connections has been debated in the literature. One advantage that a global vertical network possesses, is that it will enable referencing of regional gravity anomaly databases to a uniform system, thus freeing global anomaly fields from regional systematic errors induced by height inconsistencies (Rapp, 1983; Heck, 1990). Colombo (1985b) however, has pointed out that GPS observations and gravimetry may enable one to switch from gravity anomalies to gravity disturbances, in future gravity surveys, the latter ones being independent of orthometric height inconsistencies. Although this is true, it is also unreasonable to

believe that the wealth of gravity anomaly data acquired in the past will be simply abandoned under such operational procedures.

The approaches proposed for the unification of vertical datums are based on either one of the two following principles:
(a) Since the MSS does not coincide with an equipotential, define and realize in some manner another equipotential surface to be the reference; if both the MSS as well as its departures from the reference surface are accurately determined and monitored, the transoceanic connections based on tide gauges can be maintained.
(b) Abandon MSS as a transoceanic connection and seek alternative techniques of estimating accurately geopotential differences between points separated by ocean.

Colombo (1985b) classified the observational techniques and estimation procedures proposed up to now for the unification of vertical datums into four main categories; the first two follow principle (a) above, while the other two (b).

(1) Oceanographic Approach

This technique, outlined by Cartwright (1985) considers the reference surface to be at a fixed geopotential number above an isobaric (i.e. equipressure) surface, 2000 decibars below the annual MSS at some specified epoch. Cartwright's technique employes hydrographic measurements along profiles that extend from shallow areas near a tide gauge, to ocean depths of more than 2 km. These profiles are selected to coincide with the repeat groundtracks of an altimeter satellite that can provide estimates of the ellipsoidal height of the sea surface. Steric and geostrophic leveling are used to determine the shallow point elevation relative to the deep isobaric surface, while pressure measurements and spirit leveling are used to connect the shallow point to the nearby tide gauge.

From the theoretical point of view, arguments against this technique have been raised, related to the accuracy and suitability of the isobaric surface ("level of no motion") hypothesis (Colombo, 1985b). In addition, the geostrophic leveling used to connect the deep ocean location to the shallow one, may not be accurate enough to model the complex ocean dynamics near the continental boundary (Wunsch and Gaposchkin, 1980). From the practical point of view, several oceanographic restrictions limit the selection of sites

where the technique could be applied (e.g. sites must have narrow continental shelves, should not be affected by river discharge, strong currents etc.). In addition, at least a full year of (nearly) simultaneous observations at all sites is required to establish the transoceanic links, and the resulting vertical datum would have a rather strong time dependency and would require periodic re-definition. Although periodic maintenance would be necessary for a global vertical datum, no matter what technique is used to define and realize it (since the Earth's gravity field undergoes secular and periodic changes due to a variety of geodynamic phenomena such as post-glacial rebound, mass redistribution etc.), alternative techniques may offer better temporal stability.

(2) Altimetry-Gravimetry Approach

This technique, considered variously by Mather et al. (1978) and Wunsch and Gaposchkin (1980), utilizes altimetric observations in combination with ocean gravimetry and aims to the simultaneous recovery of the QSST and the geoidal undulation. The estimation technique proposed by Wunsch and Gaposchkin (ibid) is in essence least-squares collocation, and the separation of the geoidal from the QSST signal is aided by the use of prior information in the form of a-priori degree variances for these signals. One of the limitations of such procedures comes from the inaccurate and insufficiently sampled oceanic gravity measurements. However, the ideas of Wunsch and Gaposchkin (ibid) have been pursued further by a number of investigators (Wagner, 1986; Engelis, 1987) and recent analyses (e.g. Denker and Rapp, 1990) have verified the ability of satellite altimetry to determine the long-wavelength features of the global ocean circulation and simultaneously provide improved estimates of the long-wavelength part of the oceanic geoid, as well as, improved orbital parameters. Such solutions though, aim to resolve global features of the QSST, with wavelengths greater than about 4000 km; detailed local determinations in the shallow areas near the tide gauge locations are further complicated by the inaccuracies of the tidal models.

(3) Geodetic Approach

The main ideas in this direction have been put forward by Colombo (1980). He considered the realization of a global vertical network by a set of benchmarks whose

geocentric coordinates and geopotential differences are accurately determined. In his analysis, SLR techniques would provide the geocentric coordinates, while surface gravimetry, spirit leveling and a low-degree geopotential model would provide the geopotential differences, in a least-squares collocation solution. He has also considered a modification of the observed gravity anomalies to avoid possible contamination of the estimated geopotential differences, by systematic errors in the anomalies due to height inconsistencies. Additional error analysis performed by Hajela (1983) has indicated that Colombo's technique could provide a US - Europe connection at that time, to an accuracy of about 50 to 60 kgal cm. The reference geopotential model used at that time was the OSU81 (Rapp, 1981a). The disadvantage of Colombo's technique lies on its dependence on the reference geopotential model. That is, the transoceanic "connection" of stations is carried out analytically, through the long-wavelength information provided by the reference model. Consequently, any errors of the low-degree harmonics propagate directly to the estimated geopotential differences. This has also been manifested in the contribution of the errors of the model to the total error budget, in the error analyses performed.

Hein and Eissfeller (1985) have discussed the application of an integrated geodesy adjustment approach to the problem, considering stations at (or near) tide gauges and additional observations to those considered by Colombo (1980), such as altimeter measurements and deflections of the vertical. Brovar (1988) and Rummel and Teunissen (1988), on the other hand, have considered the analytical modification to the solution of the geodetic boundary value problem, so that vertical datum offsets can be introduced as unknowns and estimated by solving a linear system of equations. The technique of Rummel and Teunissen (ibid) requires the same type of observables as the one of Colombo (1980). However, the former, is in the strict sense applicable only if vertical datum offsets are identified worldwide and introduced as unknowns in the linear system to be solved, provided also that global coverage of gravity anomalies is available; such restrictions have been circumvented in Colombo's (ibid) approach.

(4) Relativistic Approach

Based on a different physical principle, this technique, introduced by Bjerhammar (1985), aims to the direct measurement of geopotential differences, using the effect of

gravitation on frequency standards, as predicted by the theory of general relativity. Unfortunately, this effect is too small to be detectable by the frequency standards available at present, and application of this technique has to be postponed until orders of magnitude improvements are achieved in the accuracy of frequency standards.

The scientific and technological advances that have been achieved, or are anticipated for the near future, appear to favor at present the implementation of oceanographic or geodetic type of approaches for vertical datum connections. Both techniques (but more critically the oceanographic) require some internationally co-ordinated observation campaign for their implementation (Rapp, 1987); given the limited interest (from the operational point of view) for unification of vertical datums, techniques that promise best results while taking maximum advantage of data that either exist, or will be collected for other investigations, should be preferred. Also, preference should be given to those techniques that provide longer temporal stability in the resulting unified global vertical network, and thus require less often re-definition and maintenance.

1.3 Motivation, Objective and Organization of the Present Study

Two types of geodetic projects currently under planning and/or development create a favorable situation for the implementation of geodetic techniques for vertical datum connections.

First, the incorporation of GPS receivers on-board a number of satellites scheduled for launch in the 1992-1995 time frame. Table 1 (see also (Colombo, 1990)) provides some information related to these missions. With the GPS receiver on-board the lower orbiter observing simultaneously as many as seven GPS satellites, a Multiple-High-Single-Low Satellite-to-Satellite Tracking (SST) configuration is established (Jekeli and Upadhyay, 1990). Such configuration enables one to estimate all three components of the total inertial acceleration at the altitude of the low orbiter. Provided non-gravitational accelerations can either be measured (as is proposed for ARISTOTELES), or effectively be eliminated (as in the case of the drug-free GP-B spacecraft), the result of such an observational system may be viewed as a dense grid of uniform quality "observations" of the gravitational acceleration vector at the altitude of the low orbiter. There are two ways that such "observations" can contribute to the solution of the problem at hand:

(a) Analysis of the global set of measurements collected during the lifetime of the low orbiters, is capable of producing global geopotential models whose quality is orders of magnitude better than current state-of-the-art models, and whose resolution (half wavelength) ranges from about 600 km (TOPEX/POSEIDON) to 100 km (ARISTOTELES). These figures have been assessed initially for GP-B by Smith et al. (1988) using an analytical approach, and have been verified recently through more elaborate and complete simulation studies (Pavlis, E. et al., 1990). Given the importance of an accurate geopotential model in the implementation of geodetic approaches for vertical datum connections, a major contribution to the achievable accuracies is to be expected from the above missions.

(b) The dense grid of observations at altitude may help resolve localized signatures of the gravitational field on the surface of the Earth, provided the satellite is low enough and/or instrumentation on-board provides additional measurements, more sensitive to the finer details of the field (e.g. the gravity gradiometer in the case of ARISTOTELES).

Table 1. Future Satellite Missions Expected to Carry GPS Receivers On-Board.

Name	Scheduled Launch Date	Altitude/ Inclination	Description
TOPEX/ POSEIDON	1992	~ 1336 km 66.02°	USA and French Altimeters and other oceanographic instruments. GPS receiver under development.
GRAVITY PROBE-B (GP-B)	1995	~ 600 km 90°	Stanford General Relativity Gyroscopic Experiment. Drag-Free. 2-year mission.
ARISTOTELES	1995	~ 200 km 96.3°	European Space Agency's Gravity Gradiometer. 6-month mission.

A second type of geodetic activity, pertinent to the vertical datum connection problem, is the geodetic fixing of Tide Gauge Bench Marks (TGBMs) (Carter et al., 1989), a project that has been initiated by the International Association for Physical Sciences of the Ocean (IAPSO). Highly accurate determination of the geocentric positions of the TGBMs (as well as accurate monitoring of their motions) is necessary, in order to separate the crustal motions of the TGBMs from the apparent changes of the MSL observed at their locations, and thus, provide the means of investigating the possibility that global MSL shows a rising trend resulting from global warming (IAPSO, 1985). Although monitoring changes in the global sea level does not require establishment of a global vertical network, the data that are to be collected for the former purpose, can be of use for the latter as well. In addition, if geopotential differences between TGBMs can be determined accurately, without any reliance to MSL, they can be used to provide independent control over oceanographically determined QSST differences between the TGBMs.

The above developments provided the motivation to reconsider (from the geodetic point of view) the problem of estimating geopotential differences between points separated by ocean. As mentioned already, this is equivalent to the problem of connecting different vertical datums to a common reference, thus establishing a uniform global vertical datum. Following the ideas of Colombo (1980), a "global vertical datum" is defined here as a network of benchmarks situated on various continents, between which a set of estimated geopotential differences is given. The technique used to estimate these geopotential differences is based on an observational system that attempts to improve the one considered by Colombo (ibid), and overcome some of its limitations. The basic "components" of the current observational setup are shown in Figure 1.

Two benchmarks, BMA and BMB, are considered to be situated on the same or on different continents (separated by ocean). These are VLBI or SLR stations, whose geocentric coordinates are known to sub-decimeter accuracy, and in addition they are equipped with calibrated absolute gravimeters, so that the magnitude of absolute gravity is also known accurately at these sites. Differential GPS observations, and relative gravity measurements, provide estimates of the gravity disturbance at points inside "caps"

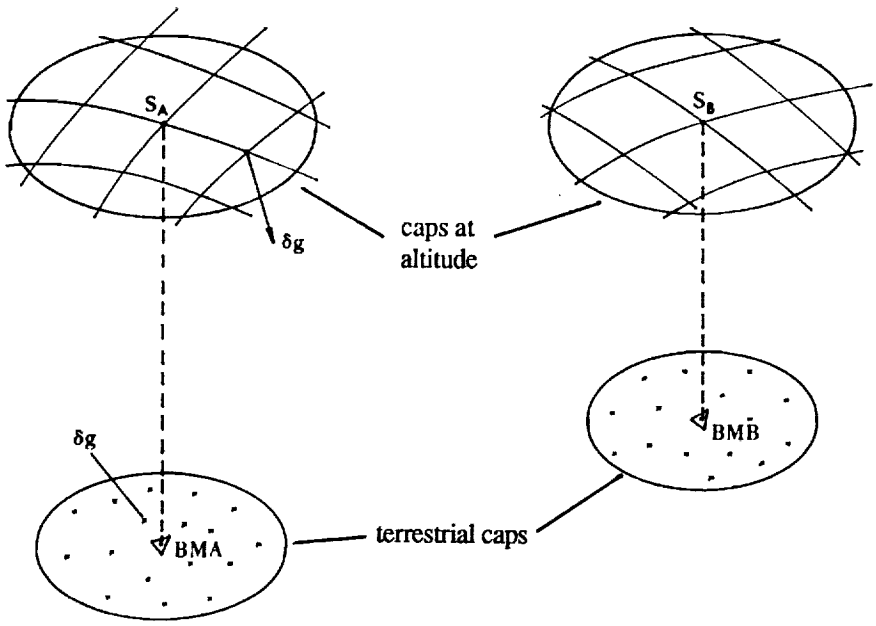

Figure 1. The Basic Observational Geometry.

centered at the corresponding benchmarks. Consider also, "caps" centered directly over these benchmarks, at the altitude of a satellite which carries a GPS receiver on-board. Inside these caps, at satellite locations whose geocentric coordinates are known from the GPS tracking, some functional of the gravitational potential has been estimated (e.g. the three components of the gravitational acceleration vector).

From the data requirement point of view, apart of information that either exists already or will be obtained as part of other geodetic activities, the additional observations required here are the absolute gravity measurements at the benchmarks and the gravity disturbances in the caps surrounding them. Careful coordination (in terms of site selection) with the project of geodetic fixing of TGBMs (Carter et al., 1989) can reduce the number of additional absolute gravity measurements required, while kinematic (or rapid static) GPS techniques can provide an efficient way of performing the gravimetric surveys inside the caps.

Based on the above information, using also a reference geopotential model, one can estimate the potential difference between the benchmarks BMA and BMB, using

least-squares collocation (Moritz, 1980). In addition, such estimation technique, enables one to derive measures of the accuracy of the resulting estimates. The main objective of this study is to provide accuracy estimates for the resulting geopotential differences, based on realistic assumptions for the errors associated with the input data, and considering the observational setup of Figure 1, or variations of it. More precisely, the error analysis to be presented, will address the following issues:

(1) The attainable accuracies for the geopotential differences, if state-of-the-art geopotential models, developed in the absence of the anticipated missions, are to be used in the estimation.

(2) The corresponding accuracies using models of the quality expected to be obtained from various future missions.

(3) The contribution of observations at altitude to the estimation of the geopotential differences, and the possible improvements in accuracy through the incorporation of such observations.

It is worth noticing that the procedure considered here does not involve spirit leveling at all. In more realistic configurations, involving more than one benchmark per continent, if geopotential differences between these benchmarks are available from leveling (combined with gravimetry), they could (and should) be used in a simultaneous adjustment, to increase the redundancy and strengthen the solution (as in the estimation scheme described by Colombo (1980)). In that sense the current error analysis corresponds to a worst-case scenario.

CHAPTER II

MODELING ASPECTS

The accuracy that can be achieved in the estimation of the geopotential differences using the configuration described in section (1.3), depends on the accuracies of the primary observables involved in the estimation, and on the way according to which random and systematic errors in the observed quantities propagate to the estimated values. The former can be assessed from information related to the performance of the sensing instruments involved in the data acquisition process (e.g. gravimeters); the latter requires the development of analytical formulations that relate the primary observables to the quantities of interest, and constitutes the subject of this chapter. More precisely, the following paragraphs focus on the modeling of the gravity disturbance observations on the surface of the Earth, and of the components of the gravitational acceleration vector at altitude as obtained from a Satellite-to-Satellite tracking configuration.

2.1 The Boundary Condition Implied by Gravity Disturbance Observations

Let (r, θ, λ) denote geocentric distance, geocentric co-latitude and longitude respectively. The following notation definitions are adopted:

$V(r, \theta, \lambda)$: true gravitational potential of the Earth.

$V^e(r, \theta)$: gravitational potential of a reference ellipsoid of revolution whose surface is an equipotential surface of its gravity field.

$V^m(r, \theta, \lambda)$: true value of the gravitational potential of the Earth, that arises from all the harmonics only up to maximum degree M.

$\Phi(r, \theta)$: true centrifugal potential of the Earth.

It is well known (Heiskanen and Moritz, 1967, p. 47) that:

$$\Phi(r, \theta) = \frac{1}{2}\omega^2 r^2 \sin^2\theta \tag{2.1}$$

where ω is the spin rate of the Earth. An estimate of $\Phi(r, \theta)$ may be obtained from estimated values of r, θ and ω. Assuming for a moment that (r, θ) are perfectly known, the error in the estimated value of $\Phi(r, \theta)$ due to an error ε_ω in ω will be:

$$\varepsilon\hat{\Phi}(r, \theta)_\omega = \hat{\omega} r^2 \sin^2\theta \varepsilon_\omega \tag{2.2}$$

Using the nominal values r = 6371 km, $\hat{\omega}$ = 7292115 x 10^{-11}rad/s, and ε_ω = 0.1 x 10^{-11} rad/s (Chovitz, 1988), one has for a point on the equator (where $\varepsilon\hat{\Phi}_\omega$ becomes maximum):

$$\max\varepsilon\hat{\Phi}(r, \theta)_\omega \approx 3 \times 10^{-3} m^2 s^{-2} = 3 \times 10^{-4} \text{ kgal m} \tag{2.3}$$

Such error in potential translates to linear ("height") error of about 0.3 mm and therefore is, in the context of this study, negligible. Hence, in all subsequent analysis, the spin rate of the actual Earth will be considered perfectly known and equal to the spin rate value used in the definition of the reference ellipsoid, i.e.

$$\varepsilon\hat{\Phi}(r, \theta)_\omega = 0\,, \tag{2.4}$$

and the centrifugal potential estimated from perfectly known (r, θ) but approximately known ω, will be considered identical to the true centrifugal potential of the actual Earth. The following notation will be used:

$$W(r, \theta, \lambda) = V(r, \theta, \lambda) + \Phi(r, \theta) \tag{2.5}$$

$$U^e(r, \theta) = V^e(r, \theta) + \Phi(r, \theta) \tag{2.6}$$

$$U^m(r, \theta, \lambda) = V^m(r, \theta, \lambda) + \Phi(r, \theta) \tag{2.7}$$

so that, W represents the true gravity potential of the Earth, U^e the gravity potential of the reference ellipsoid, and U^m the true value of the part of the gravity potential of the Earth that contains harmonics of the true gravitational potential only up to maximum degree M. V^m and U^m should not be confused with estimates $\hat{V}^m$ and $\hat{U}^m$ of these quantities, obtained e.g. through satellite perturbation analysis; the former are true values while the latter are contaminated by the commission error of the estimated harmonic coefficients.

The disturbing potential T at a point $P(r, \theta, \lambda)$, is now defined by Heiskanen and Moritz (1967, section 2-13):

$$T_P = W_P - U^e_P \tag{2.8}$$

with respect to the ellipsoidal field, and by:

$$T^m_P = W_P - U^m_P \tag{2.9}$$

with respect to the truncated field U^m. Due to the previous definitions and the assumption made concerning the centrifugal potential, one has:

$$T_P = V_P - V^e_P \tag{2.10}$$

$$T^m_P = V_P - V^m_P \tag{2.11}$$

In addition, the following quantities are introduced (Heiskanen and Moritz, ibid):

$$\text{gravity vector} : \vec{g}_P = \text{grad}(W)_P \tag{2.12}$$

$$\text{normal gravity vector} : \vec{\gamma}_P = \text{grad}(U^e)_P \tag{2.13}$$

$$\text{gravity disturbance vector} : \vec{\delta g}_P = \vec{g}_P - \vec{\gamma}_P \tag{2.14}$$

and the geometrical relations associated with these definitions are illustrated in Figure 2. According to the previous definitions and due to linearity of the gradient operator one has:

$$\vec{\delta g}_P = \text{grad}(T)_P \tag{2.15}$$

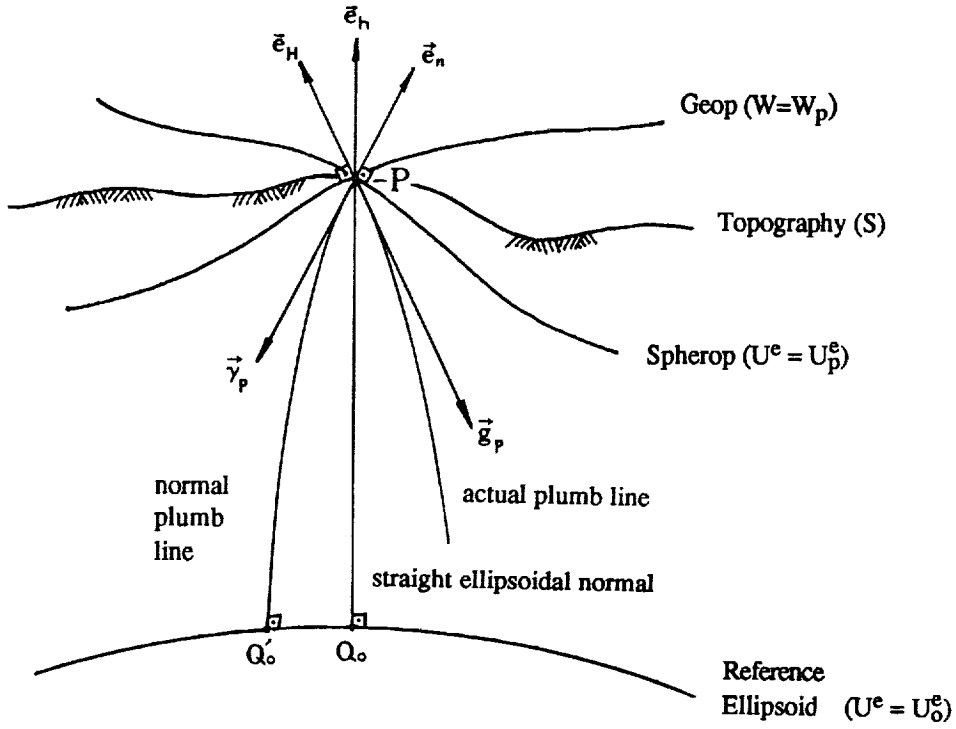

Figure 2. Geometry Associated With the Gravity Disturbance.

Now, proceeding along the same lines as Moritz (1980), if τ is the arc-length along the isozenithal (ibid, p. 345), one can derive from equation (2.15):

$$\delta g'_P = -\left(\frac{\partial T}{\partial \tau}\right)_P \tag{2.16}$$

where $\delta g'_P$ is the component of $\vec{\delta g}_P$ in the downward direction of the isozenithal passing through P. The very small curvature of the normal plumb line (Moritz, 1983, p. 7) justifies the approximation that the normal plumb line coincides with the straight ellipsoidal normal, in which case the isozenithal will also coincide with the straight ellipsoidal normal (Moritz, 1980, pp. 345-346). Under such an assumption, equation (2.16) becomes:

$$\delta g'_P = -\left(\frac{\partial T}{\partial h}\right)_P \tag{2.17}$$

and $\delta g_P'$ will be hereon understood to represent the component of $\vec{\delta g}_P$ along the downward direction of the straight ellipsoidal normal through P. If $\vec{e}_h$ is the unit vector in the direction of increasing ellipsoidal height, and $\vec{e}_n$ the unit vector along the normal plumb line (pointing outwards), then the assumption made before implies:

$$\vec{e}_h \equiv \vec{e}_n \tag{2.18}$$

and equation (2.17) may be written as:

$$\delta g_P' = (\vec{g}_P - \vec{\gamma}_P) \cdot (- \vec{e}_h) \tag{2.19}$$

where the dot denotes scalar product. According to (2.18) the last equation becomes:

$$\delta g_P' = - \vec{g}_P \cdot \vec{e}_h - |\vec{\gamma}_P|$$

$$= - \text{grad}(W)_P \cdot \vec{e}_h - |\vec{\gamma}_P| \qquad \text{or finally:}$$

$$- |\vec{\gamma}_P| = \delta g_P' + \left(\frac{\partial W}{\partial h}\right)_P \tag{2.20}$$

On the other hand, if $\vec{e}_H$ is the unit vector along the direction of increasing orthometric height, one has:

$$|\vec{g}_P| = \text{grad}(W)_P \cdot (- \vec{e}_H) \tag{2.21}$$

or, (Pavlis, 1988, equation 2.31) :

$$|\vec{g}_P| = \left(- \cos\bar{\theta} \frac{\partial W}{\partial h} - \xi \frac{\partial W}{M \partial \varphi} - \eta \frac{\partial W}{N \cos\varphi \partial \lambda} \right)_P \tag{2.22}$$

where, $\bar{\theta}$ is the total deflection of the vertical, ξ and η its latitudinal and longitudinal components respectively (Heiskanen and Moritz, 1967, p. 83), M and N the meridional and prime vertical radii of curvature respectively and φ denotes geodetic latitude.

Adding equations (2.20) and (2.22) by parts, one obtains:

$$|\vec{g}_P| - |\vec{\gamma}_P| = \delta g'_P + \varepsilon_P \tag{2.23}$$

where:

$$\varepsilon_P = \left[\left(1 - \cos\bar{\theta}\right)\frac{\partial W}{\partial h} - \xi \frac{\partial W}{M\partial\varphi} - \eta \frac{\partial W}{N\cos\varphi\partial\lambda} \right]_P \tag{2.24}$$

From equations (2.17) and (2.23) one has:

$$|\vec{g}_P| - |\vec{\gamma}_P| = -\left(\frac{\partial T}{\partial h}\right)_P + \varepsilon_P \tag{2.25}$$

However, it was shown by Pavlis (1988, equation 2.52), that:

$$\left(\frac{\partial \circ}{\partial h}\right)_P = \left(\frac{\partial \circ}{\partial r}\right)_P - e^2 \sin\theta_P \cos\theta_P \left(\frac{\partial \circ}{r\partial\theta}\right)_P + O(e^4) \tag{2.26}$$

where e is the first eccentricity of the reference ellipsoid. Hence, neglecting terms of the order e^4 and higher, one has from (2.25):

$$|\vec{g}_P| - |\vec{\gamma}_P| = -\left(\frac{\partial T}{\partial r}\right)_P + (\varepsilon_h)_P + \varepsilon_P \tag{2.27}$$

where,

$$(\varepsilon_h)_P = \left[e^2 \sin\theta\cos\theta \left(\frac{\partial T}{r\partial\theta}\right) \right]_P \tag{2.28}$$

Equations (2.25) or (2.27) represent the boundary condition of a Neumann-type boundary value problem (bvp) of potential theory (Kellogg, 1954), linearized with respect to a Somigliana-Pizzetti normal gravity field (Heiskanen and Moritz, 1967, section 2-7). From equations (2.22) and (2.24) follows that:

$$|\vec{g}_P| = -\left(\frac{\partial W}{\partial h}\right)_P + \varepsilon_P \quad . \tag{2.29}$$

Equation (2.25), when compared with (2.29), indicates that linearization with respect to the aforementioned normal field, removes the centrifugal terms from (2.29). In addition, linearization permits the truncation of the Taylor series expansion of $\partial\cdot/\partial h$, around $\partial\cdot/\partial r$, to terms of $O(e^2)$ in (2.27). Provided that the effect of the mass of the atmosphere has been taken into account analytically (see section 2.3), the disturbing potential T may be considered harmonic outside the topographic surface (S). The problem at hand then, is to determine the function T, harmonic outside (S), and regular at infinity, subject to the boundary condition (2.25) or (2.27), both valid over the known boundary (S). This is a fixed bvp; however, both (2.25) and (2.27) represent oblique derivative boundary conditions, since neither the ellipsoidal normal, nor the geocentric radius vector, are normal to the surface (S), where the boundary values are given. Equation (2.25) contains the effects of the approximation (2.18), while (2.27) contains in addition the effects of the neglected terms of $O(e^4)$ and higher in the Taylor series expansion of $\partial\cdot/\partial h$ around $\partial\cdot/\partial r$. Equation (2.27) may also be written as:

$$|\vec{g}_P| - |\vec{\gamma}_P| - [(\varepsilon_h)_P + \varepsilon_P] = -\left(\frac{\partial T}{\partial r}\right)_P \tag{2.30}$$

or, due to equations (2.10) and (2.11) :

$$|\vec{g}_P| - |\vec{\gamma}_P| - [(\varepsilon_h)_P + \varepsilon_P] + \left[\frac{\partial (V^m - V^e)}{\partial r}\right]_P = -\left(\frac{\partial T^m}{\partial r}\right)_P \tag{2.31}$$

For the purpose of future reference, equation (2.25) is also repeated here, written in the form:

$$|\vec{g}_P| - |\vec{\gamma}_P| - \varepsilon_P = -\left(\frac{\partial T}{\partial h}\right)_P \tag{2.32}$$

Regardless of the form of the boundary condition that one adopts, the primary observable from surface gravimetry is the magnitude of the gravity acceleration at the surface point P. The magnitude of the normal gravity at the same point can be computed to any degree of precision, once the reference ellipsoidal gravity field is defined and the geocentric coordinates of P are given (Heiskanen and Moritz, 1967, section 6-2). Hence, the gravity disturbance

$$\delta g_P = |\vec{g}_P| - |\vec{\gamma}_P| \quad , \tag{2.33}$$

as obtained from surface gravimetry, contains the observation errors of $|\vec{g}_P|$ and the errors in $|\vec{\gamma}_P|$ induced by the errors in the geocentric coordinates of P. The latter is a misregistration error, i.e., the actual observation refers to a different location than the one defined by the geocentric positioning results.

From the point of view of an analytical formulation for the solution of the current bvp, it is obvious that δg is related to the unknown disturbing potential, in a rather complicated manner, due to the presence of the atmospheric effects, the ellipsoidal terms $(\varepsilon_h)_P$ and ε_P, and even more critically due to the fact that it is defined over the topography, a very complex surface which cannot be describe analytically (Holota, 1985). Fortunately however, the dominant spherical character of both the shape, as well as the gravity field of the Earth, and the fact that the atmospheric mass amounts to only about 10^{-6} (Moritz and Mueller, 1987, p. 4) of the mass of the Earth (hence the atmospheric attraction is about 10^{-6} the attraction of the rest of the Earth's mass), have the consequence that the solution of the current bvp can be approximated to a high degree of accuracy by the solution of a second bvp of potential theory for the space exterior to a sphere. The latter solution can subsequently be refined by appropriate corrections that account for the differences between the real world and the idealized situation. The analytical solution of Neumann's bvp for the exterior of a sphere is the subject of the next section, while the refinements to this solution are considered afterwards.

2.2 Solution of Neumann's Boundary Value Problem for the Exterior Space of a Sphere

In the general case, the statement of the exterior Neumann's problem is given as (Kellogg, 1954, p. 246):

"Determine a function U, harmonic in the infinite region outside a closed surface S, if its normal derivatives $\partial U/\partial n$ assume on the surface S prescribed values". Harmonicity over an infinite region will be understood to include the demand for regularity at infinity (ibid, p. 217). Such demand ensures uniqueness for the solution of the exterior problem, unlike the interior one, where the unknown function can only be determined up to an additive constant (ibid, p. 246).

To develop an integral formula for the solution of the exterior problem, one must find a Green's function of the second kind G(P ; Q), such that:

$$U(P)=\frac{1}{4\pi}\iint_S \frac{1}{\ell} G(P\,;Q)\frac{\partial U}{\partial n}(Q)dS_Q \tag{2.34}$$

where, P is outside S and Q defines the location of the variable area-element dS_Q on S. In the current case the surface S will be the surface of a sphere of radius R, centered at the origin O of the coordinate system used (see Figure 3).

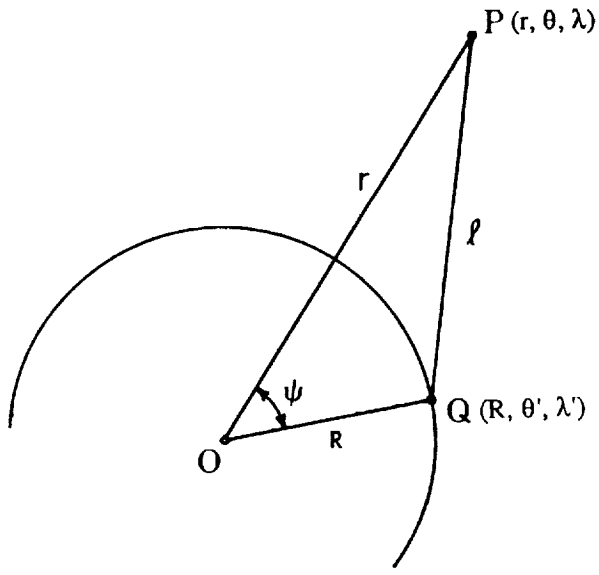

Figure 3. Geometric Relations Used in the Derivation of Hotine's Kernel.

The unknown function U will be denoted here T, while the boundary values $\partial T/\partial r$ with opposite sign will be denoted δg, i.e.

$$\delta g = -\frac{\partial T}{\partial r} \tag{2.35}$$

on the sphere (O, R). For the determination of the required Green's function one may proceed as in Hotine (1969) (see also (Sjöberg, 1990)). From Figure 3 one has:

$$\ell^2 = r^2 + R^2 - 2Rr\cos\psi \tag{2.36}$$

and setting:

$$k = \frac{R}{r} \tag{2.37}$$

yields:

$$\frac{r}{\ell} = \left(1 + k^2 - 2k\cos\psi\right)^{-1/2} \tag{2.38}$$

The right-hand side of the last equation is readily recognized to be the generating function of the Legendre polynomials (Davis, 1975, p. 365); hence:

$$\frac{r}{\ell} = \sum_{n=0}^{\infty} k^n P_n(\cos\psi) \tag{2.39}$$

where, $P_n(t)$ denotes the n^{th}-degree Legendre polynomial of the first kind with argument t (Heiskanen and Moritz, 1967, section 1-11), and the infinite series in (2.39) is absolutely and uniformly convergent for $k<1$. Considering k as an independent variable in (2.39) and integrating both sides of (2.39) with respect to k, one obtains:

$$\int \frac{r}{\ell}\,dk = \sum_{n=0}^{\infty} \frac{k^{n+1}}{n+1} P_n(\cos\psi) \tag{2.40}$$

Now, as Hotine (1969, p. 311) has observed:

$$\frac{2n+1}{n+1} = 2 - \frac{1}{n+1} \tag{2.41}$$

so that, from (2.39) and (2.40), taking also into account (2.37), one has:

$$2\frac{R}{\ell} - \int \frac{r}{\ell}\, dk = \sum_{n=0}^{\infty} \frac{2n+1}{n+1} k^{n+1} P_n(\cos\psi) \quad . \tag{2.42}$$

The indefinite integral in (2.42) may be evaluated in closed form as:

$$\int \frac{r}{\ell}\, dk = \ln 2 + \ln\left(\frac{\ell}{r} + k - \cos\psi\right) \quad . \tag{2.43}$$

Considering the limiting value of the expression on the right-hand side of equation (2.43) as r tends to infinity, it may be easily verified that:

$$\int_{\infty}^{r} \frac{r}{\ell}\, dk = \ln\left(\frac{\frac{\ell}{r} + k - \cos\psi}{1 - \cos\psi}\right) \quad . \tag{2.44}$$

In addition,

$$\lim_{r\to\infty}\left\{\frac{R}{\ell}\right\} = 0 \quad , \tag{2.45}$$

so that equation (2.42) implies:

$$2\frac{R}{\ell} - \ln\left(\frac{\frac{\ell}{r} + k - \cos\psi}{1 - \cos\psi}\right) = \sum_{n=0}^{\infty} \frac{2n+1}{n+1} k^{n+1} P_n(\cos\psi)\Big|_{\infty}^{r} \quad . \tag{2.46}$$

Since,

$$|P_n(t)| \le 1 \;\; ; \;\; -1 \le t \le 1 \;, \;\; n = 0, 1, 2, \ldots \tag{2.47}$$

one has:

$$\lim_{r\to\infty}\left\{\sum_{n=0}^{\infty}\frac{2n+1}{n+1}k^{n+1}P_n(\cos\psi)\right\}=\sum_{n=0}^{\infty}\frac{2n+1}{n+1}P_n(\cos\psi)\cdot\lim_{r\to\infty}\left\{k^{n+1}\right\}=0\ ,\tag{2.48}$$

as long as $k < 1$. Hence, equation (2.46) finally becomes:

$$H(k,\psi)=\sum_{n=0}^{\infty}\frac{2n+1}{n+1}k^{n+1}P_n(\cos\psi)\tag{2.49}$$

where:

$$H(k,\psi)=2\frac{k}{D}-\ln\left(\frac{D(k,\psi)+k-\cos\psi}{1-\cos\psi}\right)\quad;\quad\psi\neq 0\tag{2.50}$$

and:
$$D^2(k,\psi)=1-2k\cos\psi+k^2\tag{2.51}$$

The series in (2.49) has the same convergence properties as the one in (2.39), for $k < 1$. The case $k = 1$ requires special consideration in order to establish conditional convergence, except of course for $\psi = 0$ (Hotine, ibid). The function $H(k, \psi)$ will be designated hereon Hotine's function (or kernel); more precisely the form (2.50) will be referred to as Pizzetti's extension of Hotine's kernel, while the term Hotine's kernel will be reserved for the special case when $k = 1$.

The unknown function T is now identified to represent the disturbing potential (equations (2.8) and (2.10)). Assuming that T is harmonic outside the sphere (O, R), the following relation will be adopted for its expression in terms of solid spherical harmonics:

$$T(r,\theta,\lambda)=\frac{GM}{r}\sum_{n=0}^{\infty}\left(\frac{R}{r}\right)^n\sum_{m=-n}^{n}\overline{C}_{nm}\overline{Y}_{nm}(\theta,\lambda)\tag{2.52}$$

where: GM is the geocentric gravitational constant

$\bar{C}_{nm}$ are fully-normalized, unitless, disturbing potential coefficients (with respect to the ellipsoidal gravitational field)

and:

$$\bar{Y}_{nm}(\theta, \lambda) = \bar{P}_{n|m|}(\cos\theta) \cdot \begin{cases} \cos m\lambda & \text{if } m \geq 0 \\ \sin |m|\lambda & \text{if } m < 0 \end{cases} \tag{2.53}$$

where $\bar{P}_{nm}(t)$ is the fully-normalized associated Legendre function of the first kind with argument t (Heiskanen and Moritz, 1967, section 1-11). Denoting the n^{th}-degree surface spherical harmonic (ibid, section 1-10) of T by $T_n(\theta, \lambda)$, i.e.,

$$T(r, \theta, \lambda) = \frac{GM}{r} \sum_{n=0}^{\infty} \left(\frac{R}{r}\right)^n \sum_{m=-n}^{n} \bar{C}_{nm} \bar{Y}_{nm}(\theta, \lambda) \tag{2.54}$$

equation (2.52) becomes:

$$T(r, \theta, \lambda) = \sum_{n=0}^{\infty} \left(\frac{R}{r}\right)^{n+1} T_n(\theta, \lambda) \tag{2.55}$$

and both (2.52) and (2.55) are convergent for r > R (ibid, section 1-16). According to the last equation one has:

$$\frac{\partial T}{\partial r} = -\frac{1}{r} \sum_{n=0}^{\infty} (n+1) \left(\frac{R}{r}\right)^{n+1} T_n(\theta, \lambda) \tag{2.56}$$

and thus, according to (2.35):

$$\delta g(r, \theta, \lambda) = \frac{1}{r} \sum_{n=0}^{\infty} (n+1) \left(\frac{R}{r}\right)^{n+1} T_n(\theta, \lambda) \quad . \tag{2.57}$$

Note that δg here is used merely as a symbol for $-\partial T/\partial r$, with no explicit connection to the quantities that are actually observed, in contrast to the discussions of section 2.1. The relation between the current δg and the observables will be considered later.

Assuming that $\delta g(r = R, \theta, \lambda)$, on the surface of the sphere (O, R), can be expressed as a convergent series of surface spherical harmonics, $\delta g_n(\theta, \lambda)$, one has:

$$\delta g(R, \theta, \lambda) = \sum_{n=0}^{\infty} \delta g_n(\theta, \lambda) \quad . \tag{2.58}$$

and, due to (2.57) and (2.58), it follows that:

$$\delta g_n(\theta, \lambda) = \frac{n+1}{R} T_n(\theta, \lambda) \quad . \tag{2.59}$$

The surface spherical harmonics $\delta g_n(\theta, \lambda)$, may be determined by (Heiskanen and Moritz, equation 1-71) :

$$\delta g_n(\theta, \lambda) = \frac{2n+1}{4\pi} \iint_{\sigma} \delta g(R, \theta', \lambda') P_n(\cos\psi) d\sigma \quad , \tag{2.60}$$

where σ is the surface of the unit sphere, and :

$$\cos\psi = \cos\theta\cos\theta' + \sin\theta\sin\theta'\cos(\lambda - \lambda') \tag{2.61}$$

$$d\sigma = \sin\theta' d\theta' d\lambda' \quad . \tag{2.62}$$

Equation (2.60), due to (2.59), yields :

$$\frac{n+1}{R} T_n(\theta, \lambda) = \frac{2n+1}{4\pi} \iint_{\sigma} \delta g(R, \theta', \lambda') P_n(\cos\psi) d\sigma \quad \Rightarrow \text{(due to (2.55))}$$

$$T(r, \theta, \lambda) = \frac{R}{4\pi} \iint_{\sigma} \left[\sum_{n=0}^{\infty} \left(\frac{R}{r}\right)^{n+1} \frac{2n+1}{n+1} P_n(\cos\psi) \right] \delta g(R, \theta', \lambda') d\sigma \quad , \tag{2.63}$$

where in the last equation the orders of integration and summation have been interchanged. Due to (2.49), and considering (2.37), the last equation finally becomes:

$$T(r, \theta, \lambda) = \frac{R}{4\pi} \iint_{\sigma} H\left(\frac{R}{r}, \psi\right) \delta g(R, \theta', \lambda') d\sigma \quad . \tag{2.64}$$

The last equation is the desired integral formula, that determines the value of the harmonic function T, at any point P(r, θ, λ) outside the sphere (O, R), from the values of its normal (radial) derivative, given continuously over the surface of this sphere. In the limiting case where r→R, it can be shown easily that:

$$H(1, \psi) \equiv H(\psi) = \csc\frac{\psi}{2} - \ln\left(1 + \csc\frac{\psi}{2}\right) \tag{2.65}$$

and :
$$H(\psi) = \sum_{n=0}^{\infty} \frac{2n+1}{n+1} P_n(\cos\psi) \quad , \tag{2.66}$$

while equation (2.64) becomes :

$$T(\theta, \lambda) = \frac{R}{4\pi} \iint_{\sigma} H(\psi) \delta g(\theta', \lambda') d\sigma \quad , \tag{2.67}$$

where the constant radius R was omitted from the notation of the kernel H(ψ).

From equations (2.55) and (2.59) one also obtains:

$$T(r, \theta, \lambda) = R \sum_{n=0}^{\infty} \frac{1}{n+1} \left(\frac{R}{r}\right)^{n+1} \delta g_n(\theta, \lambda) \tag{2.68}$$

which represents the solution of the bvp in question, in terms of spherical harmonics (compare with (Heiskanen and Moritz, 1967, equation 1-91)); the surface spherical harmonics $\delta g_n(\theta, \lambda)$ are again obtained from equation (2.60).

Comparing equation (2.64) to (2.34), taking also into account the definition (2.35), it becomes obvious that the Green's function of the second kind G(P ; Q) for the problem at hand is :

$$G(P\,;Q) = -\,R\,H\left(\frac{R}{r}, \psi\right) \quad . \tag{2.69}$$

The function $H(k, \psi)$ possesses a number of properties which are given next :

(1) $$H(k, y) > 0 \;\; ; \;\; 0 < k \leq 1, \;\; 0 < \psi \leq \pi \tag{2.70}$$

This can be proved easily if one recognizes that for the above range of k and ψ, it holds true that :

$$\frac{2k}{D} \geq \frac{D + k - 1}{1 - t} \tag{2.71}$$

and utilizes a series expression for the quantity $\ln(1 + x)$ for $x > 1/2$.

(2) $$\nabla^2 H(k, \psi) = 0 \quad ; \quad k < 1 \quad , \tag{2.72}$$

i.e., $H(k, \psi)$ is harmonic outside the sphere (O, R), as it can be seen immediately from the expression (2.49).

(3) $$-\,r\frac{\partial H(k, \psi)}{\partial r} = \frac{R\left(r^2 - R^2\right)}{\ell^3} \quad , \tag{2.73}$$

which may be proved either by direct differentiation performed in equation (2.50), or, more simply, by differentiation of the series expression (2.49) utilizing also the relation (Heiskanen and Moritz, 1967, p. 35) :

$$\frac{R\left(r^2 - R^2\right)}{\ell^3} = \sum_{n=0}^{\infty} (2n + 1)\left(\frac{R}{r}\right)^{n+1} P_n(\cos\psi) \quad . \tag{2.74}$$

Note that the right-hand side of (2.73) is exactly the kernel function of Poisson's integral (ibid, equation 1-89). In addition, from (2.73) may be easily verified that:

$$\lim_{r \to R} \left\{ \frac{\partial H(k, \psi)}{\partial r} \right\} = 0 \quad ; \tag{2.75}$$

(the case $\psi = 0$ requires use of L'Hospital's rules to prove the last relation). This relation is actually a boundary condition that is imposed on the Green's function of the second kind, developed for the solution of the second bvp of potential theory (Roach, 1970, equation 9.88), specialized here for the case of spherical boundary.

A graph of the function $H(\psi)$ (equation (2.65)), is given in Figure 4; for comparison purposes, the figure also illustrates Stokes' function $S(\psi)$ (Heiskanen and Moritz, 1967, equation 2-164).

Although gravity disturbances are geometrically and conceptually simpler than gravity anomalies, traditional geodetic practice has relied heavily on the latter, for the determination of the external potential of the Earth. The underlying reason, is the requirement for a known boundary for the definition of the disturbances, unlike the anomalies (Hotine, 1969, p. 314). Using observations of the gravity anomaly vector and the gravity potential, all over the unknown surface of the Earth, Molodensky's bvp is formulated as a non-linear, free bvp, whose solution determines not only the external potential, but also the physical surface of the Earth. Linearization in that case requires the introduction of both a normal gravity field and an auxiliary known surface (the telluroid), in order to reduce the original problem to a linear, fixed bvp, and thus enable a tractable solution. The definition of the telluroid requires additional conditions to be imposed on either the potential anomaly ΔW (and the directions of actual and normal plumb lines) (Marussi mapping) or the gravity anomaly vector $\vec{\Delta g}$ (gravimetric mapping) (ibid, pp. 338-339). In the current case, the physical surface of the Earth is considered known, hence the introduction of the telluroid (and subsequently of the above conditions on ΔW or $\vec{\Delta g}$), is unnecessary. The normal gravity field, is introduced in order to remove centrifugal terms from equation (2.29) and enable an early truncation of series related to ellipsoidal terms.

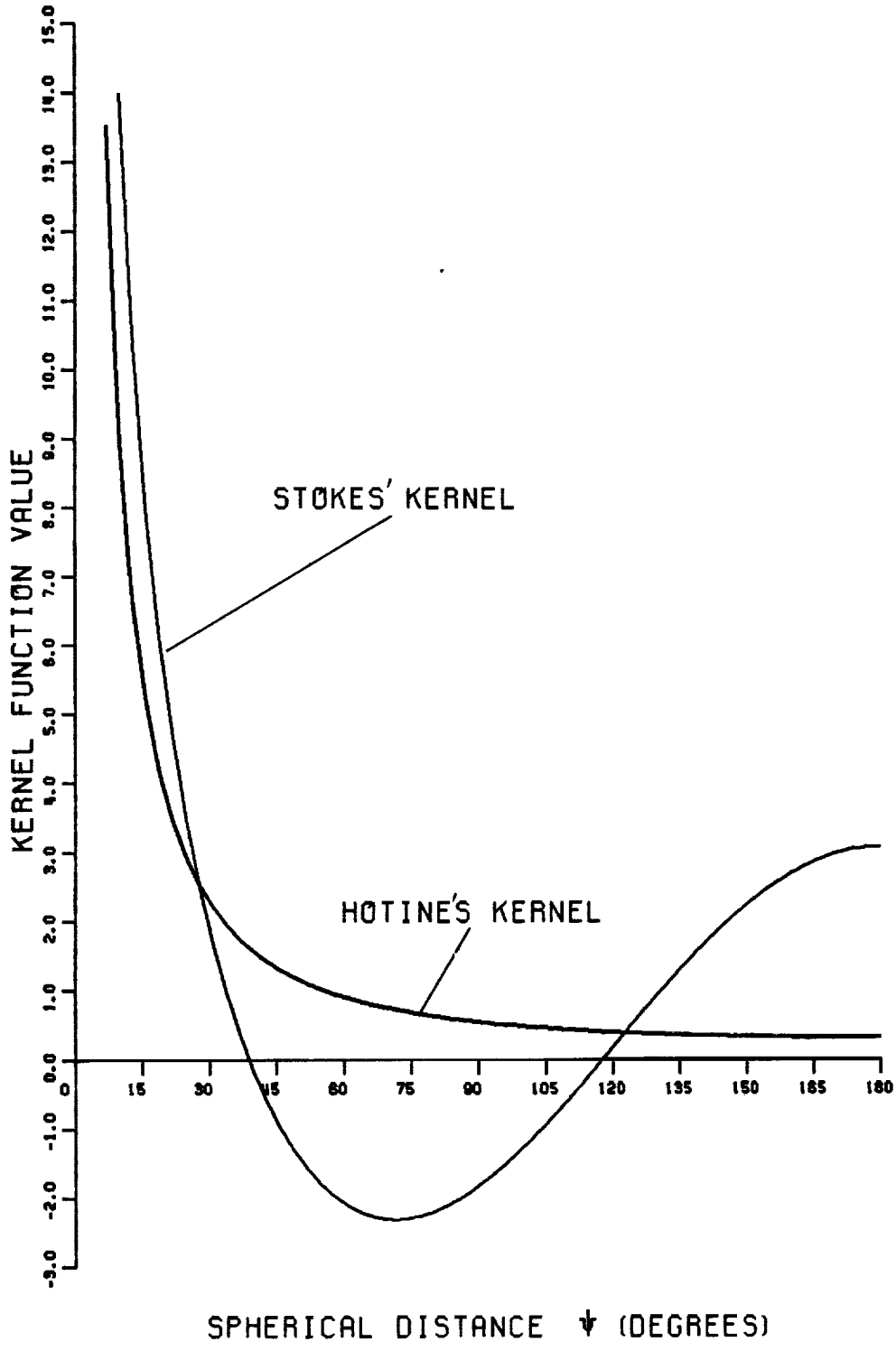

Figure 4. The Kernels of Hotine and Stokes.

Finally, from the previous derivations, it is obvious that the use of gravity disturbances circumvents the problems related to the inadmissible harmonics of degrees n = (0, 1), which have to be suppressed from the disturbing potential for the derivation of Stokes' integral (Hotine, 1969, pp. 317-318). While global gravity anomaly data, input to Stokes' integral should not contain harmonics of n = (0, 1), no such restrictions apply to the disturbances to be input to Hotine's integral formula. It should be noted here, that the absence of first-degree harmonic from T, which implies coincidence of the center of mass of the Earth with that of the reference ellipsoid, was implicitly assumed when the centrifugal terms of the true geopotential and the normal one were equated (see equations (2.8) and (2.10)). The effect however, on the centrifugal potential, of non-geocentricity of the coordinate system used, is only about 1×10^{-3} kgal m (for present accuracies on the determination of the geocenter), hence the geocentricity condition there, only mildly needs to be employed.

2.3 Consideration of Systematic Effects

The integral formula (2.64) was developed based on the assumptions:

(a) The disturbing potential T is harmonic outside the sphere (O, R) (see equation (2.52)).
(b) The boundary values δg represent radial derivatives of T (with opposite sign; see equation (2.35)).
(c) Boundary values are given on the surface of the sphere (O, R).

In the real world, the presence of the atmosphere violates assumption (a), while the available boundary data do not comply with either (b) or (c), as was discussed in section 2.1. The simplicity of the previous formulation though, and the magnitude and spectral content of the discrepancies between the real world case and the one assumed in section 2.2, suggest that it is preferable to retain the formulation developed, and modify the observable, in order to ensure the best possible compatibility with the analytical models, at the cost of degrading somewhat the integrity of the original measurements.

The primary information available from surface gravimetry combined with GPS positioning, is the magnitude of the gravity acceleration at the surface point P, and the

geocentric Cartesian coordinates of P. Normal gravity at the same point may be calculated by transforming the Cartesian coordinates to ellipsoidal ones (Heiskanen and Moritz, 1967, section 1-19), and then making use of closed formulas for the magnitude of normal gravity, as described in (ibid, section 6-2). Alternatively, Cartesian coordinates may be transformed to geodetic ones, and normal gravity may be calculated from a truncated series (ibid, section 2-10). Pavlis (1988, section 3.1.1) has shown that such series should include terms at least up to $O(h^2/a^2)$, to avoid introduction of undesirable systematic errors. That is:

$$|\vec{\gamma}_P| \approx \gamma_{Q_o}\left[1 - 2\left(1 + f + m - 2f\sin^2\varphi_{Q_o}\right)\frac{h_P}{a} + 3\left(\frac{h_P}{a}\right)^2\right] \quad , \tag{2.76}$$

where φ_{Q_o} is the geodetic latitude and h_P the ellipsoidal height of point P (see also Figure 2), and the rest of the notation is defined in (ibid, section 2.3.1).
According to the above the gravity disturbance δg_P, defined in equation (2.33), is evaluated. The systematic corrections to this quantity are described next.

1. Atmospheric Correction : δg_A

Provided the mass of the reference ellipsoid used to define the normal potential includes the total mass of the atmosphere (as in the cases of GRS '67 or GRS '80), Moritz (1980, p. 424) has shown that the atmospheric correction on measured gravity is given by:

$$\delta g_A = G\frac{M(r_P)}{r_P^2} \tag{2.77}$$

where $M(r_P)$ is the mass of the atmosphere above a sphere passing through the observation point P (see also (Pavlis, 1988, Figure 6)). To remove the atmospheric effect from δg_P, δg_A needs to be added to the gravity disturbance as given by (2.33). Obviously, since δg_A has to do with measured gravity, which enters in the same way in the definition of both disturbances and anomalies, the correction is identical for both quantities (Moritz, 1974).
For computer implementation it is convenient to evaluate dg_A from:

$$\delta g_A = 0.8658 - 9.727 \times 10^{-5} H_P + 3.482 \times 10^{-9} H_P^2 \quad \text{(mgal)} \tag{2.78}$$

where H_P is the orthometric height (or equally well the ellipsoidal one) of the gravity station in meters. This polynomial was developed by Wichiencharoen (1982), by fitting a quadratic function to the tabulated values of (IAG, 1971, p. 72). The indirect effect (shifting of equipotential surfaces due to the condensation of the atmospheric mass on the reference ellipsoid), is only about - 0.7 cm at sea level, where the correction becomes maximum (Moritz, 1980, p. 425), and thus it can be safely neglected.

2. Ellipsoidal Corrections : ε_h, ε_p

From equation (2.29) it can be seen that:

$$\varepsilon_P = \left(\frac{\partial W}{\partial h}\right)_P - \left(\frac{\partial W}{\partial H}\right)_P \tag{2.79}$$

i.e., ε_P arises due to the difference in the directional derivatives of W along the straight ellipsoidal normal (which almost coincides with the normal plumb line) and the actual plumb line. On the other hand, from (2.26) it is seen that ε_h represents the difference (up to $O(e^2)$) between the directional derivatives of T along the radial line and the straight ellipsoidal normal. Pavlis (1988, sections 2.3.3, 2.3.6) has shown that the corrections ε_h and ε_P are almost identical both in terms of magnitude and frequency content. The corrections are of the order of 10 μgals and produce long-wavelength signatures on the disturbing potential that may reach 20 kgalcm (ibid, Figure 42). The combined correction ($\varepsilon_h + \varepsilon_P$) can be computed efficiently in terms of either point values or area-mean values, from an existing geopotential coefficient set such as the OSU89B (Rapp and Pavlis, 1990), using the formulation developed by Pavlis (1988, sections 2.3.3, 2.3.4, 2.3.6).

With the above correction terms defined, making use of equations (2.30) and (2.52), one can write:

$$L_a(r_P, \theta, \lambda) = \frac{GM}{r_P^2} \sum_{n=o}^{\infty} (n+1)\left(\frac{R}{r_P}\right)^n \sum_{m=-n}^{n} \overline{C}_{nm} \overline{Y}_{nm}(\theta, \lambda) \tag{2.80}$$

where the reduced observable $L_a(r_P, \theta, \lambda)$ is given by:

$$L_a(r_P, \theta, \lambda) = |\vec{g}_P| - |\vec{\gamma}_P| + (\delta g_A - \varepsilon_h - \varepsilon_P) \quad . \tag{2.81}$$

Equation (2.80) represents a mathematical model, linear with respect to the coefficients $\overline{C}_{nm}$. A corresponding form of (2.80), written in terms of area-mean values of $L_a(r_P, \theta, \lambda)$, may be used to set up a linear system of observation equations, in order to estimate a truncated set of coefficients $\overline{C}_{nm}$, from a (preferably global) set of "observed" values of $L_a(r_P, \theta, \lambda)$. This may be done in essentially the same manner as it was done, using gravity anomalies, in (Pavlis, 1988).

However, for the current purpose, the reduced observable of (2.81) is clearly inadequate, since it refers to the surface point P, while the intention is to make use of (2.64), which requires values referring to the sphere (O, R). The continuation of the values referring to the physical surface of the Earth, to a surface that is analytically manageable, poses the most difficult problem of all other reductions, both from a theoretical as well as a numerical standpoint. The treatment described next consists of two steps; first the surface values are analytically continued to the surface of an ellipsoid and second, equation (2.67) is modified to account for the differences between the ellipsoidal and the spherical surfaces. The problem of analytical continuation is also encountered in the implementation of Stokes' integral, and due to its importance has received extensive studying by a number of investigators (e.g. Moritz (1966; 1974; 1980); Wang (1988)). Their established notation is adopted in the following discussion.

3. Analytical Continuation : g_1

For notational convenience the quantity $L_a(r_P, \theta, \lambda)$ of (2.81) will be simply denoted δg here (not to be confused with δg as used in other sections). The purpose of analytical continuation, is to determine a corresponding quantity δg^* on the ellipsoid, such that, δg is related to δg^* through Poisson's upward continuation integral (Heiskanen and Moritz, 1967, p. 35). The quantity δg^* possesses no physical meaning, as the surface value δg does, its only purpose being to enable use of convenient analytical formulas. Relating the two quantities through the upward continuation integral, ensures that the set of δg^* values on the ellipsoid, reproduces the set of δg values on the surface, and consequently the external potential determined from δg^* is identical to the one that would have been determined from δg. Strictly speaking, the use of Poisson's integral is valid only if the reference surface of δg^* is always below the physical surface of the Earth, a condition which is not satisfied (in general) by the surface of the mean-Earth ellipsoid. This problem led Bjerhammar (1962) to introduce the concept of a spherical

reference surface for δg^*, completely embedded in the Earth. The validity of Poisson's integral is also ensured if one introduces an embedded ellipsoid, confocal with the mean-Earth one, as a reference surface for δg^*. This way analytical continuation has to be performed over shorter distances, which is advantageous from the accuracy and convergence standpoints, while the embedded ellipsoid concept does not add significant complexity to the formulation; all that it requires is to reckon ellipsoidal heights from the embedded, instead of the mean-Earth ellipsoid in the following formulas.

Let now R_b denote the radius of an embedded sphere. Application of Poisson's integral to the harmonic function $r\delta g$ yields:

$$(r\delta g)_P = \frac{R_b(r_P^2 - R_b^2)}{4\pi} \iint_\sigma \frac{R_b \delta g^*}{\ell^3} d\sigma \tag{2.82}$$

where the notation could be read from Figure 3 (substituting R_b for R used there). Since δg^* is the unknown quantity, the integral equation (2.82) needs to be inverted. However, there exists no integral formula that inverts (2.82) (Heiskanen and Moritz, 1967, section 8-10), hence the solution of (2.82) can only be obtained numerically, with successive approximations. To this end, it can be shown easily (ibid, p. 318) that (2.82) may be written in the form:

$$\delta g_P - t^2 \delta g_P^* = \frac{t^2(1 - t^2)}{4\pi} \iint_\sigma \frac{\delta g^* - \delta g_P^*}{D^3} d\sigma \tag{2.83}$$

where :

$$\left.\begin{aligned} t &= \frac{R_b}{r_P} \\ D &= \frac{\ell}{r_P} \end{aligned}\right\} \tag{2.84}$$

The location of the '*' quantities on the embedded sphere is determined by projecting the surface points to this sphere along the radial line, i.e. the surface point and its projection have the same geocentric latitude. Approximating

$$r_P \approx R_b + h_P \quad , \tag{2.85}$$

expanding t^2 and D^3 in powers of h_P/R_b, and retaining only terms linear in h_P/R_b, one can easily show that (2.83) takes the form:

$$\delta g_P^* \approx \delta g_P - h_P \left[-\frac{2}{R_b} \delta g_P^* + \frac{R_b^2}{2\pi} \iint_\sigma \frac{\delta g^* - \delta g_P^*}{\ell_o^3} d\sigma \right] \tag{2.86}$$

where :

$$\ell_o = 2R_b \sin \frac{\psi}{2} \quad . \tag{2.87}$$

Equation (2.86) lends itself to an iterative scheme for the computation of δg_P^* which is initialized by setting $\delta g_P^{*(o)}$ equal to δg_P, as described for the case of gravity anomalies by Heiskanen and Moritz (1967, p. 318). Moritz (1966, p. 60) has shown that under the assumptions made above to derive (2.86), and to the first order of h_P/R_b, this equation coincides with the 'gradient solution' to the analytical downward continuation problem, i.e. the terms inside the brackets in (2.86) represent $\left(\partial \delta g^* / \partial r\right)$. The numerical implementation of (2.86) on the other hand is all but trivial, since the vertical gradient required has a very localized behavior and thus its accurate estimation requires very dense observation coverage around the computation point P. Usually, such coverage is not available. Employing assumptions regarding the correlation of the observable with elevation, and making use of available detailed elevation information, an approximate solution to (2.86) may then be evaluated, as was done by Wang (1988) for the case of gravity anomalies. The problem of analytical downward continuation is a topic on its own and further discussion will not be given here. Equation (2.86) will be written schematically:

$$\delta g_P^* = \delta g_P + g_1 \tag{2.88}$$

where :

$$g_1 = - h_P \left[-\frac{2}{R_b} \delta g_P^* + \frac{R_b^2}{2\pi} \iint_\sigma \frac{\delta g^* - \delta g_P^*}{\ell_o^3} d\sigma \right] \quad . \tag{2.89}$$

As far as the use of an embedded ellipsoid is concerned, R_b in (2.89) may be substituted by the Gaussian mean radius (Rapp, 1984, p. 43) at the computation point P, for that ellipsoid, since global integration in (2.89) is usually truncated only over a small cap centered at P.

4. Ellipsoidal to Spherical Integration : ε_t

The values δg^* obtained from the previous step refer to the surface of the embedded ellipsoid and thus are still inadequate to be used as input to Hotine's integral (2.67), which requires values on a spherical boundary surface. This problem, for the corresponding case of Stokes' integral, is usually treated with ellipsoidal correction terms as those derived by Moritz (1980, p. 314). However, as Hotine (1969) has pointed out, the problem may be treated in a conceptually simpler manner; his formulation is presented next.

First, it is observed that the result of downward continuation, δg^*, represents radial derivative of the analytical continuation of the disturbing potential (see also equation (2.81)). Ellipsoidal normal derivatives will be needed next, which formally may be obtained by adding back $(\varepsilon_h)_P$ to δg^*_P, or, without any loss of accuracy by omitting altogether $(\varepsilon_h)_P$ from (2.81). Hence, δg^*_P from (2.88) is hereon understood to represent:

$$\delta g^*_P = -\left(\frac{\partial T}{\partial h}\right)^*_P \quad . \tag{2.90}$$

With respect to the ellipsoidal coordinate system $(\alpha = \cot^{-1}u/E,\ \delta,\ \lambda)$ (see also (Heiskanen and Moritz, 1967, sections 1-19, 1-20)), the ellipsoidal harmonic expansion of the disturbing potential will be written as:

$$T(\alpha, \delta, \lambda) = \frac{GM}{R_b} \sum_{n=o}^{\infty} \sum_{m=-n}^{n} \frac{Q_{n|m}(i\cot\alpha)}{Q_{n|m}(i\cot\alpha_b)} \bar{C}^e_{nm} \bar{Y}_{nm}(\delta, \lambda) \tag{2.91}$$

where:

$$\left.\begin{aligned} i &= \sqrt{-1} \\ \cot\alpha_b &= \frac{1}{e'_b} \end{aligned}\right\} \tag{2.92}$$

and e'_b is the second eccentricity of the embedded ellipsoid, while $Q_{nm}(z)$ are associated Legendre functions of the second kind with argument z (ibid, p. 43). $\overline{Y}_{nm}(\delta, \lambda)$ are as in (2.53), but now evaluated in terms of reduced co-latitude δ. Finally $\overline{C}^e_{nm}$ are <u>real</u>, ellipsoidal harmonic coefficients of the disturbing potential, referring to scaling parameters GM and R_b. Making use of the relation (Hotine, 1969, p. 190):

$$\frac{\partial}{\partial h} = -\frac{\tan\alpha}{N}\frac{\partial}{\partial \alpha} \tag{2.93}$$

where N is the radius of curvature of the prime vertical (Rapp, 1984, p. 32), and the recurrence relation for the derivative of $Q_{nm}(z)$, one can derive easily:

$$-N\frac{\partial T}{\partial h} = \sum_{n=0}^{\infty}\sum_{m=-n}^{n}\frac{T_{nm}(\delta,\lambda)}{Q_{n|m|}(i\cot\alpha_b)}\left[(n+1)Q_{n|m|}(i\cot\alpha) + i\tan\alpha(n-m+1)Q_{n+1,|m|}(i\cot\alpha)\right] \tag{2.94}$$

where the surface ellipsoidal harmonic $T_{nm}(\delta, \lambda)$ is:

$$T_{nm}(\delta,\lambda) = \frac{GM}{R_b}\overline{C}^e_{nm}\overline{Y}_{nm}(\delta,\lambda) \quad . \tag{2.95}$$

Equation (2.94) holds true for any arbitrary point on, or outside the embedded ellipsoid. On the surface of this ellipsoid, one has $N = N_b$ and $\alpha = \alpha_b$, hence due also to (2.90), (2.94) becomes:

$$N_b\delta g^* = \sum_{n=0}^{\infty}\sum_{m=-n}^{n}(n+1)T_{nm}(\delta,\lambda) + \sum_{n=0}^{\infty}\sum_{m=-n}^{n}\left[\frac{i\tan\alpha_b(n-m+1)Q_{n+1,|m|}(i\cot\alpha_b)}{Q_{n|m|}(i\cot\alpha_b)}\right]T_{nm}(\delta,\lambda) \tag{2.96}$$

Using the series expression for $Q_{nm}(z)$, it can be shown that the bracketed term in the second summation of (2.96) is equal to:

$$\frac{e'^2_b(n-m+1)(n+m+1)}{2n+3}\left[1 + O(e'^2_b)\right] \quad . \tag{2.97}$$

The last relation is a corrected version of the misprinted relation (29.66) of Hotine (1969, p. 321). Hence, omitting terms of the fourth and higher order of the second eccentricity, equation (2.96) may be written as:

$$[N_b\delta g^*](\delta', \lambda') = \sum_{n=0}^{\infty}\sum_{m=-n}^{n}(n+1)T_{nm}(\delta', \lambda') + e_b'^2\sum_{n=0}^{\infty}\sum_{m=-n}^{n}\frac{(n-m+1)(n+m+1)}{2n+3}T_{nm}(\delta', \lambda') \quad . \tag{2.98}$$

Multiplying both sides of the last equation by $H(\psi)$ as given in (2.65) but with ψ now evaluated by:

$$\cos\psi = \cos\delta\cos\delta' + \sin\delta\sin\delta'\cos(\lambda - \lambda') \quad , \tag{2.99}$$

and integrating over the unit sphere (full solid angle), due to (2.66) one obtains:

$$T(\delta, \lambda) = \frac{1}{4\pi}\iint_{\sigma} H(\psi)[N_b\delta g^*](\delta', \lambda')d\sigma - \frac{e_b'^2}{4\pi}\iint_{\sigma}\sum_{n=0}^{\infty}\sum_{m=-n}^{n}\frac{(n-m+1)(n+m+1)}{2n+3}H(\psi)\,T_{nm}(\delta', \lambda')d\sigma \quad . \tag{2.100}$$

Denoting:

$$\varepsilon_I(\delta', \lambda') = e_b'^2\sum_{n=0}^{\infty}\sum_{m=-n}^{n}\frac{(n-m+1)(n+m+1)}{2n+3}\,T_{nm}(\delta', \lambda') \tag{2.101}$$

and collecting all the previous correction terms together, one finally obtains:

$$T(\delta, \lambda) = \frac{1}{4\pi}\iint_{\sigma} H(\psi)\left[N_b(\delta g + \delta g_A - \varepsilon_P + g_1) - \varepsilon_I\right](\delta', \lambda')\,d\sigma \quad . \tag{2.102}$$

Equation (2.102) is the desired integral formula which relates the gravity disturbance δg (as defined in equation (2.33)), to the analytical continuation of the disturbing potential on the surface of the embedded ellipsoid, accounting for the ellipticity of the boundary surface to the second order of the second eccentricity. It can be seen now that the use of spherical formulas (such as (2.67)), but evaluated in terms of reduced instead of geocentric colatitudes, introduces two errors; one due to the difference between N_b and R, and another due to the omission of ε_1. Both errors are of the second order of the (second) eccentricity (Hotine, 1969, p. 321). Also, from (2.101) and (2.95) it is obvious that the computation of ε_1 requires some a-priori knowledge of the ellipsoidal spectrum of the geopotential. To avoid the use of the ellipsoidal harmonics, and subsequently the need for transformation of geodetic latitudes (according to which measurements are usually registered), to reduced ones, Moritz (1980) used series expansions and formulated the ellipsoidal corrections, for various gravimetric quantities, in terms of geodetic latitudes and spherical harmonics (ibid, pp. 314-328). Such procedure, as Moritz himself admitted, results in more complicated expressions, than those for ellipsoidal harmonics (ibid, p. 316). At present, neither one of Moritz's motives appears to be a prohibitive factor for the formulation adopted here. The derivations of Jekeli (1988) and the computer algorithms of Gleason (1988), provide very efficient means of converting ellipsoidal to spherical spectra and vice-versa. Furthermore, in view of the computational facilities available nowadays, conversion of geodetic to reduced latitudes, even for large amounts of observation locations, can hardly be considered a prohibitive computational task.

In practical applications the integration in (2.102) is usually extended only over a small cap, centered at the computation point, while one accounts for the effect of the remote zone through the use of a global geopotential model. Such procedure requires modifications in equation (2.102), which affect the evaluation of ε_1 as well, as it will be discussed in section 3.1. However, it is instructive here to evaluate the effect of ε_1 on T, for the case of global integration.

Denote:

$$\varepsilon_1^{\pi}(\delta, \lambda) = \frac{1}{4\pi} \iint_{\sigma} H(\psi)\, \varepsilon_1(\delta', \lambda')\, d\sigma \quad . \tag{2.103}$$

Substituting in equation (2.103) $\varepsilon_I(\delta', \lambda')$ from (2.101) and $H(\psi)$ from (2.66), and making use of the decomposition formula of the Legendre polynomials (Heiskanen and Moritz, section 1-15), one obtains:

$$\varepsilon_I^{\pi}(\delta,\lambda) = e_b'^2 \sum_{n=0}^{\infty} \sum_{m=-n}^{n} \frac{(n-m+1)\,(n+m+1)}{(2n+3)\,(n+1)} T_{nm}(\delta,\lambda) \quad . \tag{2.104}$$

Given now a set of spherical harmonic coefficients of the disturbing potential, $\overline{C}_{nm}$, referring to scaling parameter $R = R^M$, one sets:

$$\overline{f}^{s}_{nm} = \frac{GM}{R_b}\left(\frac{R^M}{R_b}\right)^n \overline{C}_{nm} \quad . \tag{2.105}$$

Using the transformation formula (1.15) of Gleason (1988, p.116), one can evaluate from $\overline{f}^{s}_{nm}$, the ellipsoidal spectrum $\overline{\overline{f}}^{e}_{nm}$, while the unitless ellipsoidal coeffecients $\overline{C}^{e}_{nm}$ are finally given by:

$$\overline{C}^{e}_{nm} = \frac{R_b}{GM}\overline{\overline{f}}^{e}_{nm} \quad . \tag{2.106}$$

The term $\varepsilon_I^{\pi}(\delta,\lambda)$ may now be evaluated from equations (2.95) and (2.104), using efficient harmonic synthesis techniques such as those developed by Colombo (1981a).

Such evaluation was performed here using the OSU89B shperical harmonic coefficient set (Rapp and Pavlis, 1990), complete to degree and order 180; $\varepsilon_I^{\pi}(\delta,\lambda)$ was evaluated in terms of 1° x 1° area-mean values, while for simplicity R_b was set equal to R^M = 6378137 m, the scaling parameter to which the OSU89B model coefficients refer (ibid, p. 21,896). The ellipsoidal gravity field to which $\overline{C}_{nm}$ refer was defined through the four constants given in (ibid, p. 21,896). The values of $\varepsilon_I^{\pi}(\delta,\lambda)$ computed, range between -19 kgal cm and +17 kgal cm, with a root mean square (rms) value of 6.4 kgal cm. Their geographical variation is illustrated in Figure 5.

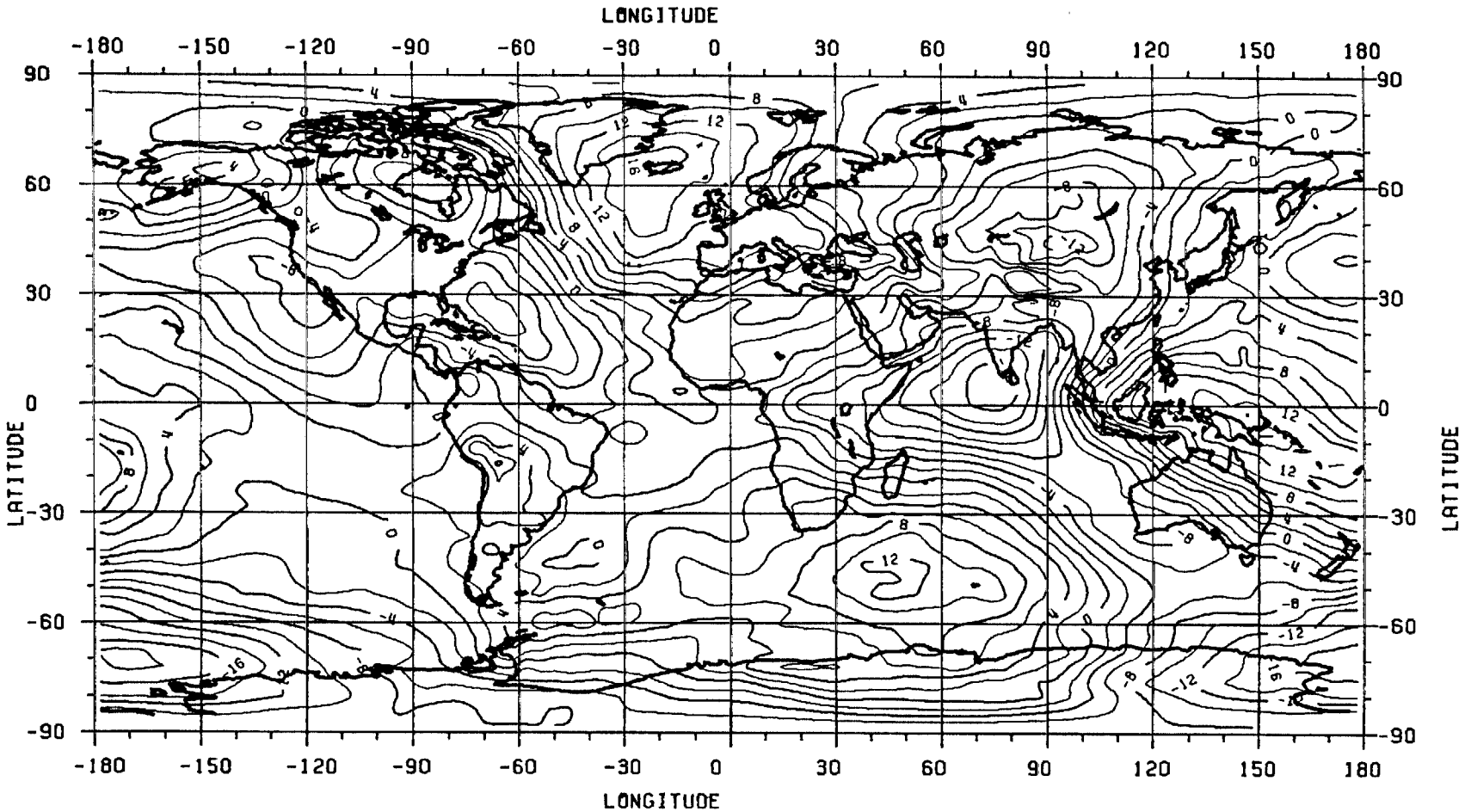

Figure 5. Disturbing Potential Correction ε_1^{π}. Area-Mean Values (1° x 1°) Computed Using OSU89B to Nmax = 180. Contour Interval is 2 kgal cm.

In a similar fashion one can derive the corresponding correction term for the case of integration of gravity anomalies (Stokes' integral); such derivation yields (see also (Hotine, 1969, p. 322)):

$$(\varepsilon_1^{\pi})_{\Delta g}(\delta, \lambda) = e_b'^2 \sum_{n=0}^{\infty}{}' \sum_{m=-n}^{n} \frac{(n-m+1)\,(n+m+1)}{(2n+3)\,(n-1)} T_{nm}(\delta,\lambda)$$

$$- \sum_{n=0}^{\infty}{}' \sum_{m=-n}^{n} \frac{1}{n-1}\left(e^2\sin^2\delta + \frac{2\omega^2 N}{\gamma}\right) T_{nm}(\delta,\lambda) \qquad (2.107)$$

where the prime indicates absence of the first-degree term from the infinite sum. Numerical values computed for the correction term of equation (2.107) (in the same manner as for the term of equation (2.104)) range between - 36 kgal cm and + 43 kgal cm, with an rms value of 14.9 kgal cm. Their geographical variation is illustrated in Figure 6. These values are in good agreement with the corresponding ones computed by Rapp (1981b), using the procedures of Moritz (1980). Both correction terms (2.104) and (2.107) are of long-wavelength nature, with more than 99% of their power concentrated below harmonic degree 36, so that one can account for their effect accurately, using an existing global geopotential model.

Finally, to evaluate the disturbing potential at the surface point P, one needs to upward continue the value computed from (2.102) (which refers to the footpoint P* on the embedded ellipsoid), to the topographic surface level. A Taylor series expansion in terms of the elevation yields:

$$T(P) = T(P^*) + \left(\frac{\partial T}{\partial h}\right)_P^* h_P + \frac{1}{2!}\left(\frac{\partial^2 T}{\partial h^2}\right)_P^* h_P^2 + \ldots \qquad (2.108)$$

hence, due to (2.90) and (2.89) one finally has:

$$T(P) \approx T(P^*) - \left(\delta g_P^* - \frac{1}{2} g_1\right) h_P \quad . \qquad (2.109)$$

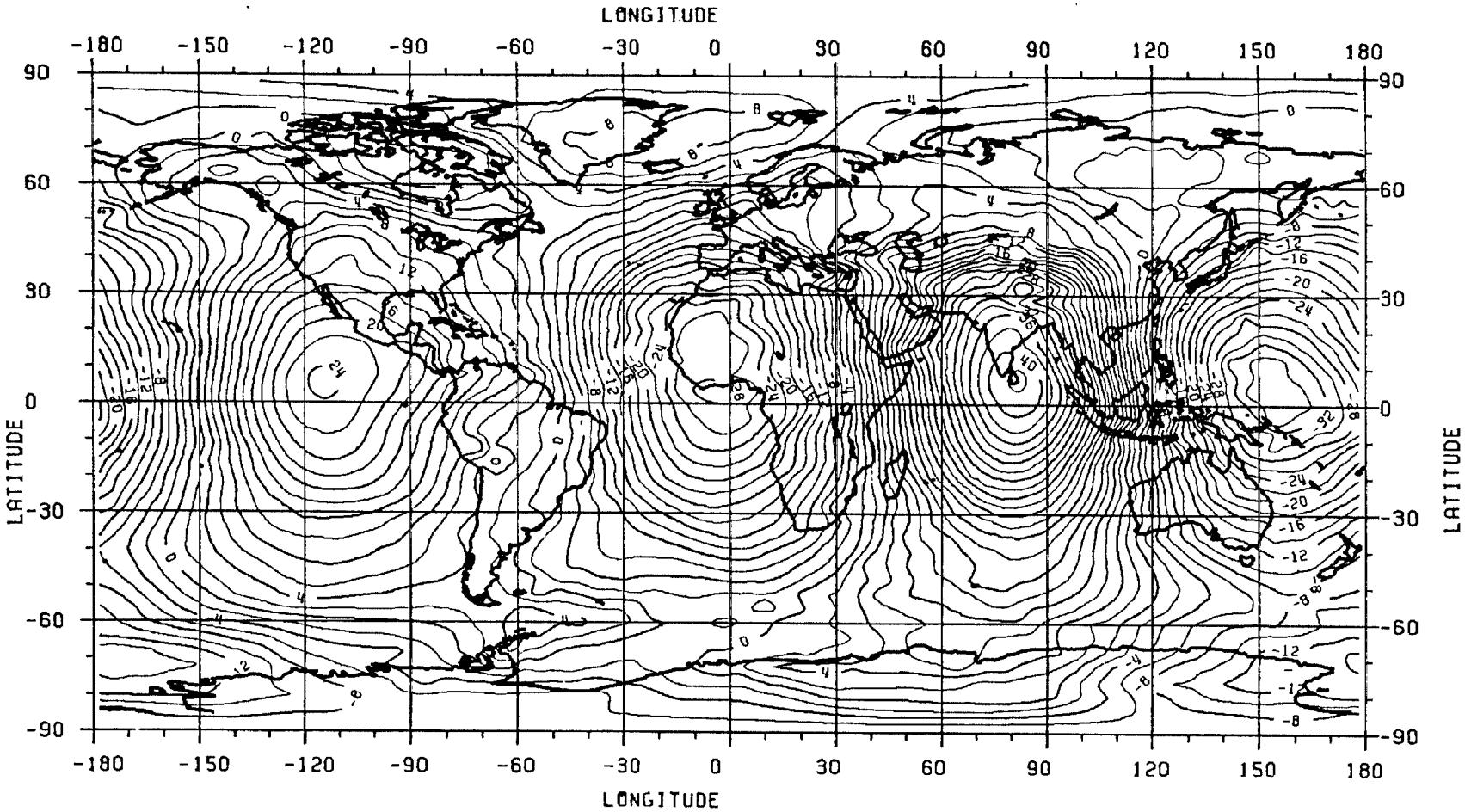

Figure 6. Disturbing Potential Correction $(\varepsilon_I^{\pi})_{\Delta g}$. Area-Mean Values (1° x 1°) Computed Using OSU89B to Nmax = 180. Contour Interval is 2 kgal cm

2.4 Gravitational Acceleration Information from a Satellite-to-Satellite Tracking Configuration

The other source of gravitational information considered here for the estimation of the geopotential differences, comes from the Multiple-High-Single-Low Satellite-to-Satellite Tracking (SST) configuration which is established when a low orbiter carrying a GPS receiver is simultaneously tracking more than one satellite of the high-altitude GPS constellation.

The idea of using SST data for geopotential modeling was originally proposed by Wolff (1969). The fact that an SST low-low mission alone, with the satellites in polar orbit, would be capable of providing a truly global, uniformly accurate and high resolution geopotential model, caused widespread attention to be given to the proposal. A number of investigations have been performed, aiming to assess the capabilities of various SST system scenarios. Some of these studies aimed to assess the quality of mean gravity anomalies and/or geoidal undulations that can be predicted on the surface of the Earth from the SST data at altitude (local solutions) (e.g. Hajela (1974; 1978; 1981), Rummel et al. (1976), Rummel (1980), Rapp and Hajela (1979) and Douglas et al. (1980)). Other studies (e.g. Colombo (1981b), Kaula (1983)) focused on the development of efficient analytical techniques, that can be used to process the large global set of observations which an SST mission will acquire during its lifetime, for the determination of harmonic coefficients of the geopotential. However, apart from early experiments of SST between ATS-6/Apollo-Soyuz and ATS-6/GEOS-3 (Kahn et al., 1982), no dedicated SST system has yet been put into orbit. This is partly due to the costly requirement for drag-free satellites at the low altitudes (e.g. 160 km), considered for SST missions of the type of the Geopotential Research Mission (GRM) (Keating et al., 1986).

In the absence of a dedicated SST mission, the possibility of using the GPS constellation as the high-altitude component, which continuously tracks a low-altitude satellite equipped with a GPS receiver, offers a viable alternative. Investigations in this direction have been already initiated through the U.S. Air Force "Shuttle-GPS Tracking for Anomalous Gravitation Estimation" (STAGE) mission (Jekeli and Upadhyay, 1990), where the Shuttle spacecraft is used as the low-orbiter, and an Inertial Measurement Unit

(IMU) is used in addition to the GPS receiver on the Shuttle, to measure and isolate non-gravitational accelerations.

The basic mathematical modeling of the observations acquired by an SST configuration remains unaltered regardless of the mission in question; in contrast, the signals represented in the observable, strongly depend on the specifications of each mission (e.g. drag-free orbit, altitude etc.). The modeling of the observable is reviewed next, while the contribution of various signals contained in it is discussed afterwards.

Consider the motion of two satellites, S_i (high) and S_o (low), as shown in Figure 7. Three mutually perpendicular unit vectors $\underline{E}_j$ (j = 1, 2, 3) span an inertial frame of reference (in this section, vectors will be denoted with underbars, for notational convenience).

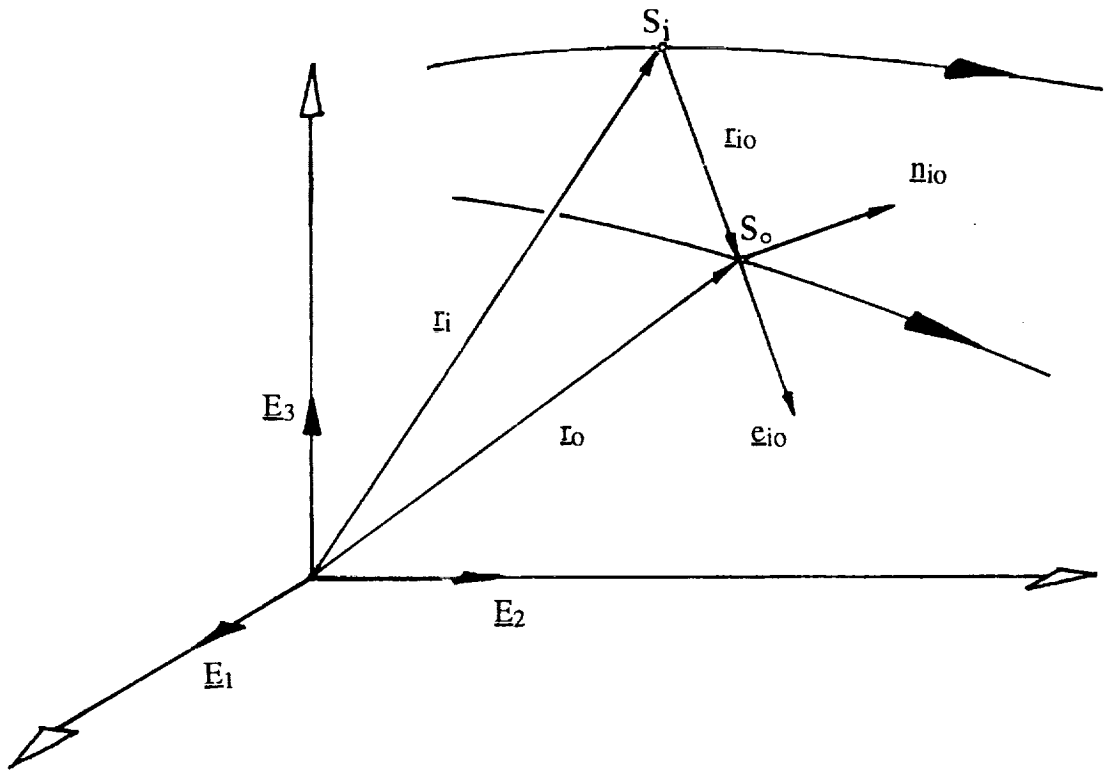

Figure 7. High-Low Satellite-to-Satellite Tracking Configuration.

The following relations are introduced:

$$|\mathbf{r}_{io}| = (\mathbf{r}_{io}^T \mathbf{r}_{io})^{1/2} = \rho_{io} \tag{2.110}$$

$$\boldsymbol{\varrho}_{io} = \frac{1}{\rho_{io}} \mathbf{r}_{io} \tag{2.111}$$

$$\boldsymbol{\varrho}_{io}^T \mathbf{n}_{io} = 0 \quad . \tag{2.112}$$

Denoting with d/dt time differentiation in the inertial frame, one has:

$$\dot{\mathbf{r}}_{io} = \frac{d}{dt}(\mathbf{r}_{io}) \quad , \tag{2.113}$$

for the inertial relative velocity between S_o and S_i, and :

$$v_{io} = \dot{\rho}_{io} = \dot{\mathbf{r}}_{io}^T \boldsymbol{\varrho}_{io} \quad , \tag{2.114}$$

for the projection of the inertial relative velocity along the direction of the "line-of-sight" (LOS) between the two spacecrafts. Designated "LOS velocity", v_{io} is a quantity that can be observed from the Doppler effect on the signal received by the low orbiter. Differentiation of (2.114), with respect to time yields:

$$\dot{v}_{io} = \ddot{\mathbf{r}}_{io}^T \boldsymbol{\varrho}_{io} + \dot{\mathbf{r}}_{io}^T \dot{\boldsymbol{\varrho}}_{io} \quad . \tag{2.115}$$

The quantity:

$$a_{io} = \ddot{\mathbf{r}}_{io}^T \boldsymbol{\varrho}_{io} \tag{2.116}$$

is the projection of the inertial relative acceleration along the LOS direction. On the other hand, $\dot{v}_{io}$ is the rate of change of the LOS velocity. The second term on the right-hand side of equation (2.115) (centrifugal acceleration) arises due to the fact that $\boldsymbol{\varrho}_{io}$ represents a direction which is rotating with respect to inertial space.

Assume now that a set of initial state-vectors for both satellites and force model parameters for the forces acting on them are approximately known. Based on such information one can compute an approximate value for $\dot{v}_{io}$ as:

$$\dot{v}^c_{io} = (\ddot{r}^c_{io})^T e^c_{io} + (\dot{r}^c_{io})^T \dot{e}^c_{io} \quad . \tag{2.117}$$

However, since neither the initial state-vectors, nor the force model parameters are known perfectly, one has:

$$\delta\dot{v}_{io} = \dot{v}_{io} - \dot{v}^c_{io} \quad , \text{ or} \tag{2.118}$$

$$\delta\dot{v}_{io} = \delta(\ddot{r}^T_{io} e_{io}) + \delta(\dot{r}^T_{io} \dot{e}_{io}) \tag{2.119}$$

where:

$$\left.\begin{aligned} \delta(\ddot{r}^T_{io} e_{io}) &= \ddot{r}^T_{io} e_{io} - (\ddot{r}^c_{io})^T e^c_{io} \\ \delta(\dot{r}^T_{io} \dot{e}_{io}) &= \dot{r}^T_{io} \dot{e}_{io} - (\dot{r}^c_{io})^T \dot{e}^c_{io} \end{aligned}\right\} \tag{2.120}$$

One may now split the total inertial relative acceleration $\ddot{r}_{io}$ into two parts:

$$\ddot{r}_{io} = \ddot{r}^G_{io} + \ddot{r}^{NG}_{io} \quad , \tag{2.121}$$

where $\ddot{r}^G_{io}$ is induced by gravitation, and $\ddot{r}^{NG}_{io}$ is due to all other forces <u>but</u> gravitation, acting on the spacecrafts S_i and S_o. Accordingly, equation (2.119) takes the form:

$$\delta\dot{v}_{io} = \delta[(\ddot{r}^G_{io})^T e_{io}] + \delta[(\ddot{r}^{NG}_{io})^T e_{io}] + \delta[\dot{r}^T_{io} \dot{e}_{io}] \quad . \tag{2.122}$$

The first term on the right-hand side of (2.122) will be the focus of the following discussion. As mentioned before, this term arises due to the errors of the approximately known gravitational model and satellite positions. Assuming that these errors are small enough to justify linearization, one has:

$$\delta(\ddot{r}^T_{io} e_{io}) \approx (\delta\ddot{r}_{io})^T e^c_{io} + \left.\frac{\partial(\ddot{r}^T_{io} e_{io})}{\partial r_o}\right|_c \delta r_o + \left.\frac{\partial(\ddot{r}^T_{io} e_{io})}{\partial r_i}\right|_c \delta r_i \tag{2.123}$$

where the superscript "G" has been omitted for notational simplicity, and in the following it will be understood that $\ddot{\underline{r}}_{io}$ refers to the component of the relative inertial acceleration induced by gravitation alone. In addition "c" indicates that the partial derivatives are evaluated at the approximately known positions.

On the other hand, by differentiating numerically the observed Doppler shifts, one obtains an "observed" value for $\dot{v}_{io}$, $\dot{v}_{io}^{obs}$, where:

$$\dot{v}_{io}^{obs} = \dot{v}_{io} + n_{io} \tag{2.124}$$

and n_{io} represents observational noise in the primary observable, unmodeled (residual) atmospheric effects, antenna multipath, as well as errors introduced by the numerical differentiation. Introducing the notation:

$$\left.\begin{aligned} \Delta\dot{v}_{io} &= \dot{v}_{io}^{obs} - \dot{v}_{io}^{c} && \text{(a)} \\ \delta a_{io}^{NG} &= (\ddot{\underline{r}}_{io}^{NG})^T \underline{e}_{io} - [(\ddot{\underline{r}}_{io}^{NG})^c]^T \underline{e}_{io}^{c} && \text{(b)} \\ \delta R_{io} &= \delta(\dot{\underline{r}}_{io}^T \dot{\underline{e}}_{io}) && \text{(c)} \end{aligned}\right\} \tag{2.125}$$

one has from (2.122), (2.123) and (2.124):

$$\Delta\dot{v}_{io} = (\delta\ddot{\underline{r}}_{io})^T \underline{e}_{io}^{c} + \left.\frac{\partial(\ddot{\underline{r}}_{io}^T \underline{e}_{io})}{\partial \underline{r}_o}\right|_c \delta\underline{r}_o + \left.\frac{\partial(\ddot{\underline{r}}_{io}^T \underline{e}_{io})}{\partial \underline{r}_i}\right|_c \delta\underline{r}_i + \delta a_{io}^{NG} + \delta R_{io} + \varepsilon_{io} \tag{2.126}$$

where ε_{io} contains now apart of the noise n_{io}, the effects of second and higher order terms omitted in equation (2.123). For the first partial derivative in (2.126), one has:

$$\frac{\partial(\ddot{\underline{r}}_{io}^T \underline{e}_{io})}{\partial \underline{r}_o} = \underline{e}_{io}^T \frac{\partial(\ddot{\underline{r}}_{io})}{\partial \underline{r}_o} + \ddot{\underline{r}}_{io}^T \frac{\partial(\underline{e}_{io})}{\partial \underline{r}_o} \quad . \tag{2.127}$$

It can be shown easily (see also (Rummel, 1980)) that:

$$\frac{\partial(\underline{e}_{io})}{\partial \underline{r}_o} = \frac{1}{\rho_{io}} (I_3 - \underline{e}_{io} \underline{e}_{io}^T) \tag{2.128}$$

where I_3 is the three-dimensional unit matrix. Rummel (ibid) also shows that:

$$\frac{\partial(\ddot{\underline{r}}_{io})}{\partial \underline{r}_o} = \frac{\partial[\text{grad}V(\underline{r}_o)]}{\partial \underline{r}_o} = M(\underline{r}_o) \quad , \tag{2.129}$$

where V is the (true) gravitational potential of the Earth, and M the three-dimensional gravitational tensor, i.e.,

$$M(\underline{r}_o) = \begin{bmatrix} \frac{\partial^2 V}{\partial x^2} & \frac{\partial^2 V}{\partial x \partial y} & \frac{\partial^2 V}{\partial x \partial z} \\ \frac{\partial^2 V}{\partial y \partial x} & \frac{\partial^2 V}{\partial y^2} & \frac{\partial^2 V}{\partial y \partial z} \\ \frac{\partial^2 V}{\partial z \partial x} & \frac{\partial^2 V}{\partial z \partial y} & \frac{\partial^2 V}{\partial z^2} \end{bmatrix}_{\underline{r}_o} \quad . \tag{2.130}$$

With corresponding derivations for the partial derivative with respect to $\underline{r}_i$, equation (2.126) after regrouping terms becomes:

$$\begin{aligned} \Delta\dot{v}_{io} = (\delta\ddot{\underline{r}}_{io})^T \underline{e}^c_{io} &+ \left\{ (\underline{e}^c_{io})^T M(\underline{r}^c_o) + \frac{1}{\rho^c_{io}} [\ddot{\underline{r}}^T_{io} - a_{io}(\underline{e}^c_{io})^T] \right\} \delta\underline{r}_o \\ &- \left\{ (\underline{e}^c_{io})^T M(\underline{r}^c_i) + \frac{1}{\rho^c_{io}} [\ddot{\underline{r}}^T_{io} - a_{io}(\underline{e}^c_{io})^T] \right\} \delta\underline{r}_i \\ &+ \delta a^{NG}_{io} + \delta R_{io} + \varepsilon_{io} \quad . \end{aligned} \tag{2.131}$$

From equation (2.131) it can be seen that the (pseudo) observable $\Delta\dot{v}_{io}$ is affected by (and thus contains information concerning) the following:

(a) The residual (with respect to the reference geopotential model used) relative gravitational acceleration along the LOS between the two spacecrafts (first term).

(b) The difference between the actual and the reference orbits of the two spacecrafts (second and third terms).

(c) The residual (with respect to the non-gravitational force models used) relative non-gravitational acceleration along the LOS, δa_{io}^{NG}.

(d) The residual relative centrifugal acceleration along the LOS, δR_{io}.

(e) The random noise on the primary observable, residual atmospheric effects, non-linear term effects etc., all these effects collectively represented in the term ε_{io}.

For the current application, of interest is only (part of) the first term in equation (2.131), while the rest of the terms represent undesired systematic and random "errors". In contrast, if for example the intention was to estimate improved orbits for the two spacecrafts, based on the (pseudo) observations $\Delta\dot{v}_{io}$, then the second and third terms in (2.131) would have been of critical importance. Since:

$$\delta\ddot{\underline{r}}_{io} = \delta\ddot{\underline{r}}_o - \delta\ddot{\underline{r}}_i \quad , \tag{2.132}$$

and:

$$\delta\underline{e}_{io} = \frac{1}{\rho_{io}^c}\left[I_3 - (\underline{e}_{io}^c)(\underline{e}_{io}^c)^T\right]\left(\delta\underline{r}_o - \delta\underline{r}_i\right) \quad , \tag{2.133}$$

one can re-write equation (2.131) as:

$$\begin{aligned}\Delta\dot{v}_{io} = {} & \left(\delta\ddot{\underline{r}}_o\right)^T\underline{e}_{io}^c - \left(\delta\ddot{\underline{r}}_i\right)^T\underline{e}_{io}^c \\ & + (\underline{e}_{io}^c)^T\left[M(\underline{r}_o^c)\delta\underline{r}_o - M(\underline{r}_i^c)\delta\underline{r}_i\right] + \ddot{\underline{r}}_{io}^T\delta\underline{e}_{io} \\ & + \delta a_{io}^{NG} + \delta R_{io} + \varepsilon_{io} \quad ,\end{aligned} \tag{2.134}$$

where the orbit error contributions were separated in the parts referring to the absolute and relative position errors of the spacecrafts respectively. The magnitude of each term on the right-hand side of (2.134) depends on the particular SST configuration in question (e.g. satellite altitudes, instrumentation etc.), the maximum degree (as well as the accuracy) of the reference geopotential model used to evaluate $\Delta\dot{v}_{io}$, and the accuracy of the satellites' ephemerides. The following considerations pertain to the case where S_o corresponds to GP-B (see Table 1), while S_i corresponds to one of the satellites of the GPS constellation, so that:

$$r_o = |\underline{r}_o| \approx 6971 \text{ km}$$

$$r_i = |\underline{r}_i| \approx 26560 \text{ km} \quad .$$

To estimate the magnitude of each term in (2.134) one needs to assume some knowledge of the terrestrial gravitational field, at least in a global average sense, as described by a global covariance model (Moritz, 1980, p. 181). The model used here will be defined by the following anomaly degree variances (see also section 3.4):

$$c_n(\text{mgal}^2) = \begin{cases} \left(\frac{GM}{a^2}\right)^2 (n-1)^2 \left(\frac{a^2}{R^2}\right)^{n+2} \sum_{m=-n}^{n} (\varepsilon \bar{C}_{nm})^2 & 2 \le n \le \text{Nmax} \\ \left(\frac{GM}{a^2}\right)^2 (n-1)^2 \left(\frac{a^2}{R^2}\right)^{n+2} \sum_{m=-n}^{n} (\bar{C}_{nm})^2 & \text{Nmax} < n \le 360 \\ \frac{343.3408\,(n-1)}{(n-2)(n+24)} (0.9988961)^{n+2} & 360 < n < \infty \end{cases} \tag{2.135}$$

where:

$GM = 3986004.36 \times 10^8$	m^3/s^2
$a = 6378137.$	m
$R = 6371000.$	m

and the $\bar{C}_{nm}$, $\varepsilon\bar{C}_{nm}$ are the fully-normalized unitless harmonic coefficients and their errors as given by the OSU89B geopotential model (Rapp and Pavlis, 1990) (even zonal harmonic coefficients are remainders after removing the ellipsoidal reference field). The c_n values defined above refer to the surface of the sphere of radius R, while Nmax represents the maximum degree of the geopotential model used to evaluate $\Delta\dot{v}_{io}$.

Considering now the first term on the right-hand side of equation (2.134) one has:

$$\left|(\delta\ddot{\underline{r}}_o)^T \underline{e}^c_{io}\right| \le |\delta\ddot{\underline{r}}_o| = \left|\text{grad}\left[\hat{T}^m(\underline{r}_\delta)\right]\right| \approx |\delta g^m(r_o)| \tag{2.136}$$

where $\hat{T}^m$ is the disturbing potential with respect to the reference model used (i.e., $\hat{T}^m$ represents the commission error of the model up to degree n = Nmax, and the omission error from n = Nmax + 1 to infinity), and δg^m is the gravity disturbance implied by the

aforementioned model (i.e. $\delta g^m = - \partial \hat{T}^m / \partial r$). The difference in direction between the actual gravitational acceleration and the one implied by the model has been disregarded in (2.136). In a spherical approximation, which is sufficient for the magnitude estimates sought here, one has (see also (Jekeli, 1979)):

$$\text{rms(o)} \equiv \left\{ \text{var}\left[\left(\delta \ddot{\underline{r}}_o\right)^T \underline{e}^c_{io} \right] \right\}^{1/2} \approx \left\{ \sum_{n=2}^{\infty} \left(\frac{n+1}{n-1} \right)^2 c_n \left(\frac{R^2}{r_o^2} \right)^{n+2} \right\}^{1/2} \tag{2.137}$$

and similarily, for the high-altitude satellite:

$$\text{rms(i)} \equiv \left\{ \text{var}\left[\left(\delta \ddot{\underline{r}}_i\right)^T \underline{e}^c_{io} \right] \right\}^{1/2} \approx \left\{ \sum_{n=2}^{\infty} \left(\frac{n+1}{n-1} \right)^2 c_n \left(\frac{R^2}{r_i^2} \right)^{n+2} \right\}^{1/2} \quad . \tag{2.138}$$

The cross-rms of the residual accelerations of the high and low satellite, assuming radial arrangement of the spacecrafts, as the $\psi = 0$ notation indicates, is given by (Jekeli, ibid):

$$\begin{aligned} \text{rms(i, o)} &= \left\{ \text{cov}\left[\left(\delta \ddot{\underline{r}}_i\right)^T \underline{e}^c_{io}, \left(\delta \ddot{\underline{r}}_o\right)^T \underline{e}^c_{io} \right]_{\psi=0} \right\}^{1/2} \\ &\approx \left\{ \sum_{n=2}^{\infty} \left(\frac{n+1}{n-1} \right)^2 c_n \left(\frac{R^2}{r_i r_o} \right)^{n+2} \right\}^{1/2} \end{aligned} \tag{2.139}$$

This cross-rms is maximized for radial arrangement of the satellites, enabling a worst case study of the effect of its omission. In addition, the rms acceleration difference between the low and high satellite (assuming radial arrangement), is given by:

$$\text{rms(o - i)} = \left\{ \text{var}\left[\left(\delta \ddot{\underline{r}}_{io}\right)^T \underline{e}^c_{io} \right] \right\}^{1/2} \approx \left[\text{rms}^2\text{(o)} - 2\,\text{rms}^2\text{(i, o)} + \text{rms}^2\text{(i)} \right]^{1/2} \quad . \tag{2.140}$$

These quantities have been evaluated using the degree variances defined in (2.135), and approximating infinity by n = 36000 in (2.137) through (2.139). The results for various degrees of truncation (the variable Nmax appearing in equation (2.135)), are given in Table 2.

Table 2. Root Mean Square (rms) Residual Acceleration Magnitude With Respect to OSU89B Model Complete to Degree Nmax (All rms values are in mgals).

Nmax	rms(i)	rms(o)	rms(i, o)	rms(o - i)
2	0.94106×10^{-2}	10.748	0.27752	10.741
4	0.32439×10^{-3}	6.391	0.37761×10^{-1}	6.391
6	0.16776×10^{-4}	4.228	0.68755×10^{-2}	4.228
8	0.55717×10^{-5}	2.784	0.11287×10^{-2}	2.784
10	0.55323×10^{-5}	1.865	0.25036×10^{-3}	1.865
20	0.55323×10^{-5}	0.583	0.18081×10^{-3}	0.583

From Table 2 it can be seen that a state-of-the-art reference gravitational model (developed in the absence of any of the missions discussed in section 1.3) and truncated to a degree as low as eight is enough to justify the assumption that the residual gravitational acceleration at GPS altitude is zero, thus introducing an error no larger than about 10^{-3} mgal (see also (Jekeli and Upadhyay, 1990)). It should be noted that Jekeli and Upadhyay (ibid), consider the reference model up to Nmax errorless, thus showing a monotonic decrease for rms(i) as Nmax increases; here rms(i) stabilizes at about 0.6×10^{-5} mgal after Nmax = 8, due to the commission error of the lower degree harmonics.

The effect on $\Delta\dot{v}_{io}$ of the orbit errors δr_o and δr_i of the low and high satellites is considered next. For this purpose, it is assumed that a global network of tracking sites on the Earth, simultaneously co-observes the GPS satellites being tracked by the low orbiter, as it will be the case for all the missions discussed in section 1.3 (Pavlis, E. et al., 1990). In such case the orbits of the GPS satellites and the low orbiter can be estimated geometrically from differential GPS observations. Yunck and Wu (1986) carried out simulation studies to assess the accuracy of such orbit determination for TOPEX, and concluded that decimeter accuracy orbits are attainable with as few as 10 globally distributed tracking stations. The orbital accuracy in such non-dynamic solutions is limited by the GPS data noise, the ground station position errors, tropospheric and higher order ionospheric effects and antenna multipath, error sources that have no significant dependence on altitude (ibid, 1986), so that 10 cm is also a realistic (and probably too conservative) estimate for the orbit error of GP-B.

Approximating the gravitational tensor $M(\underline{r})$ by:

$$M(\underline{r}) \approx -\frac{GM}{|\underline{r}|^3}\begin{bmatrix} 1 & 0 & 0 \\ 0 & 1 & 0 \\ 0 & 0 & -2 \end{bmatrix} \quad , \tag{2.141}$$

which is sufficient for order of magnitude considerations (see also (Jekeli and Upadhyay, 1990)), and denoting by ε^r the radial component (which is the most crucial for the current application) of the acceleration error induced by radial orbit error δr, one has (see equation 2.134):

Low satellite (S_o) : $\varepsilon_o^r\,(\text{mgal}) \approx 2.4 \times 10^{-1}\delta r_o(\text{m})$

High satellite (S_i) : $\varepsilon_i^r\,(\text{mgal}) \approx 4.3 \times 10^{-3}\delta r_i(\text{m})$

while the misregistration of the LOS direction, $\delta\underline{e}_{io}$, introduces an error $\varepsilon_{\delta\underline{e}_{io}}$, which does not exceed:

$$\varepsilon_{\delta\underline{e}_{io}}(\text{mgal}) \approx 4.2 \times 10^{-2}\sqrt{2}\,\delta r_o(\text{m}) \quad .$$

As it can be seen from the above estimates (which pertain to the GPS/GP-B SST configuration), the orbit error of the GPS satellite and the misregistration of the LOS direction introduce negligible acceleration errors. The orbit error of the low satellite however, introduces an acceleration error that may reach 24 μgals in amplitude (for δr_o = 10 cm) which can have a significant effect on geopotential estimation at the few centimeter accuracy level, if its power is concentrated at low frequencies. Colombo (1990) has shown that systematic errors in the satellite positions significantly affect the recovered geopotential spectrum only up to about degree 10. In addition, comparing the results of the analytical approach in the absence of such errors ("best case"), with those obtained from a complete simulation where satellite orbits were estimated dynamically in a simultaneous solution along with the geopotential spectrum (Pavlis, E. et al., 1990), Colombo (1990) verified that systematic orbit errors can be effectively decoupled from the gravitational signal in such global solutions, as long as their mathematical representation is accounted for in the adjustment. Accordingly, one way of reducing the effect of orbital errors on $\Delta\dot{v}_{io}$, is to pre-process smoothed values of the global set of

SST data in a dynamic mode where the orbital parameters of all satellites and the low-degree part of the geopotential spectrum (e.g. Nmax = 10) are simultaneously estimated from the original GPS measurements. $\Delta\dot{v}_{io}$ can then be referred to the adjusted orbits and long-wavelength geopotential spectrum obtained from such global dynamic solution. In such case, the smoothing of the original measurements is critical, since one wants to minimize leakage of the higher-frequency content of the measurements to the lower-frequency part of the estimated geopotential spectrum. However, the global character (polar GP-B orbit) and the uniform coverage of the data works favorably in the minimization of leakage effects. Obviously, as the maximum degree of the geopotential model obtained from the global adjustment increases, the contribution of the residual $\Delta\dot{v}_{io}$ (with respect to this model), to the estimation of the disturbing potential T on the Earth's surface, decreases. In the limit, if the model extends to the degree corresponding to the resolution of the data at altitude (Nmax $\approx$ 55 for GP-B), then only the ground measurements, in the caps surrounding the computation points provide additional information for the estimation of T. An alternative way of reducing the orbit error of the low satellite is the use of laser ranging combined with the GPS tracking in a geometric solution for its orbit determination (Everitt et al., 1989). In view of the magnitudes of δR_{io} and ε_{io}, which will be discussed next, the effect of orbit errors in the modeling of $\Delta\dot{v}_{io}$ does not appear to be a limiting factor. Accordingly, equation (2.134) becomes:

$$\Delta\dot{v}_{io} \approx \left(\delta\ddot{\underline{r}}_o\right)^T \underline{e}^c_{io} + \delta R_{io} + \varepsilon_{io} \quad , \tag{2.142}$$

where, in addition, it was assumed that the residual non-gravitational acceleration along the line of sight, δa^{NG}_{io}, is negligible. Such an assumption implies that non-gravitational accelerations have been modeled perfectly as a result of the global adjustment of the SST data.

The centrifugal term δR_{io} is considered next. It can be easily shown (Colombo, 1981b), that:

$$R_{io} = \dot{\underline{r}}^T_{io}\,\dot{\underline{e}}_{io} = \frac{1}{\rho_{io}}\left(\dot{\underline{r}}^T_{io}\,\underline{n}_{io}\right)^2 = \frac{1}{\rho_{io}}\left|\dot{\underline{r}}_{io}\right|^2\cos^2\gamma \tag{2.143}$$

where $\underline{n}_{io}$ is the unit vector perpendicular to the LOS direction as defined in equation (2.112), and γ is the angle between $\dot{\underline{r}}_{io}$ and $\underline{n}_{io}$. The geometry of the vectors defined on the plane generated by $\underline{r}_{io}$ and $\dot{\underline{r}}_{io}$ is illustrated in Figure 8.

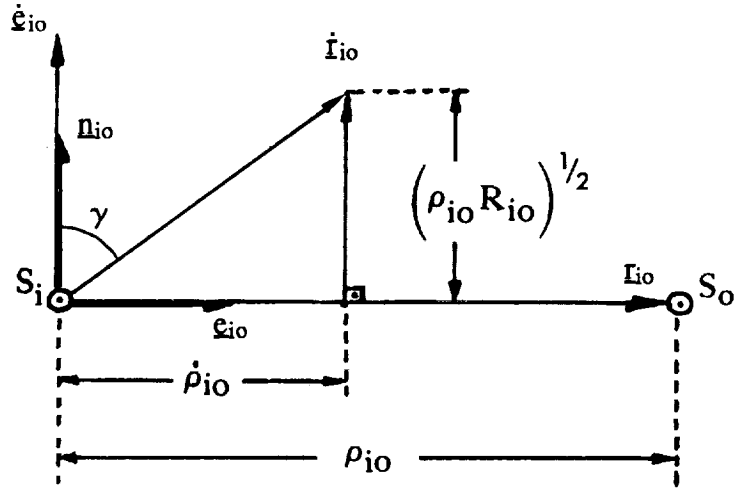

Figure 8. Geometry of the Vectors Defined on the Plane of $\underline{r}_{io}$ and $\dot{\underline{r}}_{io}$.

Subtracting the reference value R_{io}^c from the true value R_{io} one has, due to (2.143), for δR_{io}:

$$\delta R_{io} = \frac{1}{\rho_{io}} |\dot{\underline{r}}_{id}|^2 \cos^2\gamma - \frac{1}{\rho_{io}^c} |\dot{\underline{r}}_{io}^c|^2 \cos^2\gamma^c \qquad (2.144)$$

where γ^c is the angle between $\dot{\underline{r}}_{io}^c$ and $\underline{n}_{io}^c$. To obtain a magnitude estimate of δR_{io}, it is justifiable to set:

$$\rho_{io} \approx \rho_{io}^c \quad ; \quad \cos\gamma \approx \cos\gamma^c \qquad (2.145)$$

so that:

$$\delta R_{io} \approx \frac{1}{\rho_{io}^c} \{ |\dot{\underline{r}}_{io}|^2 - |\dot{\underline{r}}_{io}^c|^2 \} \cos^2\gamma^c = \frac{1}{\rho_{io}^c} \delta\{ |\dot{\underline{r}}_{io}|^2 \} \cos^2\gamma^c$$

$$= \frac{1}{\rho_{io}^c}\,\delta\left\{\dot{\underline{r}}_{io}^T\dot{\underline{r}}_{io}\right\}\cos^2\gamma^c \approx \frac{2}{\rho_{io}^c}\left(\dot{\underline{r}}_{io}^c\right)^T\delta\dot{\underline{r}}_{io}\cos^2\gamma^c \quad \Rightarrow$$

$$\delta R_{io} \approx \frac{2}{\rho_{io}^c}\left|\dot{\underline{r}}_{io}^c\right|\left|\delta\dot{\underline{r}}_{io}\right|\cos\beta\cos^2\gamma^c \quad , \tag{2.146}$$

where the total differential $\delta\left\{\dot{\underline{r}}_{io}^T\dot{\underline{r}}_{io}\right\}$ was approximated by the linear term in its Taylor series expansion (linearization), and "β" is the angle between $\dot{\underline{r}}_{io}^c$ and $\delta\dot{\underline{r}}_{io}$.

The last equation indicates that δR_{io} becomes maximum when $\gamma = 0°(180°)$, i.e. when the relative velocity of the satellites is perpendicular to the LOS direction. If in addition the satellites move in parallel and opposite directions (perpendicular to the LOS), then the magnitude of their inertial relative velocity becomes maximum, equal to the sum of the magnitudes of their individual inertial velocities. Under such circumstances the rate of rotation of the LOS direction is maximized, giving rise to the maximum possible centrifugal acceleration R_{io}, as expected. This "worst case" will be considered next, in order to estimate an upper bound for the magnitude of δR_{io}; the "best case" obviously corresponds to $\gamma = 90°(270°)$, when the satellites move towards or away from each other, so that $\underline{e}_{io}$ remains fixed with respect to inertial space and $R_{io} = 0$. For the "worst case" one has from (2.146):

$$\left|\delta R_{io}\right| \approx \frac{2}{\rho_{io}^c}\left|\dot{\underline{r}}_{io}^c\right|\left|\delta\dot{\underline{r}}_{io}\right|\left|\cos\beta\right|\cos^2\gamma^c$$

$$\leq \frac{2}{\rho_{io}^c}\left|\dot{\underline{r}}_{io}^c\right|\left|\delta\dot{\underline{r}}_{io}\right|$$

$$\leq \frac{2}{\rho_{io}^c}\left(\left|\dot{\underline{r}}_{o}^c\right| + \left|\dot{\underline{r}}_{i}^c\right|\right)\left|\delta\dot{\underline{r}}_{io}\right| \quad \Rightarrow$$

$$\max\left|\delta R_{io}\right| \approx \frac{2}{\rho_{io}^c}\left(\left|\dot{\underline{r}}_{o}^c\right| + \left|\dot{\underline{r}}_{i}^c\right|\right)\left|\delta\dot{\underline{r}}_{io}\right| \quad . \tag{2.147}$$

Making use of the energy conservation law (Jekeli and Rapp, 1980, p. 4), linearized with respect to the reference gravitational model to which δR_{io} refers, and assuming that the

motion of the high-altitude satellite is perfectly determined from that model, so that $\delta \underline{\dot{r}}_i = 0$, one has (see also (Rummel, 1980)):

$$|\delta \dot{\underline{r}}_{io}| \approx \frac{1}{|\dot{\underline{r}}_o^c|} |\hat{T}_{io}^m| \tag{2.148}$$

where:

$$\hat{T}_{io}^m = \hat{T}^m(\underline{r}_\delta) - \hat{T}^m(\underline{r}_i^c) \tag{2.149}$$

and $\hat{T}^m$ carries the same meaning as in equation (2.136) given before. Accordingly, an upper bound for the magnitude of δR_{io} is given by:

$$\max|\delta R_{io}| \approx \frac{2}{\rho_{io}^c}\left(1 + \frac{|\dot{\underline{r}}_i^c|}{|\dot{\underline{r}}_o^c|}\right)|\hat{T}_{io}^m| \quad . \tag{2.150}$$

An estimate of the disturbing potential difference $\hat{T}_{io}^m$, between the low and high satellites, may be obtained in a global average sense, considering the radial arrangement of the spacecrafts, by:

$$\mathrm{rms}(\hat{T}_{io}^m) = \left\{ \mathrm{var}\left[\hat{T}^m(r_o)\right] - 2\,\mathrm{cov}\left[\hat{T}^m(r_o), \hat{T}^m(r_i)\right]_{\psi=0} + \mathrm{var}\left[\hat{T}^m(r_i)\right] \right\}^{1/2} , \tag{2.151}$$

using the anomaly degree variance model of equation (2.135) to evaluate the disturbing potential's variances and covariances. Approximating:

$$|\dot{\underline{r}}| \approx \left(\frac{GM}{|\underline{r}|}\right)^{1/2} \tag{2.152}$$

and using the nominal values pertaining to the GPS/GP-B configuration, estimates of $\max|\delta R_{io}|$ have been computed, for various degrees of truncation, Nmax, of the reference model. These are given in Table 3.

Table 3. Estimates of the Maximum Value Attainable by δR_{io} for Various Degrees of Truncation of the Reference Model (Units are mgals).

Nmax	$\max\|\delta R_{io}\|$
2	2.201
4	0.865
6	0.444
8	0.234
10	0.127
20	0.023
1	1.910 (*)
18	0.097 (*)

(*) Values correspond to the High-Low mission considered by Rummel (1980).

For comparison purposes, two additional values are listed in Table 3. These refer to the High-Low mission considered by Rummel (1980), where the altitudes of the high and low satellites were 35500 km and 250 km respectively. These two values have been computed using the same anomaly degree variance model as in Rummel's study (ibid, p. 12). Comparing the above estimate for Nmax = 1 (i.e. when $\hat{T}^m$ represents the entire disturbing potential with respect to the ellipsoidal gravity field) to the corresponding one of Rummel's (ibid, p. 5, Table 1), it is seen that the former is about 7×10^5 times larger than the latter. Colombo (1981b, p. 15) estimated the magnitude of the centrifugal term δR_{io} for a Low-Low mission, and found a value 3×10^4 times larger than corresponding estimate of Rummel (1980, p. 5, Table 1).

The reason that both the current estimates, as well as those of Colombo, are so much larger than those of Rummel, is identified here to be an unjustifiable substitution of the term $\delta[|\dot{r}_{io}|^2]$, by the term $|\delta\dot{r}_{io}|^2$, in Rummel's derivations (ibid, pp. 4-5). Such substitution yields an expression for the average magnitude of δR_{io} (ibid, p. 5, equation 12), which is in fact independent of the relative inertial velocity of the two satellites, thus contradicting the underlying physical meaning of δR_{io}. Also apart from underestimating the magnitude of δR_{io}, such substitution implies that δR_{io} is always positive (Jekeli and Upadhyay, 1990, p. 10,984), while there is nothing dictating a fixed sign for δR_{io},

despite the fact that R_{io} itself is a non-negative quantity (see equation (2.143)). As it can be seen from equation (2.146), δR_{io} carries the same sign as $\cos\beta$, and the sign of $\cos\beta$ cannot be determined since it depends on the relative orientation of $\dot{\underline{r}}^c_{io}$ and the unknown vector $\delta\dot{\underline{r}}_{io}$. To the author's knowledge, this erroneous substitution appeared originally in Hajela's derivations (1978, p. 5, equation 2.2), and has been adopted afterwards in a number of investigations including the recent study by Jekeli and Upadhyay (1990). The maximum magnitude of δR_{io} for a reference model complete to degree and order 8 is about 0.4 mgals for the STAGE mission considered by Jekeli and Upadhyay (ibid), hence δR_{io} cannot be neglected in view of the 0.3 mgal total noise level that they have estimated for the (pseudo) observations $\Delta\dot{v}_{io}$ (ibid, p. 10,983).

The existence of the centrifugal term δR_{io} in equation (2.142) makes the analysis of the SST observational system, in terms of the pseudo observations $\Delta\dot{v}_{io}$, practically untractable. In contrast, such a problem is not encountered if the primary GPS observables (carrier phase and pseudo-range) are used in a global dynamic solution for the simultaneous estimation of satellite orbital parameters and geopotential coefficients (Pavlis, E. et al., 1990). In the current application, which is of local character, to minimize the magnitude of δR_{io}, so that its omission can be justified, one may consider the following strategies:

(a) Use of a higher degree reference geopotential model for the formation of $\Delta\dot{v}_{io}$. As it can be seen from Table 3, a model complete to Nmax = 20, implies a maximum expected value of δR_{io} of about 23 μgals, which may be considered negligible. The maximum degree of the reference model however, should be selected with due consideration to the ratio of the residual signal to the noise of the pseudo observations $\Delta\dot{v}_{io}$ as was discussed before.

(b) In a Multiple-High-Single-Low SST configuration, where as many as 8 GPS satellites are being tracked simultaneously by the low orbiter, one may select for the formation of $\Delta\dot{v}_{io}$ pseudo observations, those GPS satellites for which the quantity

$$f_{io} = \frac{2}{\rho^c_{io}} |\dot{\underline{r}}^c_{io}| \cos^2\gamma^c \qquad (2.153)$$

is minimized (and/or does not exceed a pre-established threshold value). Such editing criteria should be considered in conjunction to other geometric requirements (such as minimum elevation angles of the GPS satellites). It is obvious that such an editing procedure introduces substantial complexity to the data processing algorithm.

Finally, the noise ε_{io} of the pseudo observations $\Delta\dot{v}_{io}$ is considered following the lines of Jekeli and Upadhyay (1990). As it can be seen from their analysis (ibid, p. 10,976, Table 2), in the non-differential mode of observation, the major error source contributing to ε_{io} arises from the frequency instability of the GPS satellite oscillator. This error source effectively cancels out if single differences are formed between the phase measurements to a GPS satellite as observed by the low orbiter and a ground receiver. In such case, the total error ε_{io} of the residual acceleration along the line-of-sight, for the case of GP-B (10 cm orbit error, drag-free instrumentation), was estimated to be about 0.2 mgals.

In the following error analysis however, it will be assumed that the SST configuration contributes information on the vertical component of the gravitational acceleration at altitude. The error of the vertical component of the acceleration may be approximated by multiplying ε_{io} by the vertical dilution of precision (VDOP) (Jorgensen 1980) as described by Jekeli and Upadhyay (1990, p. 10,978). In their analysis it was found that for the Shuttle being the low orbiter, a representative value for VDOP was about 2. Adopting the same value for GP-B (which is a rather conservative assumption), one finally obtains 0.4 mgal error for the vertical component of the residual gravitational acceleration at GP-B altitude.

CHAPTER III

GLOBAL MEAN SQUARE ERROR ESTIMATION

As it was discussed in section (1.3), the geopotential differences between points separated by ocean, whose geocentric positions are known with accuracy of a few centimeters, will be estimated by combining information from:

(a) gravity disturbance measurements on the Earth's surface
(b) gravitational acceleration "observations" at the altitude of a low Earth orbiter
(c) a global geopotential model.

The development of appropriate analytical tools that can be used to estimate the expected accuracy of the resulting geopotential differences, based on assumptions related to the spatial arrangement and the uncertainties of the input data, is the subject of this chapter. In practical applications, the geopotential differences will be estimated using least-squares collocation (lsc) (Moritz, 1980) since this technique can combine efficiently observations of different functionals of the gravitational potential, and assures that the resulting estimates are based on optimal use of the information contained in the observations. In addition, lsc can be used to assess the expected uncertainty of the estimated values, and thus offers one possibility for the means with which the current error analysis could by conducted.

For given error properties of the input data, the (true) error of the estimated geopotential difference depends on the relative positions of the observation points with respect to the points to which the difference refers, as well as on the absolute positions of the latter. In that sense, the error of the estimated geopotential difference between points which lie on areas where the gravity field changes rapidly is likely to be larger than between points which lie on smoother areas of the field. The (squared) error estimate obtained from lsc on the other hand, represents a global average value, whose meaning is

as follows (Colombo, 1980). Keeping the relative positions of observation and estimation points fixed, subject the entire pattern to all possible rotations over the sphere. After each rotation measurements are taken, the lsc estimation is performed and the corresponding true estimation error is evaluated somehow. The global average of the squares of these errors, represents the squared error obtained from lsc. As a result of the use of homogeneous and isotropic covariances, if the relative geometry of observation and estimation points remains fixed, and so do the error properties of the data, the error estimate obtained through lsc will remain unchanged regardless of the absolute position and orientation of the whole observation/estimation pattern on the terrestrial sphere. Moreover, as it is well known, the lsc estimator, by its definition, ensures that this global mean square error is the minimum among the corresponding ones of any other linear estimator (Moritz, 1980, pp. 122-132). This property, as well as the ability of lsc to accommodate different data types and arbitrary spatial arrangements of measurement/estimation points, are responsible for the wide application of the lsc estimation technique.

To benefit from the above properties however, one must take up the computational effort of forming and inverting covariance matrices whose dimensions equal the number of observation points. In actual implementation where the geometry of observation/estimation points is given and one is interested in the most rigorous evaluation of the estimates themselfs, as well as their expected errors, such computational effort is well justified. However, in error analysis studies the relative geometry of observation and estimation points is more or less a matter of assumption, and one is interested only in the expected errors of the estimates and not the estimated values themselves. In addition, if one strives for estimates which will not be significantly biased by uneven data distribution, it is necessary to impose some kind of requirements pertaining to the uniformity and spatial density of the measurements. Under such circumstances, if one is willing to accept additional assumptions that result in symmetric patterns for the geometry of the observation/estimation points, efficient techniques can be used to assess the expected errors of the estimates, resulting in large computational savings. Obviously, the reliability of the error estimates evaluated this way , depends on how well the assumed symmetric data arrangements compare with actual data configurations, at least in a global average sense.

The simplest way to assess the error of a geopotential difference, estimated on the basis of a global geopotential model and terrestrial-only measurements, is through error propagation based on truncation theory. As it will be seen however, this technique cannot be used if gravitational accelerations at altitude are to be included in the estimation. On the other hand, least-squares collocation using "ring averages" (Colombo, 1980, section 4.1) can accommodate both data types (either separately or in combination) and is only restricted by assumptions related to symmetries in the measurement pattern. In that sense, the use of ring averages provides a compromise which maintains the efficiency of integral formulas while incorporating the versatility of lsc. The analytical formulation of these techniques and their intercomparison are discussed next. In addition, the covariance models for the signals and the noise of the measurements which will be used in the numerical analysis are presented afterwards.

3.1 Error Propagation Using Truncation Theory

The use of truncation theory for the assessment of the global mean square error of geoidal undulations estimated from gravity disturbances measured over a cap centered at the computation point, and a global geopotential model, has been considered variously by Jekeli (1979) and Sjöberg and Fan (1986). In the following discussion the notation used by Despotakis (1987), for the corresponding case of cap integration of gravity anomalies (Stokes' kernel), will be adopted.

Equation (2.102) of the previous chapter is written for convenience as follows:

$$T(\delta, \lambda) = \frac{1}{4\pi} \iint_{\sigma} H(\psi) D(\delta', \lambda') d\sigma \tag{3.1}$$

where:

$$D(\delta', \lambda') = \left[N_b(\delta g + \delta g_A - \varepsilon_P + g_1) - \varepsilon_1\right](\delta', \lambda') \quad . \tag{3.2}$$

The n^{th} - degree and m^{th} - order ellipsoidal harmonics of D and T are related by:

$$D_{nm}(\delta', \lambda') = (n + 1) T_{nm}(\delta', \lambda') \quad , \tag{3.3}$$

as it can be easily seen from equations (2.98) and (2.101). In addition, the solid angle corresponding to the cap centered at the computation point, is denoted by σ_c, so that:

$$\sigma \equiv \sigma_c + (\sigma - \sigma_c) \quad , \tag{3.4}$$

and a kernel modification function $W_i(\psi)$ is introduced, such that:

$$H(\psi) \equiv H_i(\psi) + W_i(\psi) \quad ; \quad 0 \le \psi \le \pi \tag{3.5}$$

and the modified kernel $H_i(\psi)$ is defined through the last equation, given the definition of $W_i(\psi)$. Due to (3.4) and (3.5), equation (3.1) becomes:

$$T(\delta, \lambda) = \frac{1}{4\pi} \iint_{\sigma} H_i(\psi) D(\delta', \lambda') d\sigma - \frac{1}{4\pi} \iint_{\sigma - \sigma_c} H_i(\psi) D(\delta', \lambda') d\sigma$$
$$+ \frac{1}{4\pi} \iint_{\sigma - \sigma_c} H_i(\psi) D(\delta', \lambda') d\sigma + \frac{1}{4\pi} \iint_{\sigma} W_i(\psi) D(\delta', \lambda') d\sigma \quad . \tag{3.6}$$

A function $\overline{H}_i(\psi)$ is now introduced, defined by:

$$\overline{H}_i(\psi) = \begin{cases} 0 & \text{if} \quad 0 \le \psi \le \psi_o \\ H_i(\psi) & \text{if} \quad \psi_o < \psi \le \pi \end{cases} \tag{3.7}$$

where ψ_o is the semi-aperture of the spherical cap σ_c. Accordingly, equation (3.6) becomes:

$$T(\delta, \lambda) = \frac{1}{4\pi} \iint_{\sigma} \left[H_i(\psi) - \overline{H}_i(\psi) \right] D(\delta', \lambda') d\sigma$$
$$+ \frac{1}{4\pi} \iint_{\sigma} \left[\overline{H}_i(\psi) + W_i(\psi) \right] D(\delta', \lambda') d\sigma \quad . \tag{3.8}$$

As long as the modification function $W_i(\psi)$ is at least piecewise continuous in the interval $0 \le \psi \le \pi$ (in which case $H_i(\psi)$ and $\overline{H}_i(\psi)$ will also be piecewise continuous), it may be expanded in a series of Legendre polynomials, as:

$$W_i(\psi) = \sum_{n=0}^{\infty} \frac{2n+1}{2} W_{in} P_n(\cos\psi) \tag{3.9}$$

where:

$$W_{in} = \int_0^{\pi} W_i(\psi) P_n(\cos\psi) \sin\psi d\psi \quad . \tag{3.10}$$

Similarly, for $\overline{H}_i(\psi)$ and $H_i(\psi)$ one has:

$$\overline{H}_i(\psi) = \sum_{n=0}^{\infty} \frac{2n+1}{2} Q_{in}(\psi_o) P_n(\cos\psi) \tag{3.11}$$

where: $$Q_{in}(\psi_o) = \int_0^{\pi} \overline{H}_i(\psi) P_n(\cos\psi) \sin\psi d\psi \quad \Rightarrow$$

$$Q_{in}(\psi_o) = \int_{\psi_o}^{\pi} H_i(\psi) P_n(\cos\psi) \sin\psi d\psi \quad , \tag{3.12}$$

and:

$$H_i(\psi) = \sum_{n=0}^{\infty} \frac{2n+1}{2} X_{in} P_n(\cos\psi) \tag{3.13}$$

$$X_{in} = \int_0^{\pi} H_i(\psi) P_n(\cos\psi) \sin\psi d\psi \quad . \tag{3.14}$$

Making use of the decomposition formula of the Legendre polynomials (Heiskanen and Moritz, section 1-15), and the orthogonality of the surface harmonics, it can be shown easily that due to (3.9), (3.11) and (3.13), equation (3.8) becomes:

$$T(\delta, \lambda) = \frac{1}{2} \sum_{n=0}^{\infty} [X_{in} - Q_{in}(\psi_o)] D_n(\delta, \lambda) + \frac{1}{2} \sum_{n=0}^{\infty} [W_{in} + Q_{in}(\psi_o)] D_n(\delta, \lambda) \tag{3.15}$$

where:

$$D_n(\delta, \lambda) = \sum_{m=-n}^{n} D_{nm}(\delta, \lambda) \quad . \tag{3.16}$$

Equation (3.15) is rigorously equivalent to (3.8) and provides the "frequency domain" counterpart of the latter. From (3.15) and (3.3) it can be seen that the quantities X_{in} and W_{in} should fulfill the relation:

$$X_{in} + W_{in} = \frac{2}{n+1} \quad ; \quad n \geq 0 \tag{3.17}$$

which provides the means of evaluating X_{in}, without performing the integration (3.14), once W_{in} has been evaluated.

For the purpose of practical implementation, one has to consider that one part of the available information (the gravity disturbance measurements) represents "space domain" quantities, while the other part (the global geopotential model) is given in terms of spectral components. It is thus reasonable to seek a combination of equations (3.8) and (3.15) such that both kinds of information can be considered simultaneously in an efficient manner. Obviously, such a combination is meaningful only if the cap measurements are more detailed and/or accurate than what can be deduced for their values from the global model, and the cap does not extend to $\psi = \pi$. In that sense, one has from (3.8) and (3.15):

$$T(\delta, \lambda) = \frac{1}{4\pi} \iint_{\sigma_c} H_i(\psi) D(\delta', \lambda') d\sigma + \frac{1}{2} \sum_{n=0}^{\infty} [W_{in} + Q_{in}(\psi_o)] D_n(\delta, \lambda) \tag{3.18}$$

whereby the integral term in (3.18) represents the cap contribution to $T(\delta, \lambda)$, implied by the modified kernel $H_i(\psi)$, and the infinite sum represents the remote zone contribution to $T(\delta, \lambda)$ implied by the original kernel $H(\psi)$ plus the cap contribution of the kernel modification $W_i(\psi)$, i.e.

$$\frac{1}{2}\sum_{n=0}^{\infty}[W_{in} + Q_{in}(\psi_o)]D_n(\delta, \lambda) = \frac{1}{4\pi}\iint_{\sigma-\sigma_c} H(\psi)D(\delta', \lambda')d\sigma + \frac{1}{4\pi}\iint_{\sigma-\sigma_c} W_i(\psi)D(\delta', \lambda')d\sigma. \tag{3.19}$$

Equation (3.18) (which is rigorously equivalent to both equations (3.8) and (3.15)), forms the basis upon which a computational formula suitable for practical implementation can be developed. Obviously, different choices of the modification kernel $W_i(\psi)$, yield different estimators of $T(\delta, \lambda)$, with varying properties. However, regardless of the choice of $W_i(\psi)$, equation (3.18) states that to determine the true value of $T(\delta, \lambda)$, requires continuous and errorless data $D(\delta', \lambda')$ inside the cap of integration σ_c, and perfect knowledge of the spectrum $D_n(\delta, \lambda)$ up to infinite degree. In practice, none of these requirements can ever be fulfilled; cap measurements can only be acquired at a finite number of discrete locations and are contaminated by observational noise, and in addition the knowledge of the spectrum extends to a finite degree and is imperfect. The errors that these imperfections induce to the estimated value $\hat{T}(\delta, \lambda)$ of the disturbing potential are examined next, along similar lines to the derivations of Christodoulidis (1976).

In practical implementation, the cap integration in (3.18), has to be replaced by a finite summation, since the function $D(\delta', \lambda')$ is not given in an analytic form but has only been sampled at discrete locations (Heiskanen and Moritz, 1967, section 2-24). To avoid biasing the result of this numerical integration, due to uneven distribution of the point measurements, one usually forms from the original point data, a set of area-mean values on a fine grid (e.g. 2' x 2'), covering the entire cap σ_c (Despotakis, 1987). It is assumed hereon that the cap data consist of area-mean values $\overline{D}^c_{ij}$, on an equiangular grid in terms of spherical distance ψ and azimuth α ($\Delta\psi = \Delta\alpha$), centered at the computation point $P(\delta, \lambda)$. Note that ψ and α are evaluated from ellipsoidal coordinates (δ, λ) and (δ', λ'). The indices (i, j) identify the location of the compartment to which the area-mean value refers, in a two-dimensional array where:

$$i = 0, 1, 2, ..., Nr - 1 \quad ; \quad j = 0, 1, 2, ..., 2N - 1 \quad . \tag{3.20}$$

As illustrated in Figure 9, the number of "rows" (or "rings") of area-mean values around the computation point is Nr, while each ring contains 2N compartments, where:

$$N = \frac{\pi}{\Delta\alpha} \quad . \tag{3.21}$$

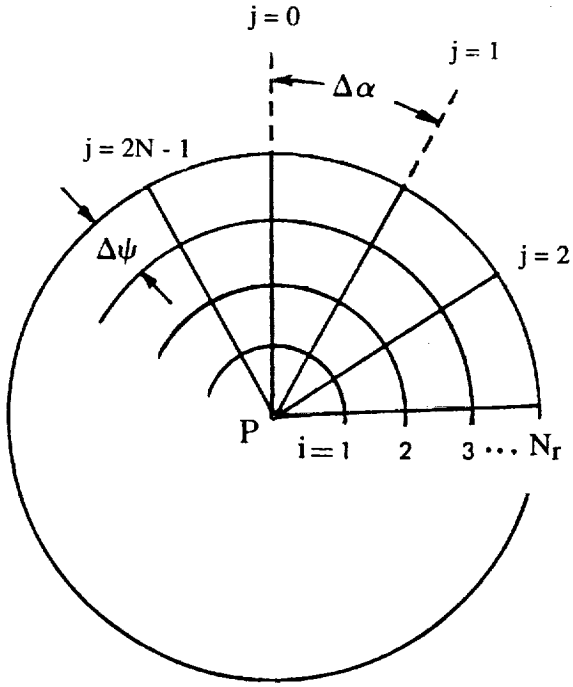

Figure 9. Arrangment of Cap Data Around the Computation Point P.

In addition, the estimated area-mean value $\overline{D}^c_{ij}$, differs from the corresponding true value $\overline{D}_{ij}$, by the true error $\varepsilon\overline{D}^c_{ij}$, so that:

$$\overline{D}_{ij} = \overline{D}^c_{ij} + \varepsilon\overline{D}^c_{ij} \quad . \tag{3.22}$$

As far as the available spectral information is concerned, a finite number of harmonics, $D^c_n(\delta, \lambda)$, up to maximum degree M, is assumed to be given. These are contaminated by commission error $\varepsilon D^c_n(\delta, \lambda)$, so that:

$$D_n(\delta, \lambda) = D_n^c(\delta, \lambda) + \varepsilon D_n^c(\delta, \lambda) \quad ; \quad n = 0, 1, ..., M \tag{3.23}$$

where $D_n(\delta, \lambda)$ represents the true value of these harmonics. Based on $\overline{D}_{ij}^c$ and $D_n^c(\delta, \lambda)$, the following estimate of the disturbing potential is evaluated:

$$\hat{T}(\delta, \lambda) = \frac{1}{4\pi} \sum_{i=0}^{Nr-1} \sum_{j=0}^{2N-1} \overline{D}_{ij}^c \iint_{\sigma_{ij}} H_k(\psi) d\sigma + \frac{1}{2} \sum_{n=0}^{M} [W_{kn} + Q_{kn}(\psi_o)] D_n^c(\delta, \lambda) \tag{3.24}$$

where σ_{ij} is the solid angle (area on the unit sphere) corresponding to the (i, j)th compartment, and the subscript k was used above to discriminate different kernel selections. The true error of the estimate $\hat{T}(\delta, \lambda)$ is given by:

$$\varepsilon\hat{T}(\delta, \lambda) = T(\delta, \lambda) - \hat{T}(\delta, \lambda) \quad , \tag{3.25}$$

so that, taking into account (3.18), and (3.22) through (3.25), one has:

$$\varepsilon\hat{T}(\delta, \lambda) = \varepsilon_1(\delta, \lambda) + \varepsilon_2(\delta, \lambda) + \varepsilon_3(\delta, \lambda) + \varepsilon_4(\delta, \lambda) \tag{3.26}$$

where:

$$\left.\begin{aligned}
\varepsilon_1(\delta, \lambda) &= \frac{1}{4\pi} \iint_{\sigma_c} H_k(\psi) D(\delta', \lambda') d\sigma - \frac{1}{4\pi} \sum_{i=0}^{Nr-1} \sum_{j=0}^{2N-1} \overline{D}_{ij} \iint_{\sigma_{ij}} H_k(\psi)\, d\sigma && \text{(a)} \\
\varepsilon_2(\delta, \lambda) &= \frac{1}{4\pi} \sum_{i=0}^{Nr-1} \sum_{j=0}^{2N-1} \varepsilon\overline{D}_{ij}^c \iint_{\sigma_{ij}} H_k(\psi)\, d\sigma && \text{(b)} \\
\varepsilon_3(\delta, \lambda) &= \frac{1}{2} \sum_{n=0}^{M} [W_{kn} + Q_{kn}(\psi_o)]\, \varepsilon D_n^c(\delta, \lambda) && \text{(c)} \\
\varepsilon_4(\delta, \lambda) &= \frac{1}{2} \sum_{n=M+1}^{\infty} [W_{kn} + Q_{kn}(\psi_o)]\, D_n(\delta, \lambda) && \text{(d)}
\end{aligned}\right\} \tag{3.27}$$

The following nomenclature will be used for the above error components (Christodoulidis, 1976):

ε_1 : sampling (or discretion) error of the cap integration

ε_2 : propagated error of the cap data

ε_3 : commission error of the geopotential model

ε_4 : omission error of the geopotential model.

It should be emphasized that $\varepsilon\bar{D}^c_{ij}$ refers to the area-mean value of the $(i, j)^{th}$ compartment, and not to the original point measurement, although in practice, for compartments as small as 2' x 2', the estimated error of such area-mean value differs very little from the corresponding error of a point measurement.

The error component $\varepsilon_1(\delta, \lambda)$ is considered next in detail. The following notation is introduced:

$$\varepsilon_1(\delta, \lambda) = a(\delta, \lambda) - b(\delta, \lambda) \tag{3.28}$$

where:

$$\left.\begin{aligned} a(\delta, \lambda) &= \frac{1}{4\pi}\iint_{\sigma_c} H_k(\psi) D(\delta', \lambda')\, d\sigma \qquad (a) \\ b(\delta, \lambda) &= \frac{1}{4\pi}\sum_{i=0}^{Nr-1}\sum_{j=0}^{2N-1}\bar{D}_{ij}\iint_{\sigma_{ij}} H_k(\psi)\, d\sigma \qquad (b) \end{aligned}\right\} \tag{3.29}$$

From equation (3.15) one has immediately:

$$a(\delta, \lambda) = \frac{1}{2}\sum_{n=0}^{\infty}[X_{kn} - Q_{kn}(\psi_o)]D_n(\delta, \lambda) \quad , \tag{3.30}$$

while for $b(\delta, \lambda)$, employing in a discretized manner the same technique used before to derive (3.8) from (3.6), one can write:

$$b(\delta, \lambda) = b_1(\delta, \lambda) - b_2(\delta, \lambda) \tag{3.31}$$

where:

$$\left.\begin{aligned} b_1(\delta, \lambda) &= \frac{1}{4\pi} \sum_{i=0}^{N-1} \sum_{j=0}^{2N-1} \overline{D}_{ij} \iint_{\sigma_{ij}} H_k(\psi)\, d\sigma \qquad (a) \\ b_2(\delta, \lambda) &= \frac{1}{4\pi} \sum_{i=0}^{N-1} \sum_{j=0}^{2N-1} \overline{D}_{ij} \iint_{\sigma_{ij}} \overline{H}_k(\psi)\, d\sigma \qquad (b) \end{aligned}\right\} \quad . \tag{3.32}$$

Consider the term $b_1(\delta, \lambda)$ first; due to equation (3.13) and the decomposition formula:

$$P_n(\cos\psi) = \frac{1}{2n+1} \sum_{m=-n}^{n} \overline{Y}_{nm}(\delta, \lambda)\, \overline{Y}_{nm}(\delta', \lambda') \quad , \tag{3.33}$$

equation (3.32a) becomes:

$$b_1(\delta, \lambda) = \frac{1}{4\pi} \sum_{i=0}^{N-1} \sum_{j=0}^{2N-1} \overline{D}_{ij} \iint_{\sigma_{ij}} \left[\sum_{n=0}^{\infty} \frac{2n+1}{2} X_{kn} \frac{1}{2n+1} \sum_{m=-n}^{n} \overline{Y}_{nm}(\delta, \lambda)\, \overline{Y}_{nm}(\delta', \lambda') \right] d\sigma \Rightarrow$$

$$b_1(\delta, \lambda) = \frac{1}{8\pi} \sum_{i=0}^{N-1} \sum_{j=0}^{2N-1} \overline{D}_{ij} \sum_{n=0}^{\infty} X_{kn} \sum_{m=-n}^{n} \overline{Y}_{nm}(\delta, \lambda) \iint_{\sigma_{ij}} \overline{Y}_{nm}(\delta', \lambda')\, d\sigma \quad . \tag{3.34}$$

The coordinates of the variable point of integration (δ', λ'), are related to the integration variables spherical distance ψ and azimuth α with respect to the computation point $P(\delta, \lambda)$, by the well known formulas (Heiskanen and Moritz, 1967, p. 113):

$$\left.\begin{aligned} \cos\psi &= \cos\delta\cos\delta' + \sin\delta\sin\delta'\cos(\lambda' - \lambda) \qquad (a) \\ \tan\alpha &= \frac{\sin\delta'\sin(\lambda' - \lambda)}{\sin\delta\cos\delta' - \cos\delta\sin\delta'\cos(\lambda' - \lambda)} \qquad (b) \end{aligned}\right\} \tag{3.35}$$

and the integral over σ_{ij} will be denoted by $I\overline{Y}_{nm}(i,j)$ so that:

$$\iint_{\sigma_{ij}} \overline{Y}_{nm}(\delta', \lambda')d\sigma = \int_{\psi_i}^{\psi_i+\Delta\psi}\int_{\alpha_j}^{\alpha_j+\Delta\alpha} \overline{Y}_{nm}(\delta', \lambda')\sin\psi d\psi d\alpha = I\overline{Y}_{nm}(i, j) \quad . \tag{3.36}$$

Re-arranging the order of the summations in (3.34) one has, due to (3.36):

$$b_1(\delta, \lambda) = \frac{1}{2}\sum_{n=0}^{\infty} X_{kn} \sum_{m=-n}^{n} \overline{Y}_{nm}(\delta, \lambda)\left[\frac{1}{4\pi}\sum_{i=0}^{N-1}\sum_{j=0}^{2N-1} \overline{D}_{ij} I\overline{Y}_{nm}(i, j)\right] \quad . \tag{3.37}$$

The expression inside the brackets in (3.37) is readily recognized to represent a quadrature formula (Colombo, 1981a), according to which an estimate $\hat{D}_{nm}$ of the true spectrum D_{nm} of $D(\delta, \lambda)$ may be obtained, given a global set (N x 2N) of errorless area mean values $\overline{D}_{ij}$, on the equiangular grid $\Delta\psi = \Delta\alpha$ with pole the computation point $P(\delta, \lambda)$. Hence:

$$\hat{D}_{nm} = \frac{1}{4\pi}\sum_{i=0}^{N-1}\sum_{j=0}^{2N-1} \overline{D}_{ij}\, I\overline{Y}_{nm}(i, j) \quad . \tag{3.38}$$

It should be mentioned here that the coefficients $\hat{D}_{nm}$ obtained from (3.38) refer to the coordinate system associated with the (δ, λ) grid, although the area-mean values $\overline{D}_{ij}$ are given on the (ψ, α) grid with pole the computation point $P(\delta, \lambda)$. Although in theory the two grids do not have to coincide, this incompatibility makes the practical evaluation of the quadrature formula (3.38) extremely inefficient, basically because the computation of integrated Legendre functions (upon which the evaluation of $I\overline{Y}_{nm}(i, j)$ depends), cannot be accomplished using efficient recursions as those derived by Paul (1978). However, equation (3.38) is used here as an intermediate step to provide insight and aid in the derivation of the final expression for the sampling error. As it will be seen, the final formula for the sampling error does not require for its evaluation the actual implementation of (3.38). Due to (3.38) equation (3.37) becomes:

$$b_1(\delta, \lambda) = \frac{1}{2}\sum_{n=0}^{\infty} X_{kn}\hat{D}_n(\delta, \lambda) \tag{3.39}$$

where:

$$\hat{D}_n(\delta, \lambda) = \sum_{m=-n}^{n} \hat{D}_{nm} \overline{Y}_{nm}(\delta, \lambda) \quad . \tag{3.40}$$

Following the same procedure for $b_2(\delta, \lambda)$, and taking into account equation (3.31), one obtains for $b(\delta, \lambda)$:

$$b(\delta, \lambda) = \frac{1}{2} \sum_{n=0}^{\infty} [X_{kn} - Q_{kn}(\psi_o)] \hat{D}_n(\delta, \lambda) \quad . \tag{3.41}$$

Hence, due to (3.28), (3.30) and (3.41) the sampling error $\varepsilon_1(\delta, \lambda)$ finally becomes:

$$\varepsilon_1(\delta, \lambda) = \frac{1}{2} \sum_{n=0}^{\infty} [X_{kn} - Q_{kn}(\psi_o)] S_n(\delta, \lambda) \tag{3.42}$$

where:

$$S_n(\delta, \lambda) = D_n(\delta, \lambda) - \hat{D}_n(\delta, \lambda) = \sum_{m=-n}^{n} [D_{nn} - \hat{D}_{nm}] \overline{Y}_{nm}(\delta, \lambda) \tag{3.43}$$

and $S_n(\delta, \lambda)$ represents the n^{th} - degree surface harmonic of the sampling error associated with the quadrature formula (3.38).

Proceeding along similar lines, one has for the propagated error $\varepsilon_2(\delta, \lambda)$:

$$\varepsilon_2(\delta, \lambda) = \frac{1}{2} \sum_{n=0}^{\infty} [X_{kn} - Q_{kn}(\psi_o)] \sum_{m=-n}^{n} \overline{Y}_{nm}(\delta, \lambda) \left[\frac{1}{4\pi} \sum_{i=0}^{N-1} \sum_{j=0}^{2N-1} \varepsilon \overline{D}_{ij}^{c} \, I\overline{Y}_{nm}(i, j) \right] \quad . \tag{3.44}$$

One may view the true errors $\varepsilon \overline{D}_{ij}^{c}$ of the area-mean values as discrete samples of an error function defined over the full solid angle (unit sphere). To be more precise, the totality of the $\varepsilon \overline{D}_{ij}^{c}$ values represents one realization of a stochastic process on the unit sphere (Moritz, 1980, p. 279). This error function can be expanded in surface (ellipsoidal) harmonics, and the coefficients ε_{nm} of such expansion may be approximated by the following quadrature expression, given the discrete samples $\varepsilon \overline{D}_{ij}^{c}$:

$$\varepsilon_{nm} \approx \frac{1}{4\pi\beta_n} \sum_{i=0}^{N-1} \sum_{j=0}^{2N-1} \varepsilon \overline{D}_{ij}^{c} \, I\overline{Y}_{nm}(i, j) \tag{3.45}$$

where β_n is the Pellinen smoothing factor of degree n, which corresponds to a spherical cap having area equal to the area of an equiangular compartment in the ring with i = N/2 (the "equator" of the (ψ, α) grid). It is acknowledged here that the use of smoothing factors β_n which are independent of ψ (or equivalently of the ring index i) is only an approximation, since the area of the equiangular compartments on the (ψ, α) grid varies with ψ as it can be seen from Figure 9 (detailed discussion of this aspect is given in Katsambalos (1979)). Using a complete (N x 2N) set of area-mean gravity anomalies on an equiangular grid, it has been verified numerically that the spectrum implied by a quadrature formula of the type (3.45) (ring-independent β_n) differs from the spectrum implied by a quadrature formula using ring-dependent β_n factors, by about 15% near the degree corresponding to the Nyquist frequency (n = N). In view of the fact that the error properties assigned to the data are to a significant extent a matter of assumption, the approximation introduced in (3.45) by using ring-independent β_n factors appears to be acceptable. Accordingly, equation (3.44) becomes:

$$\varepsilon_2(\delta, \lambda) \approx \frac{1}{2} \sum_{n=0}^{\infty} \beta_n [X_{kn} - Q_{kn}(\psi_o)] \varepsilon_n(\delta, \lambda) \tag{3.46}$$

where:

$$\varepsilon_n(\delta, \lambda) = \sum_{m=-n}^{n} \varepsilon_{nm} \overline{Y}_{nm}(\delta, \lambda) \tag{3.47}$$

The formulation suggested here to model the sampling (or discretion) and the propagated errors is slightly different than the one originally proposed by Christodoulidis (1976) and adopted by Despotakis (1987). Christodoulidis (1976) examined alternative techniques to model the sampling error, and concluded that a computationally manageable and accurate enough model would be (in the current notation):

$$\varepsilon_1(\delta, \lambda) = \frac{1}{2} \sum_{n=N+1}^{\infty} [X_{kn} - Q_{kn}(\psi_o)] D_n(\delta, \lambda) \, . \tag{3.48}$$

(The fact that the analyses cited above were made for geoidal undulations obtained from integration of gravity anomalies is immaterial, since the four error sources identified in equation (3.27) are present in both integral formula applications.) The model (3.48) is based on the assumption that the data inside the cap of integration contain spectral

information only up to degree N, which is related to the size of the data compartment by the well known rule of thumb given in (3.21). This is one possible approximation; however, equation (3.48), rigorously interpreted, represents the sampling error for the case of continuous coverage inside the cap with band-limited data (containing spectral information only up to degree N). Such an approximation of the real-world situation (where continuous coverage can never be achieved, and the spectral content of the area-mean values is rather difficult to assess), is less realistic, and does not yield a significantly simpler model, than the model (3.42) proposed here.

As far as the propagated error is concerned, the Pellinen smoothing factors have been introduced here to account for the fact that area-mean values are used for the cap integration, while error covariance models in practice usually describe error properties of point data. Despotakis (1987, equation 2.26) altered the original formula for the propagated error as given by Christodoulidis (1976, equation 150), by truncating the error spectrum at degree N, effectively assuming that all error contribution above this degree is smoothed out from the area-mean values. In the model (3.46) proposed here, the error tapers off gradually as the degree n increases, since $\beta_n \to 0$ as $n \to \infty$.

According to the above, the expected global rms value of each error component can now be derived. The following definitions are introduced first for notational brevity:

$$\left.\begin{aligned} XQ_{kn} &= X_{kn} - Q_{kn}(\psi_o) \qquad \text{(a)} \\ WQ_{kn} &= W_{kn} + Q_{kn}(\psi_o) \qquad \text{(b)} \end{aligned}\right\} \tag{3.49}$$

where it is understood that both XQ_{kn} and WQ_{kn} depend on the semi-aperture ψ_o of the cap. Taking the total average $\bar{E}$ (Moritz, 1980, p. 100) of the square of each error component $\varepsilon_\ell (\ell = 1, 2, 3, 4)$, one has due to the orthogonality of the surface harmonics:

$$\text{rms}^2(\varepsilon_1) = \bar{E}\left[\varepsilon_1^2(\delta, \lambda)\right] = \frac{1}{4}\sum_{n=0}^{\infty} XQ_{kn}^2 s_n \tag{3.50a}$$

and similarly:

$$\left.\begin{aligned} \text{rms}^2(\varepsilon_2) &= \frac{1}{4}\sum_{n=0}^{\infty}(\beta_n XQ_{kn})^2\sigma_n \qquad \text{(b)} \\ \text{rms}^2(\varepsilon_3) &= \frac{1}{4}\sum_{n=0}^{M} WQ_{kn}^2 \varepsilon d_n \qquad \text{(c)} \\ \text{rms}^2(\varepsilon_4) &= \frac{1}{4}\sum_{n=M+1}^{\infty} WQ_{kn}^2 d_n \qquad \text{(d)} \end{aligned}\right\} \qquad (3.50)$$

where the linearity of the operator $\bar{E}$ was used, and the following notation was established:

$$\left.\begin{aligned} s_n &= \bar{E}\left[S_n^2(\delta,\lambda)\right] = M\left[S_n^2(\delta,\lambda)\right] \qquad \text{(a)} \\ \sigma_n &= \bar{E}\left[\varepsilon_n^2(\delta,\lambda)\right] \qquad \text{(b)} \\ \varepsilon d_n &= \bar{E}\left[\varepsilon D_n^2(\delta,\lambda)\right] \qquad \text{(c)} \\ d_n &= \bar{E}\left[D_n^2(\delta,\lambda)\right] = M\left[D_n^2(\delta,\lambda)\right] \qquad \text{(d)} \end{aligned}\right\} \qquad (3.51)$$

The homogeneous and isotropic space averaging operator M is defined by (Moritz, 1980, p. 82):

$$M(\circ) = \frac{1}{8\pi^2}\int_{\lambda=0}^{2\pi}\int_{\delta=0}^{\pi}\int_{\alpha=0}^{2\pi}(\circ)\sin\delta\, d\delta\, d\lambda\, d\alpha \qquad (3.52)$$

In addition, the total average of the products $\varepsilon_\ell(A).\varepsilon_\ell(B)$ (ℓ = 1, 2, 3, 4) of each error component for two points A and B separated by spherical distance ψ_d is given by (Christodoulidis, 1976):

$$\begin{aligned} \text{rms}^2[\varepsilon_1(A).\varepsilon_1(B)] &= \bar{E}[\varepsilon_1(\delta_A,\lambda_A).\varepsilon_1(\delta_B,\lambda_B)] \\ &= \frac{1}{4}\sum_{n=0}^{\infty} XQ_{kn}^2 s_n P_n(\cos\psi_d) \end{aligned} \qquad (3.53a)$$

and similarly:

$$\left.\begin{aligned} \mathrm{rms}^2[\varepsilon_2(A).\varepsilon_2(B)] &= \frac{1}{4}\sum_{n=0}^{\infty}(\beta_n X Q_{kn})^2 \sigma_n P_n(\cos\psi_d) \qquad (b)\\ \mathrm{rms}^2[\varepsilon_3(A).\varepsilon_3(B)] &= \frac{1}{4}\sum_{n=0}^{M} WQ_{kn}^2 \varepsilon d_n P_n(\cos\psi_d) \qquad (c)\\ \mathrm{rms}^2[\varepsilon_4(A).\varepsilon_4(B)] &= \frac{1}{4}\sum_{n=M+1}^{\infty} WQ_{kn}^2 d_n P_n(\cos\psi_d) \qquad (d) \end{aligned}\right\} \qquad (3.53)$$

Since the error components identified in (3.27) originate from independent causes, it is reasonable to assume that these errors are uncorrelated (it needs to be assumed here that the global geopotential model has been derived independently of the cap data). In such case, the expected global rms error of the geopotential estimated by (3.24), is given by:

$$\mathrm{rms}(\varepsilon\hat{T}) = \left[\sum_{\ell=1}^{4} \mathrm{rms}^2(\varepsilon_\ell)\right]^{1/2} \quad , \qquad (3.54)$$

while the expected global rms error of the geopotential difference $\varepsilon\hat{T}_{AB}$, between the points A, B separated by spherical distance ψ_d is given by (Christodoulidis, 1976, p. 43):

$$\mathrm{rms}(\varepsilon\hat{T}_{AB}) = \sqrt{2}\left\{\sum_{\ell=1}^{4} \mathrm{rms}^2[\varepsilon_\ell(A)] - \sum_{\ell=1}^{4} \mathrm{rms}^2[\varepsilon_\ell(A).\varepsilon_\ell(B)]\right\}^{1/2} \quad . \qquad (3.55)$$

The above formulation enables one to estimate the expected global rms errors in geopotential and geopotential differences, obtained from the estimator (3.24), once appropriate models have been established for the degree variances s_n, σ_n, εd_n and d_n.

As far as the selection of the kernel modification function is concerned, two alternative principles may be followed for the definition of $W_k(\psi)$:

(a) Deterministic approach: The selection of $W_k(\psi)$ here is made in such a way, that the resulting kernel function that corresponds to the remote zone contribution ("truncation

kernel" - see equation (3.19)), possesses eigenvalues which converge to zero more rapidly than those corresponding to the unmodified kernel $H(\psi)$ (Jekeli, 1980). In this manner, one attempts to reduce the error arising from the lack of detailed data outside the cap of integration, taking also advantage of the information provided by a global geopotential model. The increased convergence rate of the eigenvalues of the truncation kernel is accomplished analytically, by removing the discontinuity of this kernel (Meissl's method) or the discontinuities of the kernel and its derivatives (Molodenskii's method) at $\psi = \psi_o$, as discussed in detail by Jekeli (ibid). Such modifications are made without considering the error properties of the cap data or of the available geopotential model.

(b) Stochastic approach: The determination of $W_k(\psi)$ here is accomplished numerically, by imposing the condition that the resulting global rms error of $\hat{T}$ is minimum. Such condition yields a linear system of equations for the eigenvalues W_{kn} of the modification kernel. This approach has been put forward by Colombo (1977), who considered the minimization of the truncation error only, and was developed further by Sjöberg (1986) to account for all error sources identified in equation (3.27). The eigenvalues W_{kn} determined in this manner depend on the assumed error properties of both the cap data and the geopotential model.

Despotakis (1987) intercompared Stokes' kernel and its modifications according to Meissl's, Molodenskii's and Sjöberg's techniques, in a global rms error analysis fashion, as well as in actual geoidal undulation computations. His analysis indicated that in a global average sense and for cap sizes smaller than about 5°, the computationally simpler technique of Meissl is expected to be almost as accurate as the more demanding techniques of Molodensky and Sjöberg. In Despotakis' actual computations, Meissl's and Sjöberg's techniques yielded results of practically the same quality (ibid, p. 97, Table 28).

For the following analysis the original kernel of Hotine ($k = 1$) and its modification according to Meissl's suggestion ($k = 2$) will only be considered. For these cases one has:

Unmodified Hotine's kernel ($k = 1$)

$$W_1(\psi) \equiv 0 \; ; \; H_1(\psi) \equiv H(\psi) \qquad 0 \le \psi \le \pi \tag{3.56}$$

and the eigenvalues of the kernels $W_1(\psi)$, $H_1(\psi)$, and $\bar{H}_1(\psi)$ are given by:

$$\left.\begin{aligned} W_{1n} &= 0 && \text{(a)} \\ X_{1n} &= \frac{2}{n+1} && \text{(b)} \\ Q_{1n}(\psi_o) \equiv Q_n(\psi_o) &= \int_{\psi_o}^{\pi} H(\psi) P_n(\cos\psi) \sin\psi d\psi && \text{(c)} \end{aligned}\right\} \qquad (3.57)$$

for $n \geq 0$. The coefficients $Q_n(\psi_o)$ should not be confused with the corresponding Molodensky truncation coefficients referring to Stokes' kernel.

Meissl's modification ($k = 2$)

$$W_2(\psi) = H(\psi_o) \equiv H_o \; ; \; H_2(\psi) = H(\psi) - H_o \qquad 0 \leq \psi \leq \pi \qquad (3.58)$$

and the corresponding eigenvalues are:

$$W_{2n} = \int_o^{\pi} H_o P_n(\cos\psi) \sin\psi d\psi \quad \Rightarrow \quad W_{2n} = \begin{cases} 2H_o & \text{if } n = 0 \\ 0 & \text{if } n > 0 \end{cases} \qquad (3.59a)$$

$$X_{2n} = \begin{cases} \frac{2}{n+1} - 2H_o & \text{if } n = 0 \\ \frac{2}{n+1} & \text{if } n > 0 \end{cases} \qquad (3.59b)$$

$$Q_{2n}(\psi_o) = \int_o^{\pi} [H(\psi) - H_o] P_n(\cos\psi) \sin\psi d\psi = Q_n(\psi_o) - H_o \int_{\psi_o}^{\pi} P_n(\cos\psi) \sin\psi d\psi \; .$$

The last equation, due to the recurrence relations of the Legendre polynomials (see Appendix A, equation A.15), can easily be reduced to:

$$Q_{2n}(\psi_o) = Q_n(\psi_o) - \begin{cases} H_o(1 + \cos\psi_o) & \text{if } n = 0 \\ \frac{H_o}{2n+1} \left[P_{n+1}(\cos\psi_o) - P_{n-1}(\cos\psi_o) \right] & \text{if } n > 0 \end{cases} \; . \qquad (3.59c)$$

The above expressions for W_{2n}, X_{2n}, and $Q_{2n}(\psi_o)$ are strictly valid for $0 < \psi_o \leq \pi$, due to the singularity of Hotine's kernel at $\psi = 0$. The case $\psi_o = 0$ implies that no cap data are used in the determination of T, hence only the commission and omission error of the geopotential model contribute to the error of $\hat{T}$. In such case the sum of the eigenvalues W_{kn} plus $Q_{kn}(\psi_o)$ (which appear in equations 3.27c and 3.27d), always equals $2/(n + 1)$, regardless of the selection of the kernel modification $W_k(\psi)$.

From the numerical point of view, it is obvious from the previous formulation, that only the evaluation of $Q_n(\psi_o)$ is a computationally complicated process. Jekeli (1979) developed an efficient recurrence relation for the evaluation of $Q_n(\psi_o)$ ($\psi_o \neq 0$). His technique was expanded in this study and a similar recurrence relation was developed for the more general case of Pizzetti's extension of Hotine's kernel, i.e. for the kernel $H(R/r, \psi)$ where $r \geq R$. The detailed derivation of the recurrence relation for the truncation coefficients $Q_n(R/r, \psi_o)$, corresponding to this kernel, is given in Appendix A. In case one postulates the absence of the zeroeth- and first-degree harmonics from the gravity disturbance, the kernel $H(R/r, \psi)$ requires corresponding modification (Jekeli, ibid), and the resulting kernel $H^*(R/r, \psi)$ (i.e., $H(R/r, \psi)$ less its zeroeth- and first-degree harmonics), implies a different set of truncation coefficients $Q_n^*(R/r, \psi_o)$. The derivation of a recurrence relation for $Q_n^*(R/r, \psi_o)$ is given in Appendix B.

The zeroeth-degree coefficients $Q_{ko}(\psi_i)$, $i = 0, 1, 2, ..., N_r$ provide an efficient way for the evaluation of the discretized integral over the cap, as long as the cap measurements are defined on the (ψ, α) grid. Denoting the cap contribution to the disturbing potential by $Cap(\psi_o)$, so that (see equation 3.24):

$$Cap(\psi_o) = \frac{1}{4\pi} \sum_{i=o}^{Nr-1} \sum_{j=o}^{2N-1} \overline{D}_{ij}^{c} \iint_{\sigma_{ij}} H_k(\psi) d\sigma \quad , \tag{3.60}$$

one can easily see that due to (3.12):

$$\iint_{\sigma_{ij}} H_k(\psi) d\sigma = \Delta\alpha [Q_{ko}(\psi_i) - Q_{ko}(\psi_{i+1})] \tag{3.61}$$

so that (with obvious notation for Q_{ko}):

$$\mathrm{Cap}(\psi_o) = \sum_{i=o}^{Nr-1} \frac{1}{2}[Q_{ko}(i) - Q_{ko}(i+1)]\left[\frac{1}{2\pi}\sum_{j=o}^{2N-1} \Delta\alpha \bar{D}_{ij}^{c}\right] \quad . \tag{3.62}$$

Denote:

$$\left.\begin{aligned} \bar{D}_i^c &= \frac{1}{2\pi}\sum_{j=o}^{2N-1} \Delta\alpha \bar{D}_{ij}^{c} = \frac{1}{2N}\sum_{j=o}^{2N-1} \bar{D}_{ij}^{c} \qquad (a) \\ \Delta Q_{ko}(i) &= \frac{1}{2}[Q_{ko}(i) - Q_{ko}(i+1)] \qquad (b) \end{aligned}\right\} \tag{3.63}$$

so that $\bar{D}_i^c$ represents the ring-average "observation" of the i-th ring, and $\Delta Q_{ko}(i)$ the semi-difference of the two values of Q_{ko} at the spherical distances ψ_i and ψ_{i+1} bordering the i-th ring. Accordingly, the cap contribution $\mathrm{Cap}(\psi_o)$ is given by:

$$\mathrm{Cap}(\psi_o) = \sum_{i=o}^{Nr-1} \Delta Q_{ko}(i)\bar{D}_i^c \tag{3.64}$$

and this equation demonstrates the fact that the cap contribution to the disturbing potential is the weighted sum of the ring-average "observations" $\bar{D}_i^c$, with weights the quantities $\Delta Q_{ko}(i)$. Equation (3.64) represents a rigorous evaluation of (3.60), and is a consequence of the isotropy of the kernel $H_k(\psi)$ (no dependence on azimuth) and of the particular selection of the data grid (ψ, α). The form of equation (3.64) is valid even if the "width" of the rings (i.e. $\psi_{i+1} - \psi_i$) and/or the number of compartments per ring (i.e. $\Delta\alpha$) vary with the distance ψ from the computation point, as described in Heiskanen and Moritz (1967, p. 120), provided of course that $\bar{D}_i^c$ and $\Delta Q_{ko}(i)$ are evaluated accordingly. As it is well known (ibid, p. 120) the disadvantage of using the (ψ, α) grid to register the data, is the need to re-evaluate $\bar{D}_{ij}^c$ (or $\bar{D}_i^c$) as one moves from one computation point to another. The alternative of course, is to register the data with respect to the (δ, λ) grid (ibid, p. 117), but then the integration of the kernel function over the data compartment has to be performed numerically. Provided the original point measurements are available (so that one can decide upon which grid to use to register the mean values) and if the computation points are few in number and randomly distributed, the (ψ, α) grid is inherently better suited for cap integration.

3.2 Error Assessment for the Over-Determined Boundary Value Problem

The formulation given in the previous section for the error estimation of the disturbing potential (or the disturbing potential difference), obtained from cap integration of gravity disturbances and a global geopotential model, is applicable only in case the computation points lie on or outside the sphere to which the gravity disturbance data refer. This is due to the fact that Hotine's integral formula (upon which the entire derivation was based) is the solution of Neumann's boundary value problem for the exterior space of a sphere. The estimation of the error of disturbing potential on the Earth's surface, obtained from gravity disturbance measurements at altitude requires alternative treatment. In addition, if observations at altitude are to be used in combination with terrestrial measurements, then the boundary value problem in question becomes over-determined, as opposed to the uniquely-determined Neumann's problem solved by Hotine's integral. The statement of such a problem, for the case where the known boundary surfaces are concentric spheres may be given as follows (see also Figure 10 for notation definitions):

"Determine a function T, harmonic in the infinite region outside the sphere (O, R_T) and regular at infinity, if its normal (radial) derivatives $(-\partial T/\partial r)$ obtain prescribed values on the two concentric spheres (O, R_T) and (O, R_S) where $R_S = R_T + h$ and $h > 0$."

Since the boundary values on (O, R_T) alone, are sufficient to determine T outside (O, R_T) uniquely (through the solution of Neumann's problem), and since the same holds true for the boundary values on (O, R_S) and the space outside (O, R_S), existence of a unique solution to the over-determined problem requires a compatibility condition to be fulfilled between the two sets of boundary data. This condition can easily be obtained from the following considerations. Let D_T^c and D_S^c denote the boundary data on the spheres (O,R_T) and (O,R_S) respectively. Let also $P(R_S, \theta, \lambda)$ be an arbitrary point on the surface of the sphere (O,R_S). Then, due to equation (2.67) one has:

$$T_P = \frac{R_S}{4\pi} \iint H(\psi)\, D_S^c(\theta', \lambda')\, d\sigma \qquad (3.65)$$

while due to equation (2.64):

$$T_P = \frac{R_T}{4\pi} \iint H\left(\frac{R_T}{R_S}, \psi\right) D_T^c(\theta', \lambda') d\sigma \quad . \tag{3.66}$$

Hence, for a unique value of T_P to exist, D_T^c and D_S^c should fulfil the compatibility condition:

$$\iint \left[H\left(\frac{R_T}{R_S}, \psi\right) R_T D_T^c(\theta', \lambda') - H(\psi)\, R_S D_S^c(\theta', \lambda') \right] d\sigma = 0 \tag{3.67}$$

for <u>every</u> point $P(R_S, \theta, \lambda)$ on the sphere (O, R_S). In that case, due to Stokes' theorem (Heiskanen and Moritz, 1967, pp. 17-18), T is also uniquely determined outside the surface of the sphere (O, R_S). Due to the relation (2.73) between the radial derivative of Hotine's kernel and the kernel of Poisson, the condition (3.67) may also be replaced by the equivalent set of conditions:

$$\left.\begin{aligned} R_S D_S^c(R_S, \theta, \lambda) &= \frac{R_T (R_S^2 - R_T^2)}{4\pi} \iint_\sigma \frac{R_T D_T^c(\theta', \lambda')}{\ell_{PQ}^3} d\sigma \qquad \text{(a)} \\ R_S^2 \frac{1}{4\pi} \iint_\sigma D_S^c(\theta', \lambda') d\sigma &= R_T^2 \frac{1}{4\pi} \iint_\sigma D_T^c(\theta', \lambda') d\sigma \qquad \text{(b)} \end{aligned}\right\} \tag{3.68}$$

Note that (3.68a) by itself is equivalent to a condition similar to (3.67), but with its right-hand side equal to a constant. Condition (3.68b) enforces such constant to be zero. The condition (3.67) (or equivalently the set of conditions (3.68a, b)) would have been fulfilled as an identity, if the measurements D_T^c and D_S^c were free of errors. In the presence of observational noise however, to enforce a unique solution to the over-determined bvp, one could use either (3.67) or (3.68a, b) and set up a least-squares adjustment of the form $F(L_a) = 0$ (condition equations), for D_T^c and D_S^c. The result of this adjustment would be a set of $\hat{D}_T$ and $\hat{D}_S$ which would fulfil the compatibility condition

and would be accompanied by a-posteriori estimates of their error properties. The a-posteriori errors of $\hat{D}_T$ could then be used in the truncation theory formulation of the previous section, to estimate the error of geopotential (T) or geopotential difference (ΔT). In this manner the additional information provided by the measurements at altitude, for the estimation of T or ΔT on the Earth's surface, can be taken into account. However, the above procedure requires the measurements $\hat{D}_T$ and $\hat{D}_S$ to provide global coverage, so that (a discretized form of) (3.67) or (3.68) can be used to set up the condition equations. The problem at hand however, is of local nature. Terrestrial measurements are given in the caps centered at the computation points A and B, while the measurements at altitude are given in the caps centered at S_A and S_B as illustrated in Figure 10.

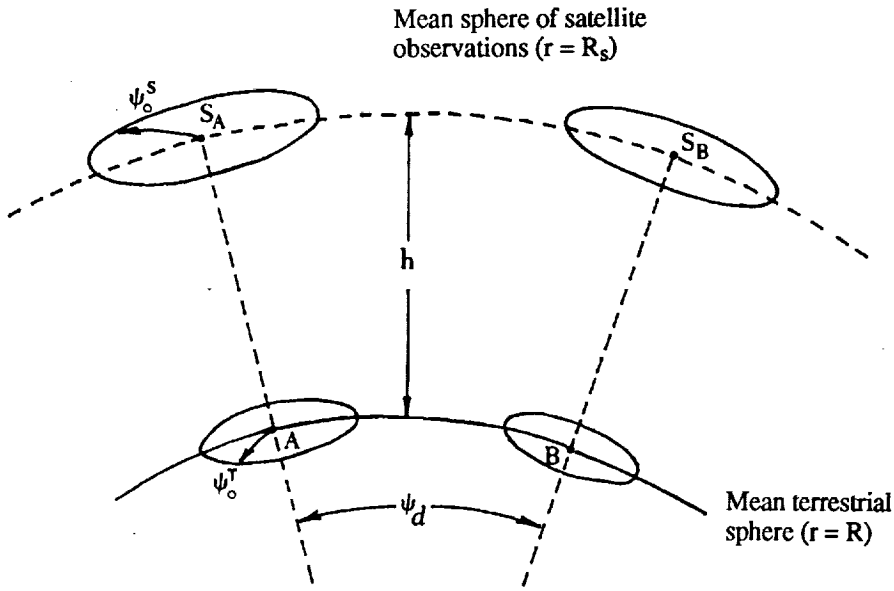

Figure 10. Geometry of the Measurement and Estimation Points.

One way to circumvent the inability to use integral formulas for downward continuation, is to perform the error analysis in two steps:

(a) Using the altitude generalized truncation coefficients derived in Appendix A, one can estimate the error $\varepsilon\Delta T^{T}_{S_A S_B}$ of $\Delta T_{S_A S_B}$ when the latter is estimated from terrestrial measurements via upward continuation (Pizzetti's extension of Hotine's integral). This error may then be compared to the corresponding error $\varepsilon\Delta T^{S}_{S_A S_B}$ obtained when $\Delta T_{S_A S_B}$ is estimated from the measurements at altitude.

(b) Significant contribution of the observations at altitude to the accuracy of ΔT_{AB} is provided when $\varepsilon\Delta T^{T}_{S_A S_B} > \varepsilon\Delta T^{S}_{S_A S_B}$. To quantify this contribution one may use least-squares collocation where the signal to be predicted is ΔT_{AB} and the two independent input signals are: $\Delta T_{S_A S_B}$ obtained from data at altitude and ΔT_{AB} obtained from terrestrial measurements, each input signal accompanied by the corresponding error as obtained from truncation theory.

Obviously the motivation for using the above procedure is to take advantage of the simplicity of error propagation through truncation theory on one hand, and of the "built-in" ability of least-squares collocation to perform the downward continuation (Moritz, 1980, p. 97) on the other. However, as it will be shown next, these properties may be exploited in a more efficient way, if least-squares collocation with "ring-averages" is used for the error analysis. In such case all measurements are used simultaneously in the error analysis and the error estimate $\varepsilon\Delta T_{AB}$ is obtained in one step.

3.3 Least-Squares Collocation Using Ring Averages

Consider the observations in the caps centered at A, S_A (see Figure 10) arranged in the vector $\underline{d}_A$ and similarly those in the caps centered at B, S_B in the vector $\underline{d}_B$. These observations consist of a signal part denoted z and a noise part denoted n, so that (Colombo, 1980):

$$\left.\begin{aligned} \underline{d}_A &= \underline{z}_A + \underline{n}_A \quad (a) \\ \underline{d}_B &= \underline{z}_B + \underline{n}_B \quad (b) \end{aligned}\right\} \qquad (3.69)$$

The signal to be estimated from the data $\underline{d}_A$ and $\underline{d}_B$ is the geopotential difference ΔT_{AB}. A linear estimate of this signal has the general form:

$$\Delta\hat{T}_{AB} = \underline{f}^T\underline{d} \tag{3.70}$$

where:

$$\underline{d} = \begin{bmatrix} \underline{d}_A \\ \cdots \\ \underline{d}_B \end{bmatrix} \tag{3.71}$$

and the estimator $\underline{f}$ can always be considered as composed of two parts:

$$\underline{f} = \begin{bmatrix} -\underline{f}_A \\ \cdots \\ \underline{f}_B \end{bmatrix} . \tag{3.72}$$

Hence, the estimate $\Delta\hat{T}_{AB}$ becomes:

$$\Delta\hat{T}_{AB} = \underline{f}_B^T\underline{d}_B - \underline{f}_A^T\underline{d}_A \tag{3.73}$$

and its error is given by:

$$\varepsilon\Delta\hat{T}_{AB} = (T_B - T_A) - \left(\underline{f}_B^T\underline{d}_B - \underline{f}_A^T\underline{d}_A\right) . \tag{3.74}$$

Applying the total averaging operator $\bar{E}$ (Moritz, 1980, p. 100) to the square of the estimation error one has:

$$\bar{E}\left[(\varepsilon\Delta\hat{T}_{AB})^2\right] = \bar{E}\left[(T_B - T_A)^2 + \underline{f}_B^T\underline{d}_B\underline{d}_B^T\underline{f}_B + \underline{f}_A^T\underline{d}_A\underline{d}_A^T\underline{f}_A - 2(T_B - T_A)\underline{d}_B^T\underline{f}_B \right.$$
$$\left. + 2(T_B - T_A)\,\underline{d}_A^T\underline{f}_A - 2\underline{f}_A^T\underline{d}_A\,\underline{d}_B^T\underline{f}_B\right] . \tag{3.75}$$

Assuming no correlation between signals and noise, i.e.

$$\bar{E}(T\underline{n}^T) = \bar{E}(\underline{z}\,\underline{n}^T) = 0 \tag{3.76}$$

and denoting:

$$\left.\begin{aligned} M(TT) &= C_{TT} \quad (a)\\ M(T\underline{z}^T) &= C_{Tz} \quad (b)\\ M(\underline{z}\underline{z}^T) &= C_{zz} \quad (c)\\ \bar{E}(\underline{n}\,\underline{n}^T) &= D \quad (d) \end{aligned}\right\} \tag{3.77}$$

one has from equation (3.75):

$$\begin{aligned} \bar{E}\left[(\varepsilon\Delta\hat{T}_{AB})^2\right] = {} & 2C_{TT}(A, A) - 2C_{TT}(A, B) + \underline{f}_B^T[C_{zz}(B, B) + D(B, B)]\underline{f}_B \\ & + \underline{f}_A^T[C_{zz}(A, A) + D(A, A)]\underline{f}_A - 2[C_{Tz}(B, B) - C_{Tz}(A, B)]\underline{f}_B \\ & + 2[C_{Tz}(B, A) - C_{Tz}(A, A)]\underline{f}_A - 2\underline{f}_A^T[C_{zz}(A, B) + D(A, B)]\underline{f}_B \end{aligned} \tag{3.78}$$

From all possible choices of linear estimators $\underline{f}$ one seeks now such an $\underline{f}$ that minimizes $\bar{E}\left[(\varepsilon\Delta\hat{T}_{AB})^2\right]$. Imposing the conditions:

$$\frac{1}{2}\frac{\partial}{\partial\underline{f}_A}\bar{E}\left[(\varepsilon\Delta\hat{T}_{AB})^2\right] = \frac{1}{2}\frac{\partial}{\partial\underline{f}_B}\bar{E}\left[(\varepsilon\Delta\hat{T}_{AB})^2\right] = 0 \tag{3.79}$$

one arrives, due to (3.78), to the following linear system of equations in $\underline{f}_A$ and $\underline{f}_B$:

$$\left.\begin{aligned} \underline{f}_A^T[C_{zz}(A, A) + D(A, A)] - \underline{f}_B^T[C_{zz}(A, B) + D(A, B)] + C_{Tz}(B, A) - C_{Tz}(A, A) = 0 \\ -\underline{f}_A^T[C_{zz}(A, B) + D(A, B)] + \underline{f}_B^T[C_{zz}(B, B) + D(B, B)] - C_{Tz}(B, B) + C_{Tz}(A, B) = 0 \end{aligned}\right\} \tag{3.80}$$

The following assumptions are now made: the observations $\underline{d}_A$ and $\underline{d}_B$ have the same configuration and are characterized by the same error properties. In addition, no correlation exists between the noise $\underline{n}_A$ and $\underline{n}_B$. If one seeks an estimate of ΔT_{AB} which should not be significantly biased towards either endpoint of the baseline AB, it is reasonable to require that at both endpoints A and B, the available measurements have similar configuration and error properties. Hence, the above assumptions are not unrealistic from the practical point of view. Under these assumptions one has:

$$\left.\begin{aligned} C_{zz}(A, A) &= C_{zz}(B, B) && \text{(a)}\\ C_{Tz}(A, A) &= C_{Tz}(B, B) && \text{(b)}\\ C_{Tz}(A, B) &= C_{Tz}(B, A) && \text{(c)}\\ D(A, A) &= D(B, B) && \text{(d)}\\ D(A, B) &= 0 && \text{(e)} \end{aligned}\right\} \qquad (3.81)$$

and the solution of the system (3.80) can easily be found to be:

$$\underline{f}_A = \underline{f}_B \qquad (3.82)$$

$$\underline{f}_A = [C_{zz}(A, A) - C_{zz}(A, B) + D(A, A)]^{-1}[C_{Tz}^T(A, A) - C_{Tz}^T(A, B)] \quad . \qquad (3.83)$$

Substituting (3.81) - (3.83) in (3.78) one finds that under the previous assumptions the global mean square error of $\Delta\hat{T}_{AB}$ is given by:

$$\overline{E}\left[(\varepsilon\Delta\hat{T}_{AB})^2\right] = 2\left[C_{TT}(A, A) - C_{TT}(A, B) - U^T\overline{C}^{-1}U\right] \qquad (3.84)$$

where the vector U and the matrix $\overline{C}$ are given by:

$$\left.\begin{aligned} U &= C_{Tz}^T(A, A) - C_{Tz}^T(A, B) && \text{(a)}\\ \overline{C} &= C_{zz}(A, A) - C_{zz}(A, B) + D(A, A) && \text{(b)} \end{aligned}\right\} \quad . \qquad (3.85)$$

Although the symmetry assumptions (3.81) significantly simplify the computation of the global mean square error of $\Delta\hat{T}_{AB}$, the formation of the covariance matrix $\overline{C}$ in (3.85b) requires computational effort proportional to the square of its dimension which is equal to the number of observations. The formation of $\overline{C}$, as well as its inversion, can be a very demanding computational process. On the other hand, as it was shown in section 3.1, the isotropy of Hotine's kernel in conjunction with the suitable selection of the (ψ, α) grid to register the cap data, resulted in very efficient formulas for the computation of $\Delta\hat{T}_{AB}$ as well as its error, in the case of the uniquely determined bvp and the integral formula approach. In that case, as it was shown in equation (3.64), the cap contribution to $\Delta\hat{T}_{AB}$ was given as a weighted sum of ring-average "observations". It is thus appropriate to consider the simplifications of equations (3.85a, b) if instead of the

original measurements, ring-averages are to be used in the least-squares collocation estimator. Obviously, in such case the number of "measurements" reduces drastically and this brings significant savings in the formation of the covariance matrices (Colombo, 1980). To follow this approach the analytical expressions for the covariances between ring-average "measurements" have to be developed first. This is done next.

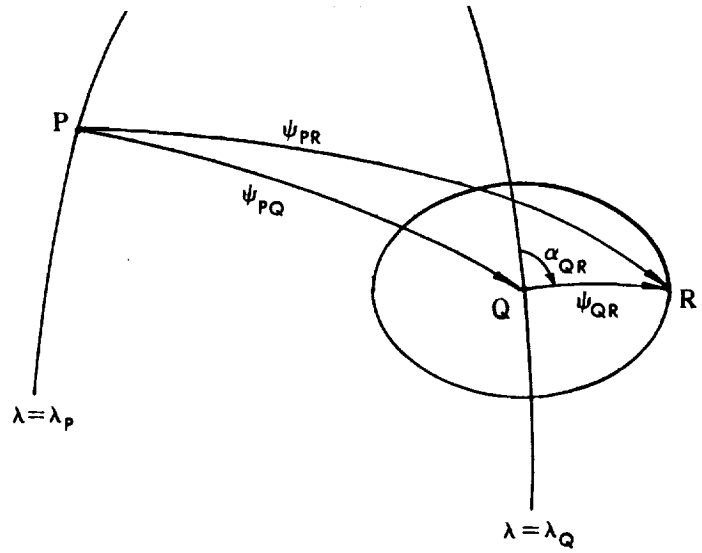

Figure 11. Geometry Associated with Ring-Averages.

Let t and s be two gravimetric quantities. The homogeneous and isotropic covariance between t and s (both considered as point values) may be expressed as:

$$\mathrm{cov}(t_P, s_R) = M(t_P s_R) = \sum_{n=0}^{\infty} \sigma_{ts}(n) P_n(\cos\psi_{PR}) \tag{3.86}$$

where the averaging operator M was defined in (3.52) and $\sigma_{ts}(n)$ (n = 0,1,2...) is the power cross-spectrum of t and s (i.e., $\sigma_{ts}(n)$ is the global average under M of the products of the surface harmonics $t_n(\delta, \lambda)$ times $s_n(\delta, \lambda)$). The ring-average of the quantity s is defined as (Jekeli, 1989):

$$\bar{s}(\psi_{QR}) = \frac{1}{2\pi} \int_{\alpha_{QR}=0}^{2\pi} s(\psi_{QR}, \alpha_{QR}) d\alpha_{QR} \tag{3.87}$$

where the notation can be read from Figure 11. The covariance between the point value t_P and the ring-average value $\bar{s}(\psi_{QR})$ is given by:

$$\begin{aligned} \mathrm{cov}[t_P, \bar{s}(\psi_{QR})] &= M\left[t_P \frac{1}{2\pi} \int_0^{2\pi} s(\psi_{QR}, \alpha_{QR})\, d\alpha_{QR} \right] \\ &= \frac{1}{2\pi} \int_0^{2\pi} M[t_P s(\psi_{QR}, \alpha_{QR})]\, d\alpha_{QR} \end{aligned} \qquad (3.88)$$

Thus the required covariance is the average over the azimuth α_{QR} of the covariance between t_P and s_R, where the point R now moves on a circle of semi-aperature ψ_{QR}, centered at Q. Substituting (3.86) in (3.88) one has:

$$\mathrm{cov}[t_P, \bar{s}(\psi_{QR})] = \frac{1}{2\pi} \left[\sum_{n=0}^{\infty} \sigma_{ts}(n) \int_0^{2\pi} P_n(\cos\psi_{PR})\, d\alpha_{QR} \right] \qquad (3.89)$$

where ψ_{PR} depends on ψ_{PQ}, ψ_{QR} and α_{QP} (which are constant), as well as on the variable azimuth α_{QR}. From the decomposition formula (Heiskanen and Moritz, 1967, equation 1-82) one has:

$$\begin{aligned} P_n(\cos\psi_{PR}) = P_n(\cos\psi_{QP}) P_n(\cos\psi_{QR}) + \\ + 2 \sum_{m=1}^{n} \frac{(n-m)!}{(n+m)!} [R_{nm}(\psi_{QP}, \alpha_{QP}) R_{nm}(\psi_{QR}, \alpha_{QR}) + \\ + S_{nm}(\psi_{QP}, \alpha_{QP}) S_{nm}(\psi_{QR}, \alpha_{QR})] \end{aligned} \qquad (3.90)$$

where R_{nm} and S_{nm} are defined in (ibid, equation 1-67). The integral in (3.89) can be written as:

$$\int_0^{2\pi} P_n(\cos\psi_{PR}) \cos(0.\alpha_{QR})\, d\alpha_{QR} \qquad (3.91)$$

so that upon replacing in (3.91) the expression (3.90) for $P_n(\cos\psi_{PR})$, due to the orthogonality of sines and cosines in the interval $[0, 2\pi]$, one has:

$$\int_0^{2\pi} P_n(\cos\psi_{PR})\, d\alpha_{QR} = 2\pi\, P_n(\cos\psi_{PQ})\, P_n(\cos\psi_{QR}) \tag{3.92}$$

and (3.89) finally becomes:

$$\mathrm{cov}[t_P, \bar{s}(\psi_{QR})] = \sum_{n=0}^{\infty} \sigma_{ts}(n) P_n(\cos\psi_{QR}) P_n(\cos\psi_{PQ}) \quad . \tag{3.93}$$

Following similar lines, the covariance between two ring-average values $\bar{t}(\psi_{PV})$ (where ψ_{PV} is the semi-aperture of a ring centered at P) and $\bar{s}(\psi_{QR})$ can easily be found to be:

$$\mathrm{cov}\left[\bar{t}(\psi_{PV}), \bar{s}(\psi_{QR})\right] = \sum_{n=0}^{\infty} \sigma_{ts}(n) P_n(\cos\psi_{PV}) P_n(\cos\psi_{QR}) P_n(\cos\psi_{PQ}) \quad . \tag{3.94}$$

The general expressions (3.93) and (3.94) can now be specialized for the current application. If d_n denotes the degree variance of the point value of gravity disturbance (more precisely of $-\partial T/\partial r$), referring to the surface of a sphere of radius R = 6371 km and $\overline{\delta g}$ denotes ring-average value of gravity disturbance, then (see also section 3.4):

$$\left.\begin{aligned}
C_{T,T}(P, Q) &= \sum_{n=2}^{\infty} \left(\frac{R}{n+1}\right)^2 d_n \left(\frac{R^2}{r_P r_Q}\right)^{n+1} P_n(\cos\psi_{PQ}) \qquad \text{(a)} \\
C_{T,\bar{\delta}_g}(P, QR) &= \sum_{n=2}^{\infty} \left(\frac{r_P}{n+1}\right) d_n \left(\frac{R^2}{r_P r_Q}\right)^{n+2} P_n(\cos\psi_{QR}) P_n(\cos\psi_{PQ}) \qquad \text{(b)} \\
C_{\bar{\delta}_g,\bar{\delta}_g}(PV, QR) &= \sum_{n=2}^{\infty} d_n \left(\frac{R^2}{r_P r_Q}\right)^{n+2} P_n(\cos\psi_{PV}) P_n(\cos\psi_{QR}) P_n(\cos\psi_{PQ}) \qquad \text{(c)}
\end{aligned}\right\} \quad . \tag{3.95}$$

Note that the summations in (3.95) start from n = 2, i.e., it is assumed that the disturbing potential does not include zeroeth- and first-degree harmonics.

It should be emphasized here that equations (3.93) through (3.95) refer to rings formed by point measurements and not to zones of area-mean values in equiangular compartments as it was the case in equation (3.64). The case of zone rings is

considerably more complicated, because it requires the use of covariances between area-mean values as discussed by Colombo (1981a, section 4). For the small size compartments (e.g., $\Delta\psi = 2'$) that will be considered in the next chapter, the difference between the case of rings formed by point measurements and zone rings will be neglected.

Based on the above formulation, it is now possible to examine the particular form that the covariance matrices in (3.85) take, in case ring-average values are used for the estimation of ΔT_{AB}. The following notation is introduced:

ψ_o^T: semi-aperture of terrestrial cap

ψ_o^S: semi-aperture of cap at altitude

$\Delta\psi^T$: spacing between rings in the terrestrial caps

$\Delta\psi^S$: spacing between rings in the caps at altitude

$\psi_d = \psi_{AB}$: angular separation between stations A and B

R(= 6371 km): mean-Earth radius

h: average altitude of satellite observations

$R_S = R + h$: radius of average sphere where satellite observations refer.

According to the above, the number of rings in each terrestrial cap is:

$$N_r^T = \frac{\psi_o^T}{\Delta\psi^T} + 1 \tag{3.96}$$

and similarly in each cap at altitude:

$$N_r^S = \frac{\psi_o^S}{\Delta\psi^S} + 1 \tag{3.97}$$

so that the total number of rings at each site (A or B) is:

$$N_r = N_r^T + N_r^S \tag{3.98}$$

Accordingly, the square symmetric matrix:

$$C = C_{zz}(A, A) - C_{zz}(A, B) \tag{3.99}$$

appearing in (3.85b), can be arranged as shown in Figure 12, after the observations on the Earth and at altitude are collected in two separate groups.

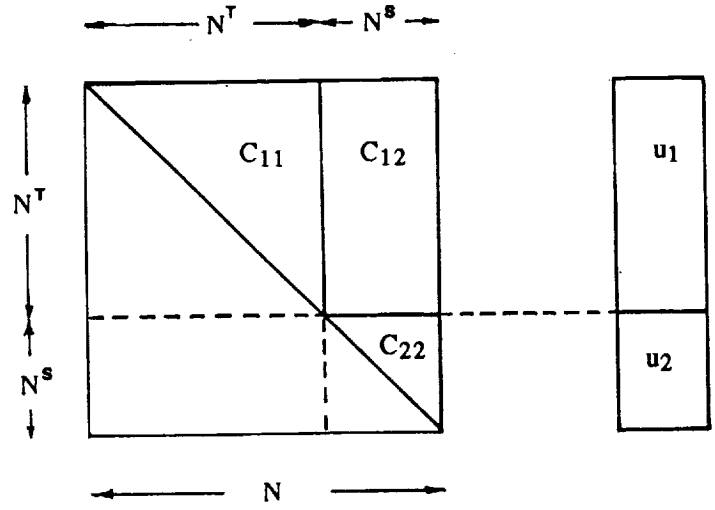

Figure 12. Structure of Covariance Matrix $C = C_{zz}(A, A) - C_{zz}(A, B)$, and Vector U of Equation (3.85).

Abbreviating by $P_n(i)$ the Legendre polynomial $P_n(\cos\psi_i)$, where ψ_i is the spherical distance from a cap center to the i-th ring around it, one can easily see that due to the equation (3.95c), the elements of C are given by:

$$\left.\begin{aligned} C_{11}(i, j) &= \sum_{n=2}^{\infty} d_n P_n(i) P_n(j)[1 - P_n(\psi_d)] \qquad (a)\\ C_{12}(i, j) &= \sum_{n=2}^{\infty} d_n \left(\frac{R}{R_S}\right)^{n+2} P_n(i) P_n(j)[1 - P_n(\psi_d)] \qquad (b)\\ C_{22}(i, j) &= \sum_{n=2}^{\infty} d_n \left(\frac{R^2}{R_S^2}\right)^{n+2} P_n(i) P_n(j)[1 - P_n(\psi_d)] \qquad (c) \end{aligned}\right\} \tag{3.100}$$

while, due to (3.95b), the elements of vector U are given by:

$$\left.\begin{aligned} u_1(i) &= \sum_{n=2}^{\infty} \frac{R}{n+1} d_n P_n(i)[1 - P_n(\psi_d)] \qquad \text{(a)} \\ u_2(i) &= \sum_{n=2}^{\infty} \frac{R}{n+1} d_n \left(\frac{R}{R_S}\right)^{n+2} P_n(i)[1 - P_n(\psi_d)] \qquad \text{(b)} \end{aligned}\right\} \quad . \tag{3.101}$$

Obviously in equations (3.100) and (3.101), $P_n(\psi_d)$, is used to abbreviate $P_n(\cos\psi_d)$. In addition ψ_i is given by:

$$\psi_i = \begin{cases} (i-1)\Delta\psi^T & \text{(terrestrial data)} \\ (i-1)\Delta\psi^S & \text{(data at altitude)} \end{cases} \quad . \tag{3.102}$$

Finally, the a-priori error variance of the difference ΔT_{AB} (i.e., the error variance before the introduction of the measurements), is twice the quantity:

$$C_{TT}(A, A) - C_{TT}(A, B) = \sum_{n=2}^{\infty} \left(\frac{R}{n+1}\right)^2 d_n[1 - P_n(\psi_d)] \quad , \tag{3.103}$$

as it can be easily deduced from (3.95a).

The last matrix which needs to be defined so that equation (3.84) can be evaluated, is the noise covariance matrix D(A, A) appearing in (3.85b). Assuming no correlation between the errors of the terrestrial data and the data at altitude, matrix D(A, A) will be block diagonal with one block having dimension N_r^T while the other N_r^S. If σ_n^T and σ_n^S are the degree variances of the error of a point gravity disturbance measurement on the Earth's surface and at altitude respectively, then the element d(i,j) of D(A, A) representing the error correlation between the i-th and j-th ring-average value is given by:

$$d(i, j) = \sum_{n=2}^{\infty} P_n(i)P_n(j) \begin{cases} \sigma_n^T & \text{(terrestrial data)} \\ \sigma_n^S & \text{(data at altitude)} \end{cases} \quad . \tag{3.104}$$

The above formulation for lsc using ring-averages treats the general case where observations on the surface of the Earth and at altitude are used simultaneously for the estimation of ΔT_{AB}. The problem of estimating ΔT_{AB} from either group of data alone, can easily be treated by forming only the pertinent part of the matrices and vectors previously defined.

3.4 Covariance Models for Signal and Noise

The implementation of the formulation given in sections 3.1 and 3.3, for the estimation of the global mean square error of the disturbing potential differences, requires appropriate covariance models to be established that describe, in a global average sense, the properties of the gravitational signal and the noise contained in the measurements. The various covariance models considered for this purpose are discussed next.

3.4.1 Global Covariance Models for the Gravity Anomaly

It is well known (Moritz, 1972) that a global covariance model for the gravity anomaly carries equivalent information with a corresponding model for the disturbing potential. Hence, covariance models for the gravity anomaly will be considered next, and the analytical relations will be given to derive the corresponding models for the disturbing potential or other linear functionals of it (e.g. the gravity disturbance). The spherical harmonic expansion of the disturbing potential is written as:

$$T(r, \theta, \lambda) = \frac{GM}{r} \sum_{n=2}^{\infty} \left(\frac{a}{r}\right)^n \sum_{m=-n}^{n} \overline{C}_{nm} \overline{Y}_{nm}(\theta, \lambda) \tag{3.105}$$

where the notation is consistent with that used in equation (2.52). In an equivalent form (3.105) may be written as:

$$T(r, \theta, \lambda) = \frac{GM}{a} \sum_{n=2}^{\infty} \left(\frac{a}{r}\right)^{n+1} \sum_{m=-n}^{n} \overline{C}_{nm} \overline{Y}_{nm}(\theta, \lambda) \quad . \tag{3.106}$$

Consistent with the form (3.106), the spherical harmonic expansion of the gravity anomaly is:

$$\Delta g(r, \theta, \lambda) = \frac{GM}{a^2} \sum_{n=2}^{\infty} (n - 1) \left(\frac{a}{r}\right)^{n+2} \sum_{m=-n}^{n} \overline{C}_{nm} \overline{Y}_{nm}(\theta, \lambda) \tag{3.107}$$

and of the gravity disturbance:

$$\delta g(r, \theta, \lambda) = \frac{GM}{a^2} \sum_{n=2}^{\infty} (n + 1) \left(\frac{a}{r}\right)^{n+2} \sum_{m=-n}^{n} \overline{C}_{nm} \overline{Y}_{nm}(\theta, \lambda) \quad . \tag{3.108}$$

The following values will be adopted here for the scaling factor "a" and the geocentric gravitational constant GM in the above and in the following equations:

$$\left.\begin{aligned} a &= 6378137. \quad m \\ GM &= 3986004.36 \times 10^8 \quad m^3/s^2 \end{aligned}\right\} \tag{3.109}$$

The surface spherical harmonic of the disturbing potential, referring to the surface of the sphere of radius:

$$r = R = 6371000. \quad m \tag{3.110}$$

is given by:

$$T_n(r = R, \theta, \lambda) \equiv T_n = \frac{GM}{a} \left(\frac{a}{R}\right)^{n+1} \sum_{m=-n}^{n} \overline{C}_{nm} \overline{Y}_{nm}(\theta, \lambda) \tag{3.111}$$

while from (3.107) and (3.108) it can be easily seen that the corresponding surface harmonics of Δg and δg are:

$$\Delta g_n(r = R, \theta, \lambda) \equiv \Delta g_n = \frac{n - 1}{R} T_n \tag{3.112}$$

$$\delta g_n(r = R, \theta, \lambda) \equiv \delta g_n = \frac{n+1}{R} T_n \quad . \tag{3.113}$$

The degree variances (Heiskanen and Moritz, 1967, p. 259) of T, Δg and δg, referring to the surface of the sphere of radius R, are given by:

$$\left.\begin{aligned} k_n = M(T_n^2) &= \left(\frac{GM}{a}\right)^2\left(\frac{a^2}{R^2}\right)^{n+1}\sum_{m=-n}^{n}\bar{C}_{nm}^2 \qquad (a)\\ c_n = M(\Delta g_n^2) &= \left(\frac{n-1}{R}\right)^2 k_n \qquad (b)\\ d_n = M(\delta g_n^2) &= \left(\frac{n+1}{R}\right)^2 k_n \qquad (c) \end{aligned}\right\} \qquad (3.114)$$

The spatial covariance function of the disturbing potential is given by (Moritz, 1972, equation 7-26):

$$K(P, Q) = \sum_{n=2}^{\infty} k_n\left(\frac{R^2}{r_P r_Q}\right)^{n+1} P_n(\cos\psi_{PQ}) \qquad (3.115)$$

while, due to the law of propagation of covariances (ibid, p. 97), the corresponding covariance functions of Δg and δg are:

$$C(P, Q) = \sum_{n=2}^{\infty} c_n\left(\frac{R^2}{r_P r_Q}\right)^{n+2} P_n(\cos\psi_{PQ}) \qquad (3.116)$$

and:

$$D(P,Q) = \sum_{n=2}^{\infty} d_n\left(\frac{R^2}{r_P r_Q}\right)^{n+2} P_n(\cos\psi_{PQ}) \quad . \qquad (3.117)$$

In the notation of section 3.3 one has:

$$C_{T,T}(P, Q) \equiv K(P, Q) \qquad (3.118)$$

$$C_{\delta g,\delta g}(P, Q) \equiv D(P, Q) \quad , \qquad (3.119)$$

while by the law of propagation of covariance:

$$C_{T,\delta g}(P, Q) = -\frac{\partial}{\partial r_Q}[C_{T,T}(P, Q)]$$

$$= \sum_{n=2}^{\infty} \left(\frac{r_P}{n+1}\right) d_n \left(\frac{R^2}{r_P r_Q}\right)^{n+2} P_n(\cos \psi_{PQ}) \quad . \tag{3.120}$$

Based on equations (3.115) through (3.120), all covariances needed in section 3.3 can be defined. Due to the relations (3.114), a model for c_n is necessary and sufficient to enable the evaluation of all the above covariances. Up to a certain maximum degree N_{max} (which at present equals 360), the anomaly degree variances c_n may be obtained from the harmonic coefficients of the disturbing potential, estimated by combining a lower-degree set of satellite-derived harmonics with the harmonics implied by a global set of gravity anomalies. A state-of-the-art global geopotential solution of this kind is the OSU89B model (Rapp and Pavlis, 1990), which is complete to degree and order 360. Hence, up to $N_{max} = 360$, c_n may be defined by:

$$c_n = \left(\frac{GM}{a^2}\right)^2 (n-1)^2 \left(\frac{a^2}{R^2}\right)^{n+2} \sum_{m=-n}^{n} \bar{C}_{nm}^2 \quad ; \quad 2 \le n \le 360 \tag{3.121}$$

where $\bar{C}_{nm}$ are the fully-normalized unitless spherical harmonic coefficients of the OSU89B model (even zonals are remainders after removing the ellipsoidal reference values). Since the disturbing potential is not band-limited to $N_{max} = 360$, one needs to adopt a model that provides the anomaly degree variances above this degree. The analytical form of degree variance models developed for this purpose, is usually selected in such a way that enables closed expressions to be derived that provide the covariance between various gravimetric quantities, facilitating in this manner the practical implementation of these models (Tscherning and Rapp, 1974). The parameters of these models are then estimated in a least-squares adjustment where "observed" degree variances are in essence the values given by (3.121) from the analysis of satellite and terrestrial data. In the following discussion two such models are considered, both of the same analytical form (ibid, 1974):

$$c_n = \frac{A(n-1)}{(n-2)(n+B)} s^{n+2} \quad ; \quad n > 2 \tag{3.122}$$

where A, B and s are parameters of the model; s is the ratio:

$$s = \frac{R_B^2}{R^2} \tag{3.123}$$

where R_B is the radius of the embedded (Bjerhammar) sphere. The first set of parameters (A, B, s) are those estimated by Tscherning and Rapp (ibid, p. 22) so that the model (3.122) is given by:

$$\left.\begin{aligned} c_2^{(1)} &= 7.5 \text{ mgal}^2 \\ c_n^{(1)} &= \frac{425.28\,(n-1)}{(n-2)(n+24)}\,(0.999617)^{n+2} \text{ mgal}^2 \quad ; \quad n > 2 \end{aligned}\right\} \tag{3.124}$$

The second set of parameters (A, B, s) was estimated by Jekeli (1978) and imply the model:

$$\left.\begin{aligned} c_2^{(2)} &= 7.5 \text{ mgal}^2 \\ c_n^{(2)} &= \frac{343.3408\,(n-1)}{(n-2)(n+24)}\,(0.9988961)^{n+2} \text{ mgal}^2 \quad ; \quad n > 2 \end{aligned}\right\} \tag{3.125}$$

In Figure 13, the anomaly degree variances implied by the OSU89B model (to $N_{max} = 360$) and by the models $c_n^{(i)}(i = 1, 2)$ above, are shown. For comparison purposes, the anomaly degree variances implied by Kaula's rule of thumb are also shown. These were computed by (Rapp and Pavlis, 1990):

$$c_n^{(k)} = \frac{192}{n + 1.5} \text{ mgal}^2 \tag{3.126}$$

Note that expressions (3.121), (3.124) - (3.126), all provide the degree variances referring to the surface of the sphere of radius R = 6371 km. As it can be seen from Figure 13, from the three models $c_n^{(k)}$, $c_n^{(1)}$, $c_n^{(2)}$ the model $c_n^{(2)}$ implies the fastest decay of the gravity anomaly spectrum at the higher degrees. In addition, one observes a very good agreement between the model $c_n^{(2)}$ and the ("observed") degree variances implied by OSU89B in the range $180 < n < 360$. Although the spectral properties of the disturbing

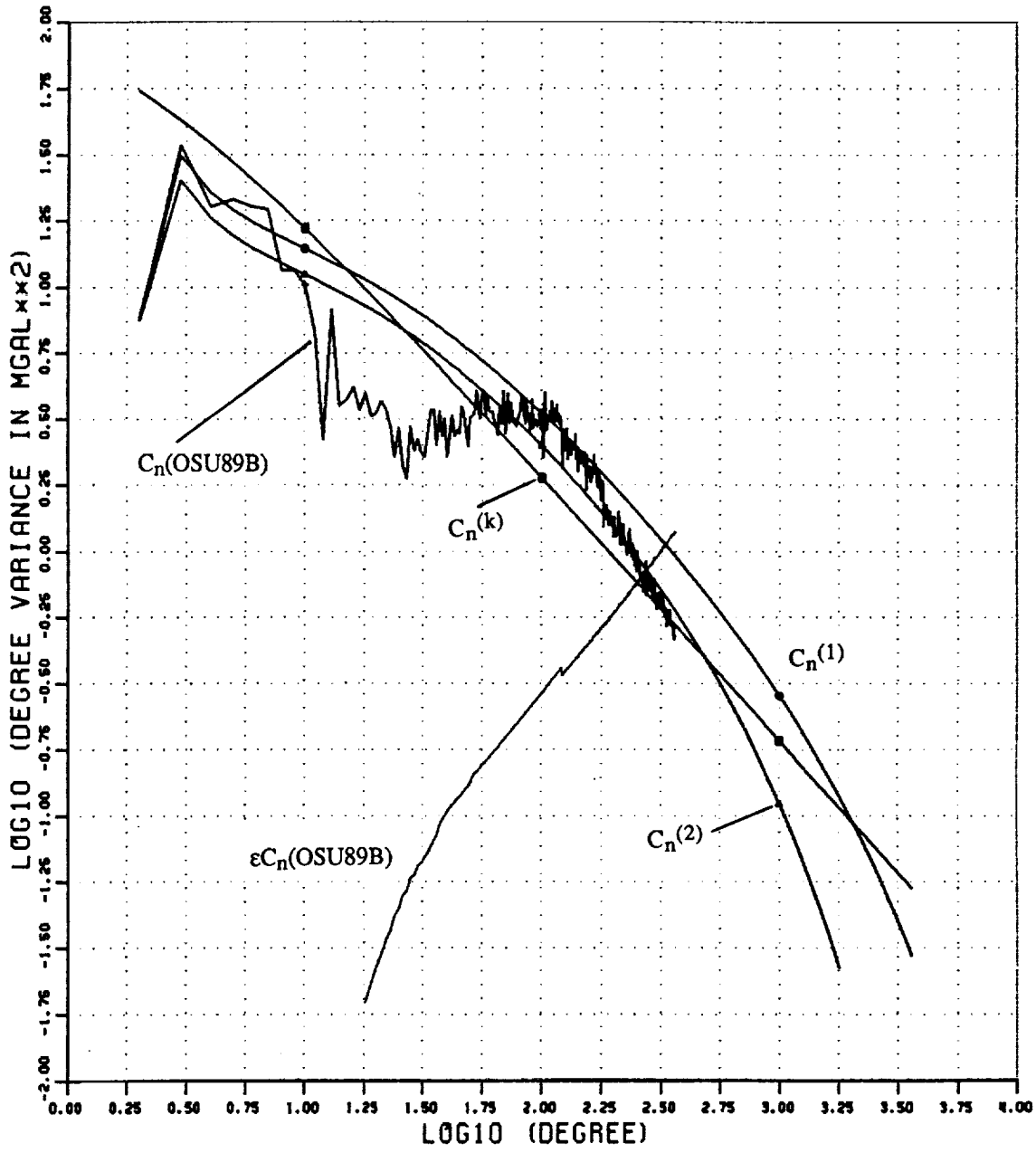

Figure 13. Anomaly Degree Variances Implied by OSU89B and the Models $c_n^{(k)}$, $c_n^{(1)}$, $c_n^{(2)}$.

potential above degree 360 are to a large extent a matter of assumption, due to the lack of detailed data on a global basis, the overall performance of a degree variance model may be judged by comparing the variance of certain gravimetric quantities, as implied by the model, to corresponding values obtained from the analysis of available measurements. For this purpose, the variance of the (point) gravity anomaly C_0, and the variance of the horizontal gradient of the gravity anomaly G_{0H} are often used (Moritz, 1980, section 22). Jekeli (1978) has shown that:

$$G_{0H} \approx \frac{1}{2} \sum_{n=2}^{\infty} g_n \tag{3.127}$$

where the degree variance of the vertical gradient, g_n is:

$$g_n = \left(\frac{\partial \Delta g}{\partial r} \right)_n = \frac{(n+2)^2}{R^2} c_n \quad . \tag{3.128}$$

To calculate C_0 and G_{0H}, four models for c_n are considered as follows:

$$\left.\begin{aligned} c_n(A) &\equiv c_n^{(1)} \\ c_n(B) &\equiv c_n^{(2)} \\ c_n(C) &= \begin{cases} c_n(\text{OSU89B}) & 2 \le n \le 360 \\ c_n^{(1)} & 360 < n < \infty \end{cases} \\ c_n(D) &= \begin{cases} c_n(\text{OSU89B}) & 2 \le n \le 360 \\ c_n^{(2)} & 360 < n < \infty \end{cases} \end{aligned}\right\} \quad . \tag{3.129}$$

Using these models and approximating infinity by n = 36000, C_0 and G_{0H} have been evaluated. The values obtained are given in Table 4.

Table 4. Gravity Anomaly (C_0) and Horizontal Anomaly Gradient (G_{0H}) Variances, Implied by Different Anomaly Degree Variance Models.

Model	C_0(mgal^2)	G_{0H}(E.U.^{2})
A	1795.0	3542.2
B	1106.0	339.3
C	1437.9	3533.2
D	1035.8	339.3

Based on extensive analysis of gravity anomalies implied by satellite altimetry, as well as of terrestrial measurements, Rapp (1985) suggested 1100 mgal^2 as an estimate for C_0. The value of G_{0H} is much more difficult to estimate, since the horizontal gradient is a signal of high-frequency content and the detailed data necessary for its determination are not currently available on a global basis. A value of 300 EU^2 (1 Eötvös Unit (EU) = 0.1 mgal/km = 10^{-9} s^{-2}) for G_{0H} is a compromise between various estimates obtained from regional data analyses (Robbins, 1985). Based on these considerations, the composite model $c_n(D)$ defined in (3.129), will be used in the numerical analysis to be presented in the next chapter.

3.4.2 Covariance Models for the Measurement Noise

The estimation of realistic error properties for the data poses an even more difficult problem than the estimation of the global properties of the gravitational signal contained in them. Provided multiple independent samples of the measurements are available, one may estimate an empirical error covariance function for the data by analyzing the differences between different samples, as it was done by Weber and Wenzel (1982) for the gravity anomaly data in Europe. In the absence of multiple independent measurements for an observable, one usually employs an analytical error covariance model to describe its error properties. The variance and the correlation length of such a model are assigned values which are representative of the measurement process under consideration. In the following, three such error covariance models are considered.

Model 1 : Dirac Impulse

The error covariance function here is given by:

$$\sigma^{(1)}(\psi) = cD(\psi) \quad ; \quad c > 0 \tag{3.130}$$

where the Dirac impulse (or delta function), $D(\psi)$, is defined on the unit sphere by Jekeli (1981):

$$\frac{1}{4\pi} \iint_{\sigma} D(\psi_{PQ}) f(\theta_P, \lambda_P)\, d\sigma = f(\theta_Q, \lambda_Q) \quad . \tag{3.131}$$

For the isotropic error covariance models that will be considered here, the n^{th} -degree variance σ_n is given in general by:

$$\sigma_n = \frac{2n+1}{2} \int_{\psi=0}^{\pi} \sigma(\psi) P_n(\cos\psi) \sin\psi d\psi \quad . \tag{3.132}$$

This equation yields for the model $\sigma^{(1)}(\psi)$, due to (3.130) and (3.131):

$$\sigma_n^{(1)} = (2n+1)c \quad ; \quad n \geq 0 \tag{3.133}$$

which implies that the rms amplitude by degree of the error is constant, equal to $c^{1/2}$, for any degree n. This property is the spherical counterpart of the corresponding spectral property of the delta function, $\delta(x)$, defined on the real line $-\infty < x < \infty$ whose Fourier transform is one (Papoulis, 1962, p. 36).

The model $\sigma^{(1)}(\psi)$, as it can be seen from (3.130) and (3.133), implies infinite variance and zero correlation length. In practical applications, where one is always considering a finite number of observations (point values or area-means), the assumption that observation errors are uncorrelated and that all observations have the same error variance, is often employed. However, as seen from the above, such assumptions, when extended to the case of infinite number of point measurements covering the entire sphere,

lead to unrealistic spectral properties of the noise. For this reason alternative error covariance models are considered next, which do not suffer from such disadvantages.

Model 2 : Gauss-Markov First-Order

The error covariance function here is given by (Rummel, 1980, p. 44):

$$\sigma^{(2)}(\psi) = ce^{-\lambda\psi} \quad ; \quad c > 0, \quad \lambda > 0 \quad . \tag{3.134}$$

The parameters c, λ are related to the variance (m_6^2) and the correlation length (ψ^c) by:

$$\left.\begin{aligned} c &= m_6^2 \qquad (a) \\ \lambda &= \frac{1}{\psi^c}\,\ell n2 \qquad (b) \end{aligned}\right\} \quad . \tag{3.135}$$

The degree variances corresponding to $\sigma^{(2)}(\psi)$ can be obtained from the following recurrence relation:

$$\sigma_n^{(2)} = \frac{2n+1}{2n-3}\,\frac{\lambda^2 + (n-2)^2}{\lambda^2 + (n+1)^2}\,\sigma_{n-2}^{(2)} \quad ; \quad n \geq 2 \tag{3.136}$$

with starting values:

$$\left.\begin{aligned} \sigma_o^{(2)} &= \frac{c}{2}\,\frac{1+e^{-\lambda\pi}}{\lambda^2+1} \qquad (a) \\ \sigma_1^{(2)} &= \frac{3c}{2}\,\frac{1-e^{-\lambda\pi}}{\lambda^2+4} \qquad (b) \end{aligned}\right\} \quad . \tag{3.137}$$

The detailed derivation of this recurrence is given in Appendix C. In case one postulates the absence of zeroeth- and first-degree harmonics from $\sigma^{(2)}(\psi)$, the resulting covariance model is given by:

$$\bar{\sigma}^{(2)}(\psi) = c\left[e^{-\lambda\psi} - \frac{1}{2}\,\frac{1+e^{-\lambda\pi}}{\lambda^2+1} - \frac{3}{2}\,\frac{1-e^{-\lambda\pi}}{\lambda^2+4}\cos\psi\right] \quad . \tag{3.138}$$

Given the correlation length ψ^c, the parameter λ for this model can be determined by solving iteratively the equation:

$$1 - 2e^{-\lambda\psi^c} + \frac{1}{2}\,\frac{1+e^{-\lambda\pi}}{\lambda^2+1} + \frac{3}{2}\,\frac{1-e^{-\lambda\pi}}{\lambda^2+4}\left(2\cos\psi^c - 1\right) = 0 \tag{3.139}$$

with initial value for λ, the one given in (3.135b). The parameter c can then be determined, given the variance m_o^2, by:

$$c = m_o^2\left[1 - \frac{1}{2}\,\frac{1+e^{-\lambda\pi}}{\lambda^2+1} - \frac{3}{2}\,\frac{1-e^{-\lambda\pi}}{\lambda^2+4}\right]^{-1} \quad . \tag{3.140}$$

Obviously, the degree variances $\bar{\sigma}_n^{(2)}$ are identical to $\sigma_n^{(2)}$ for $n \geq 2$, while $\bar{\sigma}_o^{(2)} = \bar{\sigma}_1^{(2)} = 0$.

Model 3 : Reciprocal Distance

The error covariance function here is given by:

$$\sigma^{(3)}(\psi) = c(1-\lambda)\left(1 - 2\lambda\cos\psi + \lambda^2\right)^{-1/2} \quad ; \quad c > 0\,,\ 0 < \lambda < 1 \quad . \tag{3.141}$$

Considering the notation of Figure 3, it can be easily seen that $\sigma^{(3)}(\psi)$ can be written in the form:

$$\sigma^{(3)}(\psi) = c\,\frac{r - R}{\ell} \quad , \tag{3.142}$$

where:

$$\left.\begin{aligned} r &= \frac{R}{\lambda} && \text{(a)} \\ \ell &= r\left(1 - 2\lambda\cos\psi + \lambda^2\right)^{1/2} && \text{(b)} \end{aligned}\right\} \tag{3.143}$$

and the form (3.142) explains the characterization "reciprocal distance". Given the variance m_0^2 and the correlation length ψ^c, it is easy to see that the parameter c is given by:

$$c = m_0^2 \quad , \tag{3.144}$$

while λ is obtained after solving iteratively the equation:

$$(1 - 2\lambda\cos\psi^c + \lambda^2)^{1/2} - 2(1 - \lambda) = 0 \tag{3.145}$$

with initial value for λ given by:

$$\lambda^{(o)} = 1 - \sqrt{2}\,\sin\frac{\psi^c}{2} \quad . \tag{3.146}$$

The degree variances $\sigma_n^{(3)}$ are given by the closed form expression (Sjöberg and Fan, 1986):

$$\sigma_n^{(3)} = c(1 - \lambda)\lambda^n \quad . \tag{3.147}$$

The assumption of absence of zeroeth- and first-degree harmonics from $\bar{\sigma}^{(3)}(\psi)$, yields the model (ibid, 1986):

$$\bar{\sigma}^{(3)}(\psi) = c(1 - \lambda)\left[(1 - 2\lambda\cos\psi + \lambda^2)^{-1/2} - 1 - \lambda\cos\psi\right] \quad . \tag{3.148}$$

The parameter λ for the model $\bar{\sigma}^{(3)}(\psi)$ is obtained by solving iteratively the equation:

$$2(1 - \lambda)\left[(1 - 2\lambda\cos\psi^c + \lambda^2)^{-1/2} - 1 - \lambda\cos\psi^c\right] - \lambda^2 = 0 \quad , \tag{3.149}$$

given ψ^c, and using as initial value for λ the one given in (3.146). Once λ has been determined, c is given by:

$$c = m_0^2\lambda^{-2} \quad . \tag{3.150}$$

Again, $\bar{\sigma}_n^{(3)} = \sigma_n^{(3)}$ for $n \geq 2$, while $\bar{\sigma}_0^{(3)} = \bar{\sigma}_1^{(3)} = 0$.

In order to demonstrate the different characteristics of the models $\bar{\sigma}^{(2)}(\psi)$ and $\bar{\sigma}^{(3)}(\psi)$, the parameters c and λ of these models were evaluated for a given value of the variance m_0^2 (taken here to be $m_0^2 = 1$ mgal^2) and different choices of the correlation length ψ^c (taken as 0°.1, 0°.2 and 0°.5). The results are given in Table 5. For the model $\bar{\sigma}^{(3)}(\psi)$ the radial distance r to the external point P (see Figure 3) from which the distance ℓ is reckoned is also given. The radius R in this case (see equation 3.142) was taken to be 6371 km.

Table 5. Parameters Associated with the Error Covariance Models $\bar{\sigma}^{(2)}(\psi)$ and $\bar{\sigma}^{(3)}(\psi)$, for $m_0^2 = 1$ mgal^2 and $\psi^c = 0°.1$, 0°.2 and 0°.5.

Model	ψ^c	0°.1	0°.2	0°.5
$\bar{\sigma}^{(2)}(\psi)$	λ	0.397136814873D+03	0.198557509013D+03	0.793924826289D+02
	c	1.000012680788	1.000050727516	1.000317237947
$\bar{\sigma}^{(3)}(\psi)$	λ	0.998990129118	0.997975830838	0.994906095858
	c	1.002022805406	1.004060663364	1.010266183954
	r(m)	6377440.4	6383922.1	6403619.4

As expected, for a given value of the variance m_0^2, increase of the correlation length ψ^c causes decrease of the parameter λ for both models $\bar{\sigma}^{(2)}(\psi)$ and $\bar{\sigma}^{(3)}(\psi)$ (see equations 3.135b and 3.146). As ψ^c increases, more power of the error spectrum is shifted to the lower degree harmonics, as it is illustrated in Figures 14a and 14b where the degree variances $\bar{\sigma}_n^{(2)}$ and $\bar{\sigma}_n^{(3)}$ are plotted for $\psi^c = 0°.1$ and $\psi^c = 0°.2$ respectively. For the reciprocal distance model $\bar{\sigma}^{(3)}(\psi)$, increase of ψ^c corresponds also to increase of the radial distance r, as it can be seen from Table 5.

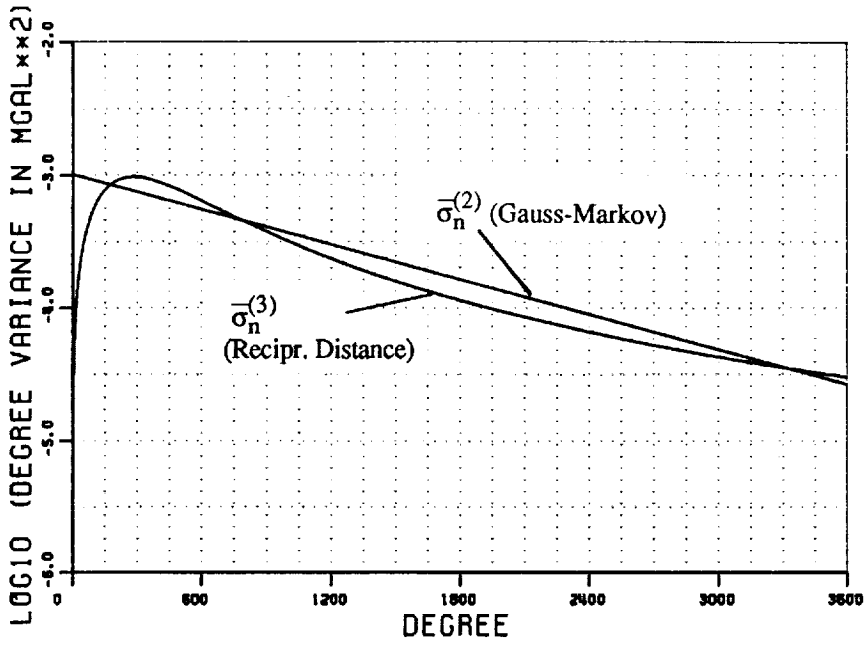

(a) Correlation Length $\psi^c = 0°.1$

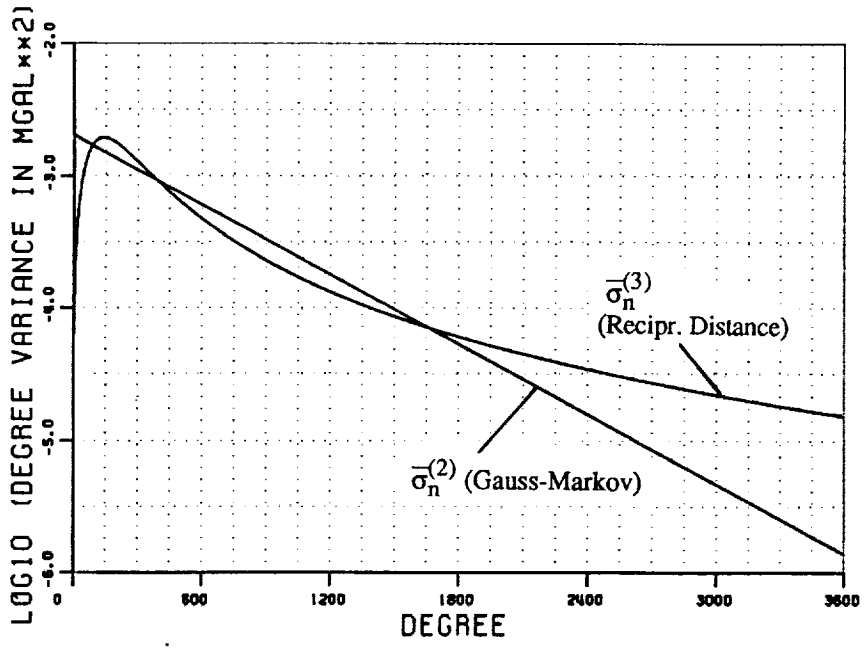

(b) Correlation Length $\psi^c = 0°.2$

Figure 14. Degree Variances $\bar{\sigma}_n^{(2)}$ and $\bar{\sigma}_n^{(3)}$ for $m_0^2 = 1$ mgal^2 and $\psi^c = 0°.1, 0°.2$.

CHAPTER IV

NUMERICAL ANALYSIS

Based on the formulation given in Chapters II and III, a number of numerical experiments were performed in order to assess the accuracy of geopotential differences estimated from the gravimetric information contained in a global spherical harmonic expansion and in the gravity disturbance data in the terrestrial and at altitude caps. The results of these computations are presented in order of increased complexity of the estimation scheme employed, starting with the geopotential differences estimated on the basis of a global geopotential model alone and concluding with the addition of gravity disturbance data on the surface of the Earth as well as at altitude.

4.1 Disturbing Potential Difference Estimated from Current and Future Global Geopotential Solutions Only

Three global geopotential solutions are considered here. These are designated:

(a) OSU89B
(b) TOPEX
(c) GPB

(a) OSU89B (Rapp and Pavlis, 1990) represents a state-of-the-art high-degree global model, available in the absence of the missions discussed in section 1.3. The estimated anomaly error degree variances associated with this model are shown in Figure 13. A number of comparisons with independent data reported by Rapp and Pavlis (ibid), indicate that the error estimates of the coefficients do provide a realistic assessment of the quality of the model. As it can be seen from Figure 13 the spectrum of the anomaly error starts exceeding the spectrum of the anomaly signal around degree 250. As the degree of the coefficients increases, validation of their error estimates becomes more difficult because precise independent information is not available on a global basis with high enough

resolution to enable comparisons. In ocean areas comparisons with GEOSAT-implied undulations indicated that, although the signal sinks below the noise above degree 250, the coefficients above this degree do contain meaningful information (ibid, p. 21,903, Table 9). In this study for the implementation of least-squares collocation, the OSU89B coefficients above degree Nmax = 250 will not be admitted as part of a reference model, with the understanding that the pessimistic error estimates above this degree may be due to shortcomings in the error assessment of the model, induced by factors such as the neglect of correlations between the 30' x 30' mean anomalies used in its development. Such neglect is at present necessitated by the inability to computationally handle a more appropriate error modeling for the 259200 mean anomalies involved in the model's development.

(b) TOPEX represents the geopotential model that is anticipated to become available from the analysis of the GPS tracking data alone on the TOPEX/Poseidon altimeter satellite (Pavlis, E., et. al., 1990). Such a model will extend to degree 50 and its expected errors were estimated in a simulation study where the GPS tracking data were used in a dynamic solution for the estimation of the geopotential spectrum, satellite orbital parameters as well as parameters related to air-drag etc. (ibid, 1990).

(c) GPB represents the geopotential model anticipated to become available from the analysis of the GPS tracking data on Gravity Probe-B spacecraft. The model from such a mission will extend to degree 55, and the expected errors of its coefficients were obtained in the simulation study by Pavlis, E., et. al. (ibid) in a similar manner as for TOPEX.

The error anomaly degree variances for OSU89B ($2 \leq n \leq 60$), TOPEX and GPB are shown in Figure 15, along with the (signal) anomaly degree variances implied by OSU89B ($2 \leq n \leq 60$). As it can be seen from this figure, TOPEX is expected to improve the current knowledge of the spectrum at degree 10 by about 3 orders of magnitude while the improvement for GPB at the same degree is by about 4 orders of magnitude. However, since TOPEX and GPB models lack the detailed terrestrial (and altimetry-implied) gravity information included in OSU89B, their error spectra yield poorer values than the error spectrum of OSU89B, after degrees ~ 25 and ~ 45 respectively.

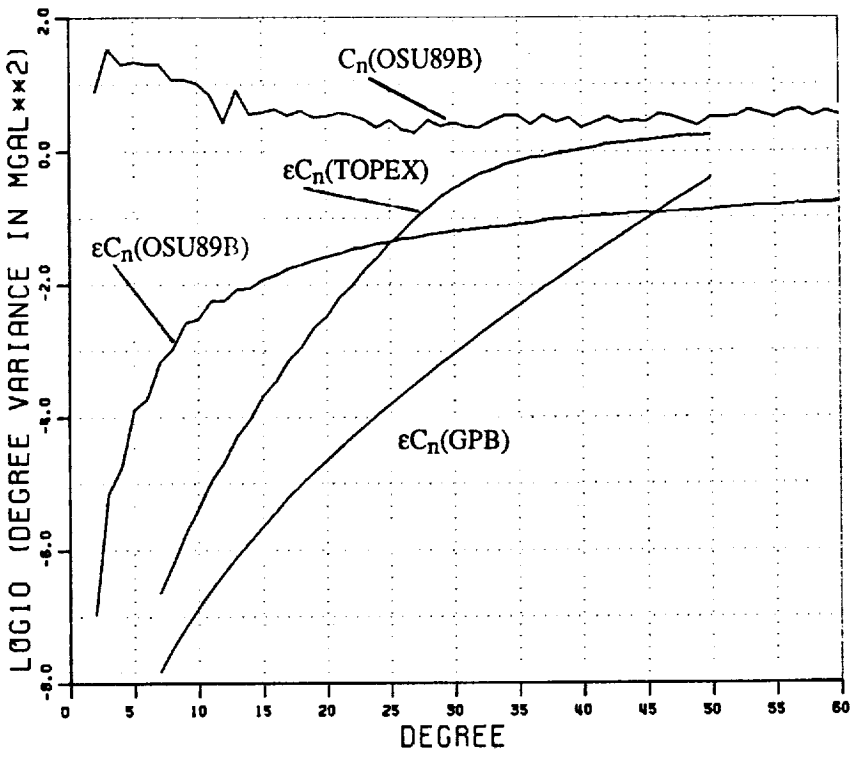

Figure 15. Anomaly Degree Variances for OSU89B and Error Anomaly Degree Variances for OSU89B, TOPEX and GPB.

Since the information based on which TOPEX and GPB are developed is independent of the information used to develop OSU89B, one can safely assume that if OSU89B is combined (in a least-squares sense) with either of the two models, the resulting solution will perform at least as good as the best of the contributing solutions performs at any given degree. In that sense, the error spectrum of a combined solution of the type TOPEX/OSU89B may be approximated by the error spectrum of TOPEX up to degree 25 and the error spectrum of OSU89B from 26 to 360. Similarly, a combined GPB/OSU89B model's error spectrum can be approximated by the error spectrum of GPB up to degree 45 and the error spectrum of OSU89B from 46 to 360. Based on these considerations, the total (commission plus omission) error in geopotential ($\psi_d = 0°$) and geopotential difference, implied by the above models, truncated at various degrees was computed using equations (3.53), (3.54) and (3.55). The results are given in Table 6. In

all numerical results to be presented hereon the radius of the reference sphere to which the estimated errors refer is R = 6371 km, and the model $c_n(D)$ of section 3.4.1 is used to represent the "true" spectrum of the gravity anomaly.

Table 6. Geopotential and Geopotential Difference Errors from Current and Future Global Spherical Harmonic Models.

			$\varepsilon\Delta T$ (kgal cm)				
Model	Nmax	$\psi_d = 0^\circ$	2°	5°	10°	30°	180°
OSU89B	25	207.7	242.2	311.0	291.6	294.0	290.7
(89B)	45	154.6	213.9	223.0	221.7	217.9	217.1
	250	60.6	77.0	85.1	86.2	85.6	85.9
TOPEX	25	206.8	242.1	310.5	290.2	292.7	289.4
(T)	50	161.3	217.4	236.4	228.0	228.5	228.9
GPB	25	206.6	242.0	310.3	289.8	292.5	289.0
(G)	50	142.5	205.5	202.1	205.6	202.1	203.0
T/89B	25/250	57.4	76.5	83.0	81.2	81.1	81.2
G/89B	45/250	52.2	74.2	74.7	73.9	73.8	73.8

As it can be seen from Table 6, the current knowledge of the geopotential spectrum implies absolute geopotential values ($\psi_d = 0°$) accurate to about 61 kgal cm, while for station separation $\psi_d = 10°$ (~1110 km) the error in ΔT is about 86 kgal cm. The future models alone, (i.e. $N_{max} = 50$), despite the great improvements they promise for the very low-degree harmonics, fail to achieve the accuracy obtainable by the currently available high-degree expansion OSU89B, due to the large omission error above the maximum degree that these models can resolve. However, when the high accuracy long-wavelength information provided by GPB, is augmented by the shorter-wavelength information contained in the high-degree model, an improvement by about 14% over the attainable accuracies using OSU89B alone (up to $N_{max} = 250$), is achieved. The corresponding improvement for the combination TOPEX/OSU89B is substantially lower (about 5%) as it is expected (see Figure 15). Apart of the higher accuracies achievable by the combination GPB/OSU89B, an additional factor that makes this combination preferable over the TOPEX/OSU89B, is that the higher resolution of GPB enables better control over the

systematic errors in the combined solution, caused by the errors in the gravity anomalies (used in the development of OSU89B), arising from vertical datum inconsistencies. As mentioned in section 1.1, Laskowski's (1983) study indicated that such errors are likely to contaminate the geopotential's spectrum up to maximum degree about 60.

4.2 Introduction of Terrestrial Gravity Disturbance Measurements

The estimation scheme of the previous section, whereby the geopotential differences were obtained on the basis of the global information contained in a geopotential model only, is now augmented by introducing detailed local gravimetric information in the form of gravity disturbances inside the caps surrounding the computation points. The characteristics and sensitivities of this estimation scheme are considerably more complicated to assess, than of the scheme of section 4.1, because here a number of inter-related factors affect the quality of the final result. Hence, to examine the individual contribution and importance of different aspects of the observation/estimation setup to the quality of the results, the following discussion is divided into three parts, addressing the choice of cap integration kernel, the cap size and data density, and the data accuracy respectively. In addition, since the error estimation of the observational setup considered here, can be performed using either truncation theory principles or least-squares collocation, a comparison of the error estimates obtained by each technique is also given in section 4.2.4.

4.2.1 The Choice of Cap Integration Kernel

The two integration kernels $H_1(\psi)$ (unmodified Hotine) and $H_2(\psi)$ (Meissl's modification) are examined here. The propagated errors in geopotential ($\psi_d = 0°$) and geopotential difference implied by the use of these kernels are given on Table 7, for two cap sizes ($\psi_0^T = 2°, 4°$) and two choices of reference geopotential model (OSU89B and the combination GPB to degree 45 augmented by OSU89B from 46 to 250).

Table 7. Geopotential and Geopotential Difference Errors Implied by Different Choices of Cap Integration Kernel. (All Errors are in kgal cm).

		OSU89B		GPB/OSU89B	
ψ_o^T	ψ_d	$H_1(\psi)$	$H_2(\psi)$	$H_1(\psi)$	$H_2(\psi)$
2°	0°	19.4	19.8	16.7	8.7
	5°	24.4	24.3	22.6	12.6
	10°	27.2	28.5	23.4	12.1
	30°	27.5	28.0	23.6	12.3
4°	0°	18.6	14.0	16.3	10.0
	5°	23.5	15.5	19.9	12.7
	10°	24.8	19.2	21.8	13.6
	30°	26.3	19.8	23.1	14.1

ψ_o^T : terrestrial cap size

ψ_d : angular separation between stations

$\Delta\psi^T = 4'$

Gravity Disturbance Error : $\bar{\sigma}^{(3)}(\psi)$; $m_o = 2$ mgal, $\psi^c = 0°.1$

Nmax = 250

In the evaluation of the errors given in Table 7 (as well as in all subsequent applications of truncation theory) the sampling error spectrum s_n, which was introduced but not specified in equation (3.51a), was evaluated from the quartic expression developed by C. Jekeli based on numerical experiments performed by Colombo (1981a, equation 3.10), i.e.

$$s_n = f^2\left(\frac{n}{N}\right) d_n \tag{4.1}$$

where:

$$f\left(\frac{n}{N}\right) = \frac{1}{100}\left\{\left[-16.19570\left(\frac{n}{N}\right) + 30.34506\right]\left(\frac{n}{N}\right) + 40.29588\right\}\left(\frac{n}{N}\right)^2 \tag{4.2}$$

and N is the Nyquist frequency implied by the sampling interval (equation 3.21), while d_n is the signal degree variance of the gravity disturbance.

Examining now the results shown in Table 7, the following comments can be made:

1. By comparing the results for the case of OSU89B and the two different cap sizes it can be seen that the kernel modification yields improved accuracy estimates by about 25% for the larger cap size (4°), but degrades slightly the results for the smaller cap size. In contrast, in the case of the combined model GPB/OSU89B, the kernel modification yields a substantial (~ 48%) reduction of the error for the smaller cap size and a less pronounced (~ 39%) for the larger one. This is due to the fact that Meissl's modification, in its attempt to accelerate the rate of convergence of the truncation coefficients, shifts part of the power of the higher-degree coefficients to the lower-degree ones (see also (Jekeli, 1980). Accordingly although the omission error decreases with the introduction of Meissl's modification, the commission error increases, and that explains the slight degradation of the results when OSU89B is used as reference model. In case the combined model is used, the lower-degree harmonics of this model are so accurately determined from GPB, that the increase of the commission error is overwhelmed by the concurrent decrease of the omission one, and that accounts for the great improvement achieved by the use of $H_2(\psi)$ instead of $H_1(\psi)$ here.

The increase of the cap size to 4° implies that additional information concerning the long-wavelengths is contributed by the cap measurements, as compared to the case $\psi_0^T = 2°$. This counterbalances the increased commission error in the case of OSU89B (going from $H_1(\psi)$ to $H_2(\psi)$), but, since the cap measurements are not error-free, reduces the 48% improvement in the case of the combined model, to 39% (increased cap size implies increased propagated error).

2. A comparison of the results for the case ($\psi_0^T = 2°$, $H_2(\psi)$, GPB/OSU89B) in Table 7, with the results given in Table 6 for GPB/OSU89B (Nmax = 250), shows the substantial improvement achieved by the incorporation of terrestrial gravity disturbances around the computation points. Such comparison implies that the present accuracies of the higher-degree harmonics, as well as the resolution that current high-degree expansions achieve, are only capable of geopotential difference determination at the accuracy level of about 75 kgal cm. If one strives for a 10 kgal cm accuracy level, then, not only terrestrial gravimetry, but the high-accuracy long-wavelength geopotential determination anticipated from the GP-B mission are needed. As it can be seen from Table 7, the present knowledge of the long-wavelength (2 to 45) part of the geopotential spectrum, can only support geopotential difference determination at the 20 to 30 kgal cm level for the cap sizes that were considered.

4.2.2 The Effect of Cap Size and Data Density

The dependence of the accuracy of the estimated geopotential differences on the extent (cap size) and density of the gravity disturbance measurements in the caps surrounding the computation points is very important, since precise gravimetric surveys required to gather the data are rather costly undertakings. In order to examine these aspects, the error of the estimated geopotential ($\psi_d = 0°$) and geopotential difference was evaluated for three cap sizes (ψ_0^T = 1°, 2° and 4°) and three grid spacings ($\Delta\psi^T$ = 2', 6' and 10'), with the combined GPB/OSU89B model to Nmax = 250 used in all cases as the reference and with $H_2(\psi)$ as the cap integration kernel. In all cases a reciprocal distance error covariance model with variance 4 mgal^2 and correlation length 0°.1 was used. The results are given in Table 8.

Table 8. Influence of Data Extent (Cap Size) and Data Density on the Error of Estimated Geopotential and Geopotential Difference. (All Errors are in kgal cm).

		$\Delta\psi^T$		
ψ_0^T	ψ_d	2'	6'	10'
1°	0°	15.9	16.0	16.4
	5°	23.8	23.9	24.4
	10°	22.5	22.6	23.2
	30°	22.5	22.6	23.2
2°	0°	8.7	8.8	9.5
	5°	12.6	12.8	13.7
	10°	12.0	12.2	13.2
	30°	12.3	12.5	13.5
4°	0°	10.0	10.1	10.7
	5°	12.7	12.9	13.8
	10°	13.6	13.8	14.7
	30°	14.1	14.3	15.1

ψ_0^T : terrestrial cap size

ψ_d : angular separation between stations

Geopotential Model : GPB/OSU89B (45/250)

Integration Kernel : $H_2(\psi)$

Gravity Disturbance Error : $\bar{\sigma}^{(3)}(\psi)$; m_0 = 2 mgal, ψ^c = 0°.1

As it can be seen from Table 8 the grid spacing ($\Delta\psi^T$) has only a minor effect on the quality of the result. As one passes from the very dense sampling ($\Delta\psi^T = 2'$), to the coarser one ($\Delta\psi^T = 10'$), a degradation of the results by only about 1 kgal cm is observed. This is due to the fact that the sampling error, for sampling intervals smaller than ~ 10', has the smallest contribution to the total error of the geopotential and the geopotential difference. For the cap sizes under consideration (up to ~ 5°) and the reference high-degree spherical harmonic models used here, the two major sources of error contributing to the total error budget are the propagated error of the cap data and the commission error of the model. The little dependence of the total error on the sampling interval (for $\Delta\psi^T <$ 10'), is rather fortunate because it implies cost savings in the data acquisition process.

As far as the cap size is concerned, as it can be seen from Table 8, $\psi_0^T = 2°$ yields the best results for the particular selection of reference gravity model (and its higher degree) and error properties of the data. It is important to notice that due to the accumulation of propagated error of the data, the increase of the cap size beyond a certain value does not improve but degrades the results. Although this appears strange at first glance (introduction of additional information should not worsen the determination of T and ΔT), it is well explained if one takes into account that the kernel $H_2(\psi)$, used to evaluate the errors in Table 8, is designed based on deterministic principles with no explicit requirement to minimize the total error of the geopotential. This aspect will be reconsidered in section 4.2.4, since it constitutes a major difference between integral formulae techniques using deterministic kernels and least-squares collocation.

4.2.3 The Effect of the Error Properties of the Gravity Disturbance Data

In view of the difficulties encountered in estimating realistic error properties for the gravity disturbance data inside the caps, it is important to examine the effect of various assumptions concerning the behavior of the data errors, on the errors of the estimated quantities (T and ΔT). For this purpose, the two error covariance models $\overline{\sigma}^2(\psi)$ and $\overline{\sigma}^3(\psi)$ were used, with different variances (m_0^2 = 1, 4 mgals^2) and correlation lengths (ψ_0^c = 0°.1, 0°.5) for the estimation of $\varepsilon T(\psi_d = 0°)$ and $\varepsilon\Delta T$. The results are given in Table 9. In all cases, the cap size was 2°, the sampling interval was 4', the geopotential model GPB/OSU89B to N_{max} = 250 was used as reference model and $H_2(\psi)$ was used as integration kernel. Examining the results in Table 9, the following comments can be made:

Table 9. Influence of the Error Properties of the Gravity Disturbance Data on the Error of Estimated Geopotential and Geopotential Difference. (All Errors are in kgal cm).

	m_0 = 1 mgal		m_0 = 2 mgal		ERROR
ψ_d	$\psi^c = 0°.1$	$\psi^c = 0°.5$	$\psi^c = 0°.1$	$\psi^c = 0°.5$	MODEL
0°	5.9	8.3	7.1	13.8	
5°	9.2	12.4	10.8	19.9	$\bar{\sigma}^{(2)}(\psi)$
10°	8.2	11.7	9.9	19.4	
30°	8.3	11.8	10.1	19.5	
0°	6.4	8.6	8.7	14.4	
5°	9.8	12.3	12.6	19.5	$\bar{\sigma}^{(3)}(\psi)$
10°	8.9	11.8	12.1	19.8	
30°	9.1	12.1	12.3	20.3	

$\psi_0^T = 2°$; $\Delta\psi^T = 4'$
Geopotential Model : GPB/OSU89B (45/250)
Integration Kernel : $H_2(\psi)$

1. In all cases considered the Gauss-Markov model $\bar{\sigma}^{(2)}(\psi)$ yields more optimistic results than the reciprocal distance model $\bar{\sigma}^{(3)}(\psi)$. Observing Figure 14a, one can see that the first-order Gauss-Markov model contains more power of the error below harmonic degree ~ 150, than the reciprocal distance error model does, for the same degree range. Since the cap data error contribution at the lower degrees is greatly attenuated, due to the very small magnitude of the coefficients XQ_{kn} (see equation (3.50b)) at these degrees, for a given variance m_0^2, the Gauss-Markov model $\bar{\sigma}^{(2)}(\psi)$ implies a smaller propagated error, than the reciprocal distance does. In addition, the difference of the errors implied by the two models becomes smaller as the correlation length increases, because the increase of ψ^c shifts more power of the error $\bar{\sigma}^{(3)}$ at lower degrees as it can be seen from Figure 14b. For example, for m_0^2 = 1 mgal^2 and $\psi^c = 0°.1$, $\bar{\sigma}^{(3)}(\psi)$ yields an error ~ 8% larger than $\bar{\sigma}^{(2)}(\psi)$, while the difference is only ~ 3% for $\psi^c = 0°.5$ (for the same error variance).

2. The error of T and ΔT is affected more by changes of the error correlation length, than by changes of the error variance. For example, for m_0^2 = 4 mgal^2, the error nearly doubles as the correlation length increases from 0°.1 to 0°.5, while for $\psi^c = 0°.1$, increasing the

variance from 1 to 4 mgal^2 causes only an increase of the error of approximately 26%. Note also that for the larger variance, an increase of the correlation length causes a quite larger increase of εT and $\varepsilon \Delta T$, than for the smaller variance.

According to the above, larger but less correlated errors in the cap measurements can be tolerated more than smaller but heavily correlated ones (e.g., systematic errors in the cap data), as far as the determination of the geopotential differences is concerned.

4.2.4 Comparison Between Error Estimates from Truncation Theory and from Least-Squares Collocation

The two different techniques for assessing the global rms error of the geopotential differences, obtained on the basis of a global spherical harmonic model and gravity disturbance data in the terrestrial caps, are intercompared in this section. For this purpose, the parameters given in Table 10 were used in the implementation of truncation theory, and the error $\varepsilon \Delta T$ was evaluated with both techniques, for two cap sizes ($\psi_0^T = 2°, 4°$), using the two different error covariance models, for three station separations ($\psi_d = 5°, 10°, 30°$).

Table 10. Comparison Between Error Estimates of Geopotential Differences Obtained from Truncation Theory and Least-Squares Collocation (All Errors are in kgal cm).

	$\psi_0^T = 2°$				$\psi_0^T = 4°$			
	TRUNCATION		LSC		TRUNCATION		LSC	
ψ_d	$\bar{\sigma}^{(2)}$	$\bar{\sigma}^{(3)}$	$\bar{\sigma}^{(2)}$	$\bar{\sigma}^{(3)}$	$\bar{\sigma}^{(2)}$	$\bar{\sigma}^{(3)}$	$\bar{\sigma}^{(2)}$	$\bar{\sigma}^{(3)}$
5°	10.8	12.6	8.7	11.4	8.1	12.7	7.3	10.9
10°	9.9	12.1	8.4	11.4	8.1	13.6	7.2	10.9
30°	10.1	12.3	8.5	11.7	8.1	14.1	7.3	11.2

$\Delta\psi^T = 4'$

Gravity Disturbance Error : $m_0 = 2$ mgal, $\psi^c = 0°.1$

Geopotential Model : GPB/OSU89B (45/250)

Integration Kernel : $H_2(\psi)$

Examining the results given in Table 10, the following observations can be made:

1. The use of least-squares collocation (with ring averages) always yields smaller error $\varepsilon\Delta T$ than the use of the integral formula. This is as expected, since lsc is by definition the optimal linear estimator, in the sense that it minimizes the rms error of the estimates, among all the other linear estimators, one of which is the integral of Hotine.

2. Increase of the cap size can never cause increase of $\varepsilon\Delta T$ in the case of lsc, no matter what the error properties of the data are. This is not the case when the integral formula is used, as it was also seen in section 4.2.2, due to the accumulation of propagated error caused by the increase of the number of measurements.

3. The reciprocal distance error covariance model yields more pessimistic results than the Gauss-Markov model in the case of lsc, as it was also the case when the truncation theory was used to estimate the error $\varepsilon\Delta T$.

4. The error estimates from the two techniques are generally in good agreement, the largest difference being on the order of 3 kgal cm (~ 21%).

Finally, summarizing the results of the previous sections, the error analysis performed here indicates that with the combination GPB/OSU89B model, used to $N_{max} = 250$, and with gravity disturbance data on a 2° cap, accurate to 2 mgals, geopotential differences accurate to ~ 12 kgal cm are achievable for stations separated by 30° (about 3300 km). If the error of the cap data reduces to 1 mgal, the corresponding $\varepsilon\Delta T$ becomes about 8.5 kgal cm, which is a comparable figure with the current accuracies of geocentric positions estimated using satellite techniques.

4.3 Introduction of Gravity Disturbance Data at Altitude

The GPS/GPB SST configuration is considered here, as the observational system that provides the gravity disturbance data at altitude. The long-wavelength reference geopotential model used in the least-squares collocation (with ring averages) error analysis that is presented next, is assumed to be the product of a global dynamic solution, based on smoothed values of the SST data, as was discussed in section 2.4. The maximum degree of this model is taken initially equal to 20 for two reasons. First, to avoid the systematic errors on the gravity disturbance at altitude, arising from the residual centrifugal acceleration term δR_{io} as explained in section 2.4 (see Table 3), and second, to permit a higher signal-to-noise ratio for the data at altitude, as opposed to higher degrees of

truncation. Two different caps sizes ($\psi_0^S = 5°, 10°$) were considered for the data at altitude, and for each case two different ring spacings were used ($\Delta\psi^S = 30', 60'$). Data density of one observation per square degree at altitude, implies an integration interval of about 13 seconds, for the polar 10-day repeat orbit of GPB, based on an approximate formula given by Jekeli and Rapp (1980). Considering also terrestrial gravity disturbance data in caps of semi-aperature 2° and ring spacing 6', the error estimates $\varepsilon\Delta T$ for station separation $\psi_d = 30°$ were computed, using also different assumptions for the error properties of the data at altitude ($m_0^S = 0.4, 0.2$ mgal). The results are given in Table 11.

Table 11. Geopotential Difference Errors Implied by the Combination of Gravity Disturbance Data on the Earth and at Altitude. (All Errors are in kgal cm).

		$\bar{\sigma}^{(2)}(\psi)$ ($\psi^c = 0°.1$)		$\bar{\sigma}^{(3)}(\psi)$ ($\psi^c = 0°.1$)	
ψ_0^S	$\Delta\psi^S$	$m_0^S = 0.4$ mgal	0.2 mgal	0.4 mgal	0.2 mgal
5°	30'	16.1	13.5	21.2	15.8
	60'	17.6	14.4	21.9	16.2
10°	30'	15.7	12.9	20.2	15.4
	60'	17.2 (15.0)	13.9 (13.2)	20.8 (15.7)	15.8 (14.0)

ψ_0^S : cap size at altitude
angular separation between stations $\psi_d = 30°$, $h_{GP\text{-}B} = 600$ km
Terrestrial Caps : $\psi_0^T = 2°$, $\Delta\psi^T = 6'$
Terrestrial Gravity Disturbance Error : $\bar{\sigma}^{(3)}(\psi)$, $m_o = 2$ mgal, $\psi^c = 0°.1$
Reference Geopotential Model : GPB to Nmax = 20 (Parenthetical Values Computed with $N_{max} = 45$).

As it can be seen from Table 11, the reciprocal distance error covariance model $\bar{\sigma}^{(3)}(\psi)$ yields again the most pessimistic results. This can be attributed to the fact that the downward continuation process involving the data at altitude, amplifies the error power in the degree range 150-750, in which range the reciprocal distance error model has more power concentrated than the first-order Gauss-Markov model (see Figure 14a). Although the downward continuation amplifies the error power throughout the band, the lower-degree part is dominated in the above estimation scheme by the reference model, while the very high part of the error spectrum has small effect on the estimated geopotential differences.

Overall, the error estimates given in Table 11 are of comparative magnitude with those obtained in the absence of the data at altitude. In order to enable a more systematic comparison between the two cases, in Table 12 the error estimates $\varepsilon\Delta T$ obtained on the basis of terrestrial data only, and various reference geopotential models, are summarized. These were computed using least-squares collocation with ring averages to enable a fair comparison with the estimates of Table 11. Comparing now the error $\varepsilon\Delta T$ from Table 11 for the case $N_{max} = 45$, $\bar{\sigma}^{(3)}(\psi)$, $m_0 = 0.4$ mgal, $\psi_0^S = 10°$, $\Delta\psi^S = 60'$ (15.7 kgal cm), to the corresponding 16.9 kgal cm from Table 12, one can see that an improvement of about 7% is achievable by the introduction of the data at altitude. Although small, such an improvement indicates two things:

(a) The error properties assigned to the data at altitude according to the reciprocal distance error covariance model with variance 0.4 mgal and correlation length 0°.1, appear to provide a realistic assessment of the quality of them. A larger improvement would imply that the error properties assigned to these data are too optimistic and in disagreement with the error budget based on which the error estimates of the global geopotential solution GPB were derived.

Table 12. Geopotential Difference Error $\varepsilon\Delta T$ Implied by Current and Future Reference Models and Terrestrial Gravity Disturbance Data in a 2° Cap.

		$\varepsilon\Delta T$ (kgal cm)		
Model	ψ_d	$N_{max} = 25$	$N_{max} = 45$	$N_{max} = 250$
	5°	46.7	22.7	18.8
OSU89B	10°	48.9	26.7	23.2
	30°	47.4	26.5	23.3
TOPEX/	5°	45.8	20.1	16.0
OSU89B	10°	46.8	20.5	16.9
(25/250)	30°	45.0	20.3	16.5
GPB/	5°	45.6	16.9	11.4
OSU89B	10°	46.5	16.7	11.4
(45/250)	30°	44.8	16.9	11.7

$\psi_0^T = 2°$, $\Delta\psi^T = 6'$

Gravity Disturbance Error : $\bar{\sigma}^{(3)}(\psi)$, $m_0 = 2$ mgal, $\psi^c = 0°.1$

(b) The introduction of the data at altitude provide a better configuration for the estimation of the geopotential differences, as compared to the use of terrestrial measurements only.

Using pessimistic error estimates as a guideline, one can conclude that measurements from the Gravity Probe B mission (in combination with terrestrial gravity disturbance data in 2° caps) are capable of providing geopotential differences over intercontinental distances, accurate to about 15 to 17 kgal cm. This estimate is an order of magnitude better than what can be achieved using the traditional vertical connections based on MSL monitoring (about 150 kgal cm). However, lacking gravitational information in the medium frequency band ($45 < n < 250$), the results from GPB are about 5 kgal cm worse that those obtained when GPB is augmented by OSU89B in this spectral band ($\varepsilon\Delta T \approx 12$ kgal cm). It should be mentioned though that such augmentation does not guarantee that the estimated geopotential differences are totally free of systematic errors arising from vertical datum inconsistencies, since the harmonics of OSU89B above degree 45 may be contaminated by such errors. To enrich the satellite observations with medium frequency gravitational signal, requires either a lower flying altitude, or additional on-board instrumentation capable of measuring higher-order gradients of the gravitational potential, and in this direction the ARISTOTELES mission may provide a significant contribution.

Finally, it should be emphasized here that the error estimates evaluated for the geopotential differences in this chapter, account for errors of the reference geopotential model and the gravity disturbance data only. Additional error contribution to the geopotential difference will arise due to random errors of the geocentric positions of the stations and due to a systematic offset of the origin of the coordinate system from the geocenter, as discussed by Colombo (1980) and Hajela (1983). Random position errors at the $\pm$ 5 cm level (Smith et al., 1985) have small effect on the estimated geopotential differences, while the systematic error due to non-geocentricity of the reference frame can have significant effect on the intercontinental connections.

CHAPTER V

SUMMARY, CONCLUSIONS AND RECOMMENDATIONS

The problem of estimation of geopotential differences over intercontinental locations was re-examined, in order to assess currently achievable accuracies and future anticipated improvements. Accurate estimation of the geopotential differences between points located at different continents, imply the unification of the vertical datums established in them, which at present are defined based on MSL monitoring and thus are (in general) inconsistent due to the presence of the Quasi-stationary Sea Surface Topography.

A review of the proposed techniques for the unification of vertical datums, in conjunction with anticipated future satellite missions and in view of the accuracies achievable at present for geocentric positioning, indicated that approaches based on the combination of gravitational information with high accuracy geocentric positioning, are favored at present and in the near future for practical implementation. In this direction, extending the ideas put forward by Colombo (1980), an observational setup was proposed, whereby gravity disturbance measurements on the Earth's surface, in caps surrounding the estimation points, are combined with corresponding data in caps directly over these points at the altitude of a low orbiting satellite, for the estimation of the geopotential difference between the terrestrial stations. The gravity disturbance data at altitude are inferred from GPS measurements made from the low orbiter to the high-altitude GPS satellites, in a multiple-high-single-low Satellite-to-Satellite Tracking configuration. In the absence of actual measurements, the performance of such an observation/estimation scheme was evaluated by conducting an error analysis study.

The mathematical modeling required to relate the primary observables to the parameters to be estimated, was studied both for the terrestrial data and the data at altitude. Emphasis was placed on the examination of systematic effects and the corresponding reductions that need to be applied to the measurements to avoid systematic errors. For the gravitational accelerations inferred from SST data, it was discovered that the magnitude of

a centrifugal acceleration term (δR_{io}) was underestimated by several orders of magnitude in the past as a result of an erroneous derivation. The previous formulation implied a magnitude of δR_{io} about 7×10^5 times smaller than the current corrected formulation. It was shown in this study that in order to keep the systematic effect arising from δR_{io} at the 20 μgal level, a reference geopotential model complete to degree 20 is required (high-low SST configuration). Previous analyses, based on the erroneous formulation, were indicating that a reference model complete to degree 4 is adequate to keep the residual systematic effect of δR_{io} at the 10 μgal level. For a given noise level (0.4 mgal) of the data at altitude, increase of the maximum degree of the reference model, significantly affects the ratio of the residual signal to the noise.

Two different techniques were considered for the estimation of the global mean square error of the geopotential differences. Error propagation using truncation theory, as applied to Hotine's integral formula, and the least-squares collocation using ring averages as input data. Both techniques are applicable in case observations on the Earth's surface only are involved in the geopotential difference estimation, but only lsc can handle efficiently the over-determined case when observations at altitude are added. Alternative formulations related to the sampling (or discretion) and the propagated errors arising in the truncation theory considerations were derived. These are characterized by the same computational requirements as the previous formulation by Christodoulidis (1976), while they provide a more consistent interpretation of the underlying physical principles that give rise to these errors. In an attempt to apply truncation theory principles for the assessment of the contribution of gravitational acceleration data at altitude, to the estimation of geopotential differences on the Earth's surface, recurrence relations for the altitude generalized truncation coefficients implied by Hotine's kernel were developed for the first time.

Both techniques (truncation theory and lsc) require for their implementation a-priori knowledge of the global properties of the signals and the noise involved in the estimation and to this end different covariance models were considered and their spectral characteristics were compared. In addition, an efficient recurrence relation for the degree variances implied by a first-order Gauss-Markov covariance model was developed for the first time in this study.

For the numerical analysis, three global geopotential solutions were considered as reference models. The currently available OSU89B high-degree harmonic expansion, and the global models anticipated to become available from GPS tracking data of the TOPEX/Poseidon and the Gravity Probe B spacecrafts respectively. Augmentations of the latter two models with higher-degree harmonics from OSU89B were also considered. A number of numerical experiments were performed that lead to the following conclusions:

(a) The currently available global geopotential model OSU89B alone is expected to yield geopotential differences between stations separated by 30°, accurate to about 86 kgal cm. The future models (augmented by OSU89B) can improve this accuracy to about 81 kgal cm (TOPEX/OSU89B) and 74 kgal cm (GPB/OSU89B) respectively.

(b) Introduction of gravity disturbance measurements in terrestrial 2° caps reduces the previous error estimates to the following: 23 kgal cm (OSU89B), 17 kgal cm (TOPEX/OSU89B) and 12 kgal cm (GPB/OSU89B), when pessimistic error estimates are used for the gravity disturbance measurements ($m_0 = 2$ mgal). With $m_0 = 1$ mgal the case GPB/OSU89B yields an error of about 9 kgal cm for 30° station separation. The error estimates for these cases were computed using both truncation theory and lsc (ring averages) and the results from the two techniques were compared. It was found that the lsc error estimates are always smaller than the ones obtained from truncation theory, as mandated from theory. The largest difference between the two error estimates was found to be about 21%.

(c) When gravity disturbance data at the altitude of GP-B (about 600 km) were introduced, a moderate (7%) improvement in accuracy, over the corresponding case without such data, was found. In both cases, the reference geopotential model used was complete to degree 45, obtained from the analysis of the GPS tracking data on GP-B. However, gravity disturbance data at this altitude are unable to resolve medium and high frequency variations of the gravity field and thus the result in this case is inferior by about 5 kgal cm to the result obtained from the combined GPB/OSU89B high-degree model (complete to degree 250).

To enrich the data at altitude with more high-frequency information, it is recommended here that additional measurements of a higher-order gradient of the

disturbing potential made from a lower flying spacecraft, be incorporated in the estimation. In this direction, the gradiometer data from ARISTOTELES mission can provide a significant contribution. In addition, it should be emphasized that the error estimates reported here correspond to a "worst-case" scenario where only one pair of benchmarks is considered for the intercontinental connection. Additional benchmarks on each continent, connected with leveling lines, can provide a better network configuration and yield an improvement on the accuracy of the intercontinental connections up to 25%, as the study by Hajela (1983) has indicated.

Finally, the results reported here are promising enough to warrant an actual testing of the technique. For this purpose, stations whose geocentric coordinates are accurately known (e.g. SLR sites or VLBI stations connected to a geocentric system using GPS) and between which the geopotential difference has been estimated independently using spirit leveling and gravimetry can be used as test sites. At present (1991), collection of gravity disturbance measurements (using relative GPS positioning and gravimetry) in caps surrounding these test sites, will enable testing of the procedure described in section 4.2. As it was discussed in that section, a cap size of 2° and an approximate spacing of 6' between the points where the gravity disturbances are determined, are optimum parameters for the observational setup, provided a state-of-the-art high-degree global geopotential model (e.g. OSU89B) is used as reference. In the actual implementation, least-squares collocation using the original gravity disturbance data (as opposed to ring-averages) should be used to maintain highest computational rigor. In addition, detailed elevation information around the test sites should be used for the consideration of the terrain effects by means of analytical continuation, as it was discussed in section 2.3.

In a more future time frame (1995), the availability of the data from the anticipated satellite missions (TOPEX/Poseidon, Gravity Probe-B, ARISTOTELES), will enable to improve the above scheme in two ways. First, by the use of global geopotential models with more accurately estimated lower-degree harmonics than those of OSU89B, as such models will become available from the analysis of the global sets of observations collected by these missions, and second by the use of gravitational information in caps at altitude (GP-B, ARISTOTELES), as discussed in section 4.3.

APPENDIX A

RECURRENCE RELATIONS FOR THE TRUNCATION COEFFICIENTS IMPLIED BY PIZZETTI'S EXTENSION OF HOTINE'S KERNEL

The development of recurrence relations for the coefficients $Q_n(R/r, \psi_o)$, defined by:

$$Q_n(R/r, \psi_o) = \int_{\psi_o}^{\pi} H(R/r, \psi) P_n(\cos\psi) \sin\psi d\psi \qquad ; \; r \geq R \tag{A.1}$$

is based on recurrence relations of the Legendre polynomials. Denoting $P_n(t)$ (or simply P_n) the n^{th} - degree Legendre polynomial, and $P_n'(t)$ (or simply P_n') its first derivative with respect to the argument t, the following relations hold true (Hobson, 1965, Ch. II, Sect. 20):

$$nP_n = -(n-1)P_{n-2} + (2n-1)tP_{n-1} \tag{A.2}$$

$$(2n+1)P_n = P_{n+1}' - P_{n-1}' \tag{A.3}$$

$$(1 - t^2)P_n' = n(P_{n-1} - tP_n) \tag{A.4}$$

$$P_n(-1) = (-1)^n \tag{A.5}$$

The following notation is introduced:

$$k = \frac{R}{r} \qquad ; \; 0 < k \leq 1 \tag{A.6}$$

$$t = \cos\psi \qquad ; \; -1 \leq t < 1 \tag{A.7}$$

$$D^2 = 1 - 2kt + k^2 \tag{A.8}$$

Accordingly, Pizzetti's extension of Hotine's kernel takes the closed form:

$$H(k,t) = \frac{2k}{D} - \ln\left(\frac{D + k - t}{1 - t}\right) \qquad ; \; t \neq 1 \tag{A.9}$$

and the series expansion form:

$$H(k,t) = \sum_{n=0}^{\infty} \frac{2n+1}{n+1} k^{n+1} P_n(t) \quad . \tag{A.10}$$

With the change of integration variable from ψ, to $t = \cos\psi$, and the substitution $x = \cos\psi_o$, equation (A.1) becomes:

$$Q_n(k,x) = \int_{-1}^{x} H(k,t)\, P_n(t)dt \tag{A.11}$$

or, due to (A.9):

$$Q_n(k,x) = 2k\int_{-1}^{x} \frac{P_n(t)}{D}dt - \int_{-1}^{x} \ln\left(\frac{D+k-t}{1-t}\right) P_n(t)dt \quad . \tag{A.12}$$

It will be understood in all subsequent derivations that $\psi_o \neq 0$ so that $x \neq 1$. The case $\psi_o = 0$ will be considered separately at the end.

For the purposes of the subsequent derivations, a number of auxiliary quantities are defined next:

$$\left.\begin{aligned} I_n(x) &= \int_{-1}^{x} P_n(t)dt && \text{(a)} \\ L_n'(k,x) &= \int_{-1}^{x} \frac{P_n(t)}{D}dt && \text{(b)} \\ K_n'(k,x) &= \int_{-1}^{x} \frac{P_n(t)}{D^3}dt && \text{(c)} \\ M_n(k,x) &= \int_{-1}^{x} \frac{P_n'(t)}{D}dt && \text{(d)} \end{aligned}\right\} \tag{A.13}$$

To develop recurrence relations for $Q_n(k, x)$, one starts with recurrence relations for some of the auxiliary quantities defined before.

From (A.2) one has:

$$P_n(x) = \frac{1}{n}[(2n - 1)\,xP_{n-1}(x) - (n-1)P_{n-2}(x)] \qquad ; n \geq 2 \tag{A.14a}$$

which, with starting values:

$$P_0(x) = 1 \qquad ; \quad P_1(x) = x \tag{A.14b}$$

establishes a recurrence relation for the Legendre polynomials.

From (A.3) and (A.5) one has:

$$I_n(x) = \frac{1}{2n + 1}[P_{n+1}(x) - P_{n-1}(x)] \qquad ; n \geq 1 \tag{A.15}$$

Although equation (A.15), along with the recurrence (A.14a,b), are sufficient to evaluate $I_n(x)$, an independent recurrence for $I_n(x)$ may be developed as follows. Equation (A.15) is written as:

$$-(n - 2)I_{n-2}(x) = -\frac{n-2}{2n-3}P_{n-1}(x) + \frac{n-2}{2n-3}P_{n-3}(x) \tag{A.16}$$

In addition, from (A.15) one has:

$$(2n - 1)xI_{n-1}(x) = xP_n(x) - xP_{n-2}(x) \tag{A.17}$$

Now, from equation (A.2) one may write:

$$xP_n(x) = \frac{n+1}{2n+1}P_{n+1}(x) + \frac{n}{2n+1}P_{n-1}(x) \tag{A.18a}$$

and:

$$-xP_{n-2}(x) = -\frac{n-1}{2n-3}P_{n-1}(x) - \frac{n-2}{2n-3}P_{n-3}(x) \tag{A.18b}$$

Adding by parts (A.16), (A.18a) and (A.18b), and taking into account (A.17), one has:

$$(2n - 1)xI_{n-1}(x) - (n - 2)I_{n-2}(x) = \frac{n + 1}{2n + 1}[P_{n+1}(x) - P_{n-1}(x)]$$

which, due to (A.15), finally establishes the following recurrence for $I_n(x)$:

$$I_n(x) = \frac{1}{n + 1}[(2n - 1)xI_{n-1}(x) - (n - 2)I_{n-2}(x)] \quad ; \quad n \geq 2 \qquad (A.19a)$$

with starting values:

$$I_0(x) = 1 + x \quad ; \quad I_1(x) = \frac{1}{2}(x^2 - 1) \quad . \qquad (A.19b)$$

For $L_n'(k, x)$, due to (A.3), one has:

$$L_n'(k, x) = \frac{1}{2n + 1}\left[\int_{-1}^{x} \frac{P_{n+1}'}{D}\,dt - \int_{-1}^{x} \frac{P_{n-1}'}{D}\,dt\right]$$

so, due to (A.13d):

$$L_n'(k, x) = \frac{1}{2n + 1}[M_{n+1}(k, x) - M_{n-1}(k, x)] \qquad (A.20)$$

With $dv = P_n'(t)dt$ ($v = P_n(t)$), and $w = D^{-1}$ ($dw = kD^{-3}dt$), integration by parts yields for $M_n(k, x)$:

$$M_n(k, x) = \frac{P_n(x)}{D_x} - \frac{(-1)^n}{(1 + k)} - kK_n'(k, x) \qquad (A.21)$$

where:

$$D_x = (1 - 2kx + k^2)^{1/2} \quad . \qquad (A.22)$$

Equations (A.20), (A.21) and (A.15), yield for $L_n'(k, x)$:

$$L_n'(k, x) = \frac{-k}{2n + 1}\left[K_{n+1}'(k, x) - K_{n-1}'(k, x)\right] + \frac{I_n(x)}{D_x} \quad ; \quad n \geq 1 \qquad (A.23)$$

Consider $K_n'(k, x)$ next. The definition (A.13c) and equation (A.2) imply:

$$(n + 1)K_{n+1}' + nK_{n-1}' = (2n + 1)\int_{-1}^{x} \frac{tP_n(t)}{D^3}\,dt \tag{A.24}$$

However, it can be easily verified that:

$$\frac{t}{D^3} = \frac{1 + k^2}{2k}\left[\frac{1}{D^3} - \frac{1}{D(1 + k^2)}\right] \tag{A.25}$$

Due to (A.25), the right-hand side of (A.24), becomes:

$$(2n + 1)\int_{-1}^{x} \frac{tP_n(t)}{D^3}dt = (2n + 1)\frac{1 + k^2}{2k}K_n' - \frac{2n + 1}{2k}\int_{-1}^{x} \frac{P_n(t)}{D}dt$$

so that, taking also into account the definition of $L_n'(k, x)$, equation (A.24) becomes:

$$2k\left[(n + 1)K_{n+1}' + nK_{n-1}'\right] = (2n + 1)\left[(1 + k^2)K_n' - L_n'\right] \tag{A.26}$$

Eliminating L_n' from equations (A.23) and (A.26), one obtains:

$$kK_{n+1}'(k, x) - (1 + k^2)K_n'(k, x) + kK_{n-1}'(k, x) = -\frac{I_n(x)}{D_x} \quad ; \; n \geq 1 \tag{A.27}$$

In addition, direct integration yields:

$$\left.\begin{aligned} &\int \frac{dt}{D^3} = \frac{1}{kD} && \text{(a)} \\ &\int \frac{tdt}{D^3} = \frac{1}{k^2 D}(1 - kt + k^2) && \text{(b)} \end{aligned}\right\} \tag{A.28}$$

Hence, a recurrence relation for $K_n'(k, x)$ may be established as follows:

$$K_n'(k, x) = \frac{1 + k^2}{k}K_{n-1}'(k, x) - K_{n-2}'(k, x) - \frac{I_{n-1}(x)}{kD_x} \quad ; \; n \geq 2 \tag{A.29a}$$

with starting values:

$$K_o'(k, x) = \frac{1}{kD}\Big|_{-1}^{x} \quad ; \quad K_1'(k, x) = \frac{1}{k^2 D}(1 - kt + k^2)\Big|_{-1}^{x} \tag{A.29b}$$

One may now express $K_{n+1}'(k, x)$ in terms of $K_n'(k, x)$ and $K_{n-1}'(k, x)$ from equation (A.29a), and then substitute this expression in equation (A.23), so that finally the following recurrence relation is established for $L_n'(k, x)$:

$$L_n'(k, x) = \frac{1}{2n + 1}\left[2kK_{n-1}'(k, x) - (1 + k^2)K_n'(k, x) + 2(n + 1)\frac{I_n(x)}{D_x}\right] \quad ; \; n \geq 2 \tag{A.30a}$$

with starting values:

$$L_o'(k, x) = -\frac{D}{k}\Big|_{-1}^{x} \quad ; \quad L_1'(k, x) = -\frac{D}{3k^2}(1 + kt + k^2)\Big|_{-1}^{x} \tag{A.30b}$$

which were obtained by direct integration applied to the definition of $L_n'(k, x)$ given in (A.13b). Notice that the recurrence (A.30a) may actually start from n = 1, however, it is computationally convenient to start it from n = 2, the same degree from which the $P_n(x)$, $I_n(x)$, $K_n'(x)$ recurrence relations start.

With the previous derivations as a background, one proceeds now with the development of recurrence relations for $Q_n(k, x)$, as follows. From equations (A.12) and (A.13b) one has:

$$Q_n(k, x) = 2kL_n'(k, x) - \int_{-1}^{x} \ln\left(\frac{D + k - t}{1 - t}\right) P_n(t)dt \quad .$$

Define:

$$R_n'(k, x) = -\int_{-1}^{x} \ln\left(\frac{D + k - t}{1 - t}\right) P_n(t)dt \tag{A.31}$$

so that the previous equation becomes:

$$Q_n(k, x) = 2kL_n'(k, x) + R_n'(k, x) \quad ; \; n \geq 0 \tag{A.32}$$

Due to equation (A.2), equation (A.31) becomes:

$$R_n' = -\frac{n-1}{n} R_{n-2}' - \frac{2n-1}{n} \int_{-1}^{x} \ln\left(\frac{D+k-t}{1-t}\right) t P_{n-1}(t)dt$$

which due to (A.4) becomes:

$$R_n' = R_{n-2}' + \frac{2n-1}{n(n-1)} \int_{-1}^{x} (1-t^2) P_{n-1}'(t) \ln\left(\frac{D+k-t}{1-t}\right)dt \qquad (A.33)$$

The integral on the right-hand side of (A.33) may be evaluated using integration by parts. Let:

$$dv = P_{n-1}'(t)dt \Rightarrow v = P_{n-1}(t) \qquad (A.34)$$

and:

$$w = (1-t^2)\ln\left(\frac{D+k-t}{1-t}\right) \qquad (A.35a)$$

It is a matter of algebraic manipulations, to show that:

$$dw = \left[-2t\ln\left(\frac{D+k-t}{1-t}\right) + \frac{kt}{D} - \frac{1}{D} + 1\right]dt \qquad (A.35b)$$

Hence, integration by parts in equation (A.33) yields:

$$R_n' = R_{n-2}' + \frac{2n-1}{n(n-1)}(1-x^2)\ln\left(\frac{D_x+k-x}{1-x}\right)P_{n-1}(x)$$

$$+ \frac{2(2n-1)}{n(n-1)} B_{n-1}' - \frac{2n-1}{n(n-1)} A_{n-1}' - \frac{2n-1}{n(n-1)} I_{n-1}(x) \qquad (A.36)$$

where:

$$A_n' = \int_{-1}^{x} \frac{kt-1}{D} P_n(t)dt \qquad (A.37)$$

and:

$$B_n' = \int_{-1}^{x} \ln\left(\frac{D+k-t}{1-t}\right) t P_n(t)dt \qquad (A.38)$$

For B_n', due to equation (A.2) and the definition (A.31) one has:

$$B'_{n-1} = -\frac{n}{2n-1} R'_n - \frac{n-1}{2n-1} R'_{n-2} \tag{A.39}$$

For A_n', due to the definition (A.13b) one has:

$$A'_{n-1} = k\int_{-1}^{x} \frac{t}{D} P_{n-1}(t)dt - L'_{n-1} ,$$

which due to equation (A.2) becomes:

$$A'_{n-1} = k\left[\frac{n}{2n-1}\int_{-1}^{x}\frac{P_n(t)}{D}dt + \frac{n-1}{2n-1}\int_{-1}^{x}\frac{P_{n-2}(t)}{D}dt\right] - L'_{n-1}$$

which finally becomes:

$$-\frac{2n-1}{n(n-1)} A'_{n-1} = -k\left[\frac{1}{n-1} L'_n + \frac{1}{n} L'_{n-2}\right] + \frac{2n-1}{n(n-1)} L'_{n-1} \tag{A.40}$$

Substituting (A.39) and (A.40) in equation (A.36), one obtains the following recurrence relation for $R_n'(k, x)$:

$$R'_n(k, x) = \frac{1}{n(n+1)}\Big\{(n-2)(n-1) R'_{n-2}(k, x) + (2n-1)(1-x^2)\ln\left(\frac{D_x + k - x}{1-x}\right) P_{n-1}(x)$$

$$-k\left[nL'_n(k, x) + (n-1)L'_{n-2}(k, x)\right]$$

$$+(2n-1)\left[L'_{n-1}(k, x) - I_{n-1}(x)\right]\Big\} ; \quad n \geq 2 \tag{A.41}$$

which requires starting values for $R_0'(k, x)$ and $R_1'(k, x)$. These may be obtained by direct integration applied to equation (A.31) that defines $R_n'(k, x)$. Let:

$$r'_o(k, t) = -\int \ln\left(\frac{D + k - t}{1 - t}\right) dt$$

$$r_1'(k, t) = -\int t \ln\left(\frac{D + k - t}{1 - t}\right) dt$$

It can be shown that:

$$r_o'(k, t) = \frac{1}{2k}\left[D^2 \ln\left(\frac{D + k - t}{1 - t}\right) - (1 + k)^2 \ln(D + k + 1) + (1 - k)^2 \ln(D - k + 1) + 2kD\right] \tag{A.42a}$$

$$r_1'(k, t) = \frac{1}{2k}\left\{k\left[\ln(D + k + 1) - \ln(D - k + 1)\right] - \frac{1}{2}\left[\frac{D^3}{3} - D^2 + (1 - k^2) D\right] - kt^2 \ln\left(\frac{D + k - t}{1 - t}\right)\right\} \tag{A.42b}$$

so that the starting values $R_o'(k, x)$ and $R_1'(k, x)$ are given by:

$$\left.\begin{aligned} R_o'(k, x) &= r_o'(k, t)\Big|_{-1}^{x} \qquad (a) \\ R_1'(k, x) &= r_1'(k, t)\Big|_{-1}^{x} \qquad (b) \end{aligned}\right\} \tag{A.43}$$

The recurrence relation for $R_n'(k, x)$ was the last relation required to establish a recursive algorithm for the computation of the truncation coefficients $Q_n(k, x)$. In summary, for $\psi_o \neq 0$ ($x = \cos\psi_o \neq 1$), the recursive evaluation of $Q_n(k, x)$ is accomplished by computing the following quantities:

1. $P_n(x)$ from equations (A.14a, b)
2. $I_n(x)$ from equations (A.19a, b)
3. $K_n'(k, x)$ from equations (A.29a, b)
4. $L_n'(k, x)$ from equations (A.30a, b)
5. $R_n'(k, x)$ from equations (A.41) through (A.43)
6. Finally $Q_n(k, x)$ is given by equation (A.32)

Two issues concerning the above recurrence should be mentioned:

a) The recurrence for $K_n'(k, x)$ is only required for the evaluation of $L_n'(k, x)$. In the special case that r = R (i.e. k = 1), Jekeli (1979) has succeeded in eliminating $K_n'(k, x)$ from the recursive algorithm, by manipulating equations corresponding to (A.29a) and (A.30a). However, this technique cannot be applied in the current case where k assumes arbitrary values in the interval (0, 1].

b) Although mathematically correct, and useful for low altitude applications, the recurrence presented here for $Q_n(k, x)$ has numerical instability problems for high altitude cases. The instability is introduced to the algorithm through the use of equation (A.29a) that determines $K_n'(k, x)$. As it can be seen from (A.29a), the division by k introduces numerical problems as $k \to 0$ (i.e. as the altitude increases). Through numerical tests (using double precision arithmetic) it was verified that for altitude equal to 600 km, and ψ_0 as small as one degree, the coefficients $Q_n(k, x)$ become unreliable after $n \approx 600$. This problem is of the same nature with the numerical instability encountered by Shepperd (1979) in the recurrence relation which he derived for the altitude generalized truncation coefficients corresponding to Stokes' kernel (ibid, p. B-3).

Finally , to complete the determination of $Q_n(k, x)$, one needs to derive the expression for $Q_n(k, 1)$, i.e. consider the case $\psi_0 = 0$ (x = 1), which was excluded from the above algorithm. Although H(k, t) has a singularity at t = 1 (see equation (A.9)), $Q_n(k, x)$ is nevertheless well-defined for x = 1. Taking into account equation (A.10), it can be easily seen that:

$$Q_n(k, 1) = \frac{2}{n+1} k^{n+1} \quad ; \quad n \geq 0 \quad . \tag{A.44}$$

APPENDIX B

TRUNCATION COEFFICIENTS IMPLIED BY THE KERNEL $H^*(k, t) = H(k, t) - k - \frac{3}{2}k^2t$

In case the gravity disturbance, $\delta g(r, \theta, \lambda)$, contains no zeroeth- and first-degree terms, one needs to determine the truncation coefficients $Q_n^*(k, x)$ implied by the kernel function $H^*(k, t)$, where:

$$H^*(k, t) = H(k, t) - k - \frac{3}{2}k^2t \tag{B.1}$$

or, in series expansion form:

$$H^*(k, t) = \sum_{n=2}^{\infty} \frac{2n + 1}{n + 1} k^{n+1} P_n(t) \quad . \tag{B.2}$$

The truncation coefficients $Q_n^*(k, x)$ are defined by:

$$Q_n^*(k, x) = \int_{-1}^{x} H^*(k,t) P_n(t) dt \tag{B.3}$$

or,

$$Q_n^*(k, x) = Q_n(k, x) - k\int_{-1}^{x} P_n(t) dt - \frac{3}{2}k^2 \int_{-1}^{x} tP_n(t) dt \tag{B.4}$$

Utilizing the results of Appendix A, one has from (A.13a):

$$\int_{-1}^{x} P_n(t) dt = I_n(x) \tag{B.5a}$$

while, due to equation (A.2):

$$\int_{-1}^{x} tP_n(t)dt = \frac{n+1}{2n+1} I_{n+1}(x) + \frac{n}{2n+1} I_{n-1}(x)$$

The last equation, due to (A.19a), may be rewritten as:

$$\int_{-1}^{x} tP_n(t)dt = \frac{n+1}{n+2} xI_n(x) + \frac{1}{n+2} I_{n-1}(x) \qquad \text{(B.5b)}$$

Due to (B.5a,b) equation (B.4) finally becomes:

$$Q_n^*(k, x) = Q_n(k, x) - \left\{ kI_n(x) + \frac{3k^2}{2n+4} [(n+1)xI_n(x) + I_{n-1}(x)] \right\} \quad ; \; n \geq 2 \qquad \text{(B.6)}$$

and, along with the starting values:

$$\left.\begin{aligned} Q_o^*(k, x) &= Q_o(k, x) - \left[k(x+1) + \frac{3k^2}{4} (x^2 - 1) \right] \qquad \text{(a)} \\ Q_1^*(k, x) &= Q_1(k, x) - \left[\frac{k}{2} (x^2 - 1) + \frac{k^2}{2} (x^3 + 1) \right] \qquad \text{(b)} \end{aligned}\right\} \qquad \text{(B.7)}$$

(which have been obtained by direct integration performed in equation (B.4)) defines the recurrence relation required to evaluate the coefficients $Q_n^*(k, x)$, from the already derived recurrences for $Q_n(k, x)$ and $I_n(x)$ (see Appendix A).

The recurrence relation (B.6) is valid regardless of the value of ψ_o. If $\psi_o = 0$, then $Q_n(k,1)$ in (B.6) are obtained from equation (A.44); otherwise the $Q_n(k, x)$ are obtained from equation (A.32). If one rewrites equation (B.4) as:

$$Q_n^*(k, x) = Q_n(k, x) - k \int_{-1}^{x} P_o(t) P_n(t)dt - \frac{3}{2} k^2 \int_{-1}^{x} P_1(t) P_n(t)dt \qquad \text{(B.8)}$$

which is valid for $n \geq 0$, then it can be seen easily that:

(a) $Q_n^*(k, 1) = Q_n(k, 1)$ for every $n \geq 2$

(b) $Q_o^*(k, 1) = Q_1^*(k, 1) = 0$, while $Q_o^*(k, x)$ and $Q_1^*(k, x)$ are not equal to zero for $x \neq 1$.

APPENDIX C

DEGREE VARIANCES OF A FIRST-ORDER GAUSS-MARKOV PROCESS ON THE SPHERE

Consider the homogeneous and isotropic first-order Gauss-Markov stochastic process on the sphere, defined through its covariance function:

$$\sigma(\psi) = c.e^{-\lambda\psi} \qquad ; \qquad c > 0\,,\, \lambda > 0 \tag{C.1}$$

where ψ is the spherical distance in radians. The degree variances of the above covariance function constitute the power spectrum of the process, and are given by the Legendre transform of $\sigma(\psi)$. Using unnormalized spherical harmonics, due to isotropy, one has for the degree variance at degree n:

$$\sigma_n = \frac{2n+1}{4\pi} \int_{\psi=0}^{\pi} \int_{\alpha=0}^{2\pi} \sigma(\psi) P_n(\cos\psi) \sin\psi \, d\psi \, d\alpha \tag{C.2}$$

or, due to (C.1):

$$\sigma_n = \frac{2n+1}{2} c \int_0^{\pi} e^{-\lambda\psi} P_n(\cos\psi) \sin\psi \, d\psi \tag{C.3}$$

Let:

$$A_n(\lambda) = \int_0^{\pi} \exp(-\lambda\psi) P_n(\cos\psi) \sin\psi \, d\psi \tag{C.4}$$

so that σ_n is given by:

$$\sigma_n = \frac{2n+1}{2} c A_n(\lambda) \tag{C.5}$$

One proceeds next with the derivation of an expression for $A_n(\lambda)$. Changing the variable from ψ to $t = \cos\psi$, one has from (C.4):

$$A_n(\lambda) = \int_{-1}^{1} \exp(-\lambda\cos^{-1}t)P_n(t)dt$$

which, due to equation (A.3) of Appendix A, yields:

$$A_n(\lambda) = \frac{1}{2n+1}\int_{-1}^{1} \exp(-\lambda\cos^{-1}t)(P'_{n+1} - P'_{n-1})dt \quad . \tag{C.6}$$

With $w = \exp(-\lambda\cos^{-1}t)$ (hence $dw = \lambda w\,(1 - t^2)^{-1/2}dt$), and $dv = (P'_{n+1} - P'_{n-1})dt$ (hence $v = P_{n+1}(t) - P_{n-1}(t)$), integration by parts in equation (C.6), yields:

$$A_n(\lambda) = \frac{\lambda}{2n+1}\int_{-1}^{1} \exp(-\lambda\cos^{-1}t)(1 - t^2)^{-1/2}\,(P_{n-1} - P_{n+1})dt \tag{C.7}$$

where, in deriving (C.7), use was made of equation (A.5) of Appendix A. From Hobson (1965, equation 20.36), one has:

$$(2n+1)(t^2 - 1)P'_n = n(n+1)(P_{n+1} - P_{n-1}) \tag{C.8}$$

according to which, equation (C.7) becomes:

$$A_n(\lambda) = \frac{\lambda}{n(n+1)}\int_{-1}^{1} \exp(-\lambda\cos^{-1}t)(1 - t^2)^{1/2}P'_n dt \quad . \tag{C.9}$$

Now let:

$$w = \exp(-\lambda\cos^{-1}t)(1 - t^2)^{1/2}$$

so that:

$$dw = \exp(-\lambda\cos^{-1}t)\left[\lambda - t(1 - t^2)^{-1/2}\right]dt$$

and, $dv = P'_n\,dt$ (hence, $v = P_n(t)$). Then, integration by parts in equation (C.9) yields:

$$A_n(\lambda) = \frac{\lambda}{n(n+1)}\left[\int_{-1}^{1} \exp(-\lambda\cos^{-1}t)(1-t^2)^{-1/2} t P_n dt - \lambda A_n(\lambda)\right]$$

which, due to equation (A.4) of Appendix A, yields:

$$A_n(\lambda) = \frac{\lambda}{n(n+1)}\left[\int_{-1}^{1} \exp(-\lambda\cos^{-1}t)(1-t^2)^{-1/2} P_{n-1} dt \right.$$

$$\left. - \frac{1}{n}\int_{-1}^{1} \exp(-\lambda\cos^{-1}t)(1-t^2)^{1/2} P_n' dt - \lambda A_n(\lambda)\right]$$

which, taking into account equation (C.9), reduces finally to:

$$[(n+1)^2 + \lambda^2]A_n(\lambda) = \lambda\int_{-1}^{1} \exp(-\lambda\cos^{-1}t)(1-t^2)^{-1/2} P_{n-1} dt \qquad (C.10)$$

Evaluating (C.10) for n = n - 2 and subtracting (C.10) from the corresponding equation, one obtains:

$$[(n-1)^2 + \lambda^2]A_{n-2}(\lambda) - [(n+1)^2 + \lambda^2]A_n(\lambda) = \lambda\int_{-1}^{1} \exp(-\lambda\cos^{-1}t)(1-t^2)^{-1/2}(P_{n-3} - P_{n-1})\, dt$$

The right-hand side of the last equation equals, due to (C.7), to (2n - 3) $A_{n-2}(\lambda)$ so that the preceding equation, after the algebraic simplifications, yields:

$$A_n(\lambda) = \frac{\lambda^2 + (n-2)^2}{\lambda^2 + (n+1)^2} A_{n-2}(\lambda) \qquad (C.11)$$

Considering now equation (C.5), it can be easily seen that the degree variances of $\sigma(\psi)$ may be evaluated from the following recurrence relation:

$$\sigma_n = \frac{2n+1}{2n-3}\frac{\lambda^2 + (n-2)^2}{\lambda^2 + (n+1)^2}\sigma_{n-2} \quad ; \quad n \geq 2 \qquad (C.12)$$

which requires starting values for σ_0 and σ_1. These are obtained by direct integration performed in equation (C.3) which yields:

$$\left.\begin{aligned} \sigma_o &= \frac{c}{2}\frac{1+e^{-\lambda\pi}}{\lambda^2+1} \qquad (a) \\ \sigma_1 &= \frac{3c}{2}\frac{1-e^{-\lambda\pi}}{\lambda^2+4} \qquad (b) \end{aligned}\right\} \qquad (C.13)$$

LIST OF REFERENCES

Bjerhammar, A., Gravity Reduction to a Spherical Surface, Technical Report, The Royal Institute of Technology, Geodesy Division, Stockholm, 1962.

Bjerhammar, A., On a Relativistic Geodesy, Bulletin Geodesique, Vol. 59, No. 3, pp. 207-220, 1985.

Brovar, V.V., On the potentials of origins of isolated levelling nets, manuscripta geodaetica, Vol. 13, pp. 29-32, 1988.

Carter, W.E., et al., Geodetic Fixing of Tide Gauge Bench Marks, Technical Report, Woods Hole Oceanographic Institution, Woods Hall, Massachusetts 02543, 1989.

Cartwright, D.E., A Practical Oceanographic Approach to the Problem of Defining a World Vertical Datum, in Proc. of the Third International Symposium on the North American Vertical Datum, Rockville, Maryland, April 21-26, 1985.

Chovitz, B.H., Parameters of Common Relevance of Astronomy, Geodesy, and Geodynamics, Bulletin Geodesique, Vol. 62, No. 3, pp. 359-367, 1988.

Christodoulidis, D.C., On the Realization of a 10 cm Relative Oceanic Geoid, Report No. 247, Dept. of Geodetic Science, The Ohio State University, Columbus, November 1976.

Colombo, O.L., Optimal Kernels for Band-Limited Data, Unisurv G27, Univ. NSW, Sydney, Australia, 1977.

Colombo, O.L., A World Vertical Network, Report No. 296, Dept. of Geodetic Science, The Ohio State University, Columbus, February 1980.

Colombo, O.L., Numerical Methods for Harmonic Analysis on the Sphere, Report No. 310, Dept. of Geodetic Science, The Ohio State University, Columbus, March 1981a.

Colombo, O.L., Global Geopotential Modelling From Satellite-to-Satellite Tracking, Report No. 317, Dept. of Geodetic Science and Surveying, The Ohio State University, Columbus, October 1981b.

Colombo, O.L., Levelling with the Help of Space Techniques, in Proc. of the Third International Symposium on the North American Vertical Datum, Rockville, Maryland, April 21-26, 1985a.

Colombo, O.L., Dear Colleague, letter to the members of Special Study Group 1.75 (SSG 1.75), 1985b.

Colombo, O.L., Charting the Gravity Field With GPS Receivers in Moving Vehicles, paper presented at The Second International Symposium on Precise Positioning With the Global Positioning System, Ottawa, Canada, September 3-7, 1990.

Davis, P.J., Interpolation and Approximation, Dover Publications, New York, 1975.

Denker, H. and R.H. Rapp, Geodetic and Oceanographic Results From the Analysis of 1 Year of Geosat Data, J. Geophys. Res., Vol. 95, No. C8, pp. 13151-13168, August, 1990.

Despotakis, V.K., Geoid Undulation Computations at Laser Tracking Stations, Report No. 383, Dept. of Geodetic Science and Surveying, The Ohio State University, Columbus, September 1987.

Douglas, B.C., C.C. Goad, and F.F. Morrison, Determination of the Geopotential From Satellite-to-Satellite Tracking Data, J. Geophys. Res., Vol. 85, No. B10, pp. 5471-5480, October, 1980.

Engelis, T., Radial Orbit Error Reduction and Sea Surface Topography Determination Using Satellite Altimetry, Report No. 377, Dept. of Geodetic Science and Surveying, The Ohio State University, Columbus, June 1987.

Engelis, T., R.H. Rapp, and Y. Bock, Measuring orthometric height differences with GPS and gravity data, manuscripta geodaetica, Vol. 10, pp. 187-194, 1985.

Everitt, C.W.F., et al., Gravity Probe B as a Geodesy Mission and its Implications for TOPEX, in CSTG Bulletin No. 11, New Satellite Missions for Solid Earth Studies - Status and Preparations, Deutsches Geodatisches Forschungsinstitut (DGFI), Munchen, Fed. Rep. of Germany, June 1989.

Gleason, D.M., Comparing ellipsoidal corrections to the transformation between the geopotential's spherical and ellipsoidal spectrums, manuscripta geodaetica, Vol. 13, pp. 114-129, 1988.

Hajela, D.P., Direct Recovery of Mean Gravity Anomalies From Satellite to Satellite Tracking, Report No. 218, Dept. of Geodetic Science, The Ohio State University, Columbus, December 1974.

Hajela, D.P., Improved Procedures for the Recovery of 5° Mean Gravity Anomalies From ATS-6/GEOS-3 Satellite to Satellite Range-Rate Observations Using Least Squares Collocation, Report No. 276, Dept. of Geodetic Science, The Ohio State University, Columbus, September, 1978.

Hajela, D.P., A Simulation Study to Test the Prediction of 1° x 1° Mean Gravity Anomalies Using Least Squares Collocation From the GRAVSAT Mission, Report No. 316, Dept. of Geodetic Science and Surveying, The Ohio State University, Columbus, September, 1981.

Hajela, D.P., Accuracy Estimates of Gravity Potential Differences Between Western Europe and the United States Through Lageos Satellite Laser Ranging Network, Report No. 345, Dept. of Geodetic Science and Surveying, The Ohio State University, Columbus, February, 1983.

Heck, B., An Evaluation of Some Systematic Error Sources Affecting Terrestrial Gravity Anomalies, Bulletin Geodesique, Vol. 64, No. 1, pp. 88-108, 1990.

Hein, G.W. and B. Eissfeller, Vertical Datum Definition by Integrated Geodesy Adjustment, in Proc. of the Third International Symposium on the North American Vertical Datum, Rockville, Maryland, April 21-26, 1985.

Heiskanen, W.A. and H. Moritz, Physical Geodesy, W.H. Freeman, San Francisco, 1967.

Herring, T.A., Precision of Vertical Position Estimates From Very Long Baseline Interferometry, J. Geophys. Res., Vol. 91, No. B9, pp. 9177-9182, August, 1986.

Hobson, E.W., The Theory of Spherical and Ellipsoidal Harmonics, Chelsea Publishing Company, New York, 1965.

Holota, P., Boundary Value Problems in Physical Geodesy: Present State, Boundary Perturbation and the Green-Stokes Representation, 1st Hotine-Marussi Symp. on Math. Geod., Rome, 1985.

Hotine, M., Mathematical Geodesy, ESSA Monograph No. 2, U.S. Department of Commerce, Washington, D.C., 1969.

International Association of Geodesy (IAG), Geodetic Reference System 1967, Special Publication of Bulletin Geodesique, Paris, 1971.

International Association for Physical Sciences of the Ocean (IAPSO), Advisory Committee on Tides and Mean Sea Level, Changes in Relative Mean Sea Level, Eos Trans. AGU, Vol. 66, No. 45, November 1985.

Jekeli, C., Global Accuracy Estimates of Point and Mean Undulation Differences Obtained From Gravity Disturbances, Gravity Anomalies and Potential Coefficients, Report No. 288, Dept. of Geodetic Science, The Ohio State University, Columbus, 1979.

Jekeli, C., Reducing the Error of Geoid Undulation Computations by Modifying Stokes' Function, Report No. 301, Dept. of Geodetic Science, The Ohio State University, Columbus, May, 1980.

Jekeli, C., The exact transformation between ellipsoidal and spherical harmonic expansions, manuscripta geodaetica, Vol. 13, pp. 106-113, 1988.

Jekeli, C., Error Spectrum vs. Spectrum Errors in Least-Squares Collocation, in Festschrift to Torben Krarup, E. Kejlso, K. Poder and C.C. Tscherning editors, Geodaetisk Institut, Copenhagen, Denmark, 1989.

Jekeli, C., T.N. Upadhyay, Gravity Estimation From STAGE, a Satellite-to-Satellite Tracking Mission, J. Geophys. Res., Vol. 95, No. B7, pp. 10973-10985, July, 1990.

Jorgensen, P.S., NAVSTAR/Global Positioning System 18-Satellite Constellations, Navigation, Vol. 27, No. 2, pp. 89-100, 1980.

Kahn, W.D., S.M. Klosko, and W.T. Wells, Mean Gravity Anomalies From a Combination of Apollo/ATS 6 and GEOS 3/ATS 6 SST Tracking Campaigns, J. Geophys. Res., Vol. 87, No. B4, pp. 2904-2918, April, 1982.

Katsambalos, K.E., The Effect of the Smoothing Operator on Potential Coefficient Determinations, Report No. 287, Dept. of Geodetic Science, The Ohio State University, Columbus, March, 1979.

Kaula, W.M., Inference of Variations in the Gravity Field From Satellite-to-Satellite Range Rate, J. Geophys. Res., Vol. 88, No. B10, pp. 8345-8349, October, 1983.

Kearsley, A.H.W., Data Requirements for Determining Precise Relative Geoid Heights From Gravimetry, J. Geophys. Res., Vol. 91, No. B9, pp. 9193-9201, August, 1986.

Keating, T., P. Taylor, W. Kahn, F. Lerch, Geopotential Research Mission Science, Engineering, and Program Summary, NASA Techn. Memo., 86240, May, 1986.

Kellogg, O.D., Foundations of Potential Theory, Dover Publications, New York, 1954.

Kelm, R., Vertical Datum Definitions Discussed in View of European Vertical and Horizontal Networks, in Proc. of the Third International Symposium on the North American Vertical Datum, Rockville, Maryland, April 21-26, 1985.

Laskowski, P., The Effect of Vertical Datum Inconsistencies on the Determination of Gravity Related Quantities, Report No. 349, Dept. of Geodetic Science and Surveying, The Ohio State University, Columbus, August 1983.

Lisitzin, E., The Mean Sea Level of the World Ocean, Comment. Phys.-Math. Helsingf., pp. 30-35, 1965.

Mather, R.S., C. Rizos and T. Morrison, On the Unification of Geodetic Levelling Datums Using Satellite Altimetry, NASA Techn. Memo., 79533, April, 1978.

Moritz, H., Linear Solutions of the Geodetic Boundary-Value Problem, Report No. 79, Dept. of Geodetic Science, The Ohio State University, Columbus, December, 1966.

Moritz, H., Precise Gravimetric Geodesy, Report No. 219, Dept. of Geodetic Science, The Ohio State University, Columbus, December, 1974.

Moritz, H., Advanced Physical Geodesy, Abacus Press, Kent, U.K., 1980.

Moritz, H., Local Geoid Determination in Mountain Regions, Report No. 352, Dept. of Geodetic Science and Surveying, The Ohio State University, Columbus, December 1983.

Moritz, H. and I.I. Mueller, Earth Rotation Theory and Observation, Ungar, New York, 1987.

Mueller, I.I., Reference Coordinate Systems, The Interdisciplinary Role of Space Geodesy, I.I Mueller and S. Zerbini (Eds.), Lecture Notes in Earth Sciences, Springer-Verlag, pp. 217-238, Erice, Sicily, Italy, July 23-29, 1988.

Paul, M.K., Recurrence Relations for Integrals of Associated Legendre Functions, Bulletin Geodesique, Vol. 52, pp. 177-190, 1978.

Pavlis, N.K., Modeling and Estimation of a Low Degree Geopotential Model From Terrestrial Gravity Data, Report No. 386, Dept. of Geodetic Science and Surveying, The Ohio State University, Columbus, March 1988.

Pavlis, E.C., D.E. Smith, O.L. Colombo, Gravity Field Estimation From Future Space Missions: Aristoteles, Gravity Probe-B and Topex/Poseidon, paper presented at the XV General Assembly of the European Geophysical Society, Copenhagen, Denmark, April 23-27, 1990.

Rapp, R.H., The Earth's Gravity Field to Degree and Order 180 Using SEASAT Altimeter Data, Terrestrial Gravity Data, and Other Data, Report No. 322, Dept. of Geodetic Science and Surveying, The Ohio State University, Columbus, December 1981a.

Rapp, R.H., Ellipsoidal Corrections for Geoid Undulation Computations, Report No. 308, Dept. of Geodetic Science, The Ohio State University, Columbus, March 1981b.

Rapp, R.H., The Need and Prospects for a World Vertical Datum, in Proc. of the IAG Symposia, XVII General Assembly, Hamburg, Vol. 2, pp. 432-445, Dept. of Geodetic Science and Surveying, The Ohio State University, 1983.

Rapp, R.H., Geometric Geodesy Part I, Dept. of Geodetic Science and Surveying, The Ohio State University, Columbus, March 1984.

Rapp, R.H., Report of Special Study Group No. 1.75, World Vertical Reference System, XIX General Assembly of IUGG, International Association of Geodesy, Vancouver, B.C., Canada, June 1987.

Rapp, R.H. and D.P. Hajela, Accuracy Estimates of 1° x 1° Mean Anomaly Determinations From a High-Low SST Mission, Report No. 295, Dept. of Geodetic Science, The Ohio State University, Columbus, September 1979.

Rapp, R.H. and M. Kadir, A Preliminary Geoid for the State of Tennessee, Surveying and Mapping, Vol. 48, No. 4, pp. 251-260, 1988.

Rapp, R.H. and N.K. Pavlis, The Development and Analysis of Geopotential Coefficient Models to Spherical Harmonic Degree 360, J. Geophys. Res., Vol. 95, No. B13, pp. 21885-21911, December 1990.

Roach, G.F., Green's Functions - Introductory Theory with Applications, Van Nostrand Reinhold Company, London, 1970.

Rummel, R., Geoid Heights, Geoid Height Differences, and Mean Gravity Anomalies From "Low-Low" Satellite-to-Satellite Tracking - An Error Analysis, Report No. 306, Dept. of Geodetic Science, The Ohio State University, Columbus, June 1980.

Rummel, R. and P. Teunissen, Height Datum Definition, Height Datum Connection and the Role of the Geodetic Boundary Value Problem, Bulletin Geodesique, Vol. 62, No. 4, pp. 477-498, 1988.

Rummel, R., D.P. Hajela, R.H. Rapp, Recovery of Mean Gravity Anomalies From Satellite-Satellite Range Rate Data Using Least Squares Collocation, Report No. 248, Dept. of Geodetic Science, The Ohio State University, Columbus, September 1976.

Schwarz, K.P., M.G. Sideris, R. Forsberg, Orthometric Heights Without Leveling, J. Surveying Eng., Vol. 113, No. 1, 1987.

Shepperd, S.W., Molodenskii-Type Coefficients with Application to Gravity Disturbance Vector Truncation Errors at Altitude, R-1329, The Charles Stark Draper Laboratory Inc., Cambridge, Massachusetts, October 1979.

Sjöberg, L.E., Comparison of Some Methods of Modifying Stokes' Formula, paper presented at the International Symposium on the Definition of the Geoid, Florence, May 26-30, 1986.

Sjöberg, L.E., Generalization of Stokes's and Hotine's formulas to a non-spherical Earth, manuscripta geodaetica, Vol. 15, pp. 74-82, 1990.

Sjöberg, L.E., H. Fan, A Comparison of the Modified Stokes' Formula and Hotine's Formula in Physical Geodesy, Report No. 4, Dept. of Geodesy, The Royal Institute of Technology, Stockholm, November 1986.

Smith, D.E., et al., A Global Geodetic Reference Frame From LAGEOS Ranging (SL5.1AP), J. Geophys. Res., Vol. 90, No. B11, pp. 9221-9233, September 1985.

Wichiencharoen, C., FORTRAN Programs for Computing Geoid Undulationsfrom Potential Coefficients and Gravity Anomalies, Internal Report, Dept. of Geodetic Science and Surveying, The Ohio State University, Columbus, 1982.

Wolff, M., Direct Measurements of the Earth's Gravitational Potential Using a Satellite Pair, J. Geophys. Res., Vol. 74, No. 22, October 1969.

Wunsch, C. and E.M. Gaposchkin, On Using Satellite Altimetry to Determine the General Circulation of the Oceans With Applications to Geoid Improvement, Rev. Geophys. and Space Physics, Vol. 18, No. 4, pp. 725-745, November 1980.

Zilkoski, D.B., The North American Vertical Datum of 1988 (NAVD 88) - Tasks, Impacts, and Benefits, Proceedings of the Symposium on Height Determination and Recent Vertical Crustal Movements in Western Europe, Hannover, Fed. Rep. of Germany, September 15-19, 1986.